DOCTOR OF PHILOSOPHY

The biology of reproduction in two British pulmonate slugs.

Nicholas, J.

Award date:
1984

Awarding institution:
Bangor University

THE BIOLOGY OF REPRODUCTION IN TWO BRITISH PULMONATE SLUGS

by

Jane Nicholas

A thesis submitted in partial fulfilment of the requirements for the degree of Philosophiae Doctor in the University of Wales.

In three volumes

VOLUME II

School of Animal Biology,
University College of North Wales,
Bangor, Gwynedd,
United Kingdom.

October 1984.

KEY

a	acinus	agd	albumen gland ducts
ah	anterior, slender region of hermaphrodite duct	al	ascending limb of carrefour loop
alb	albumen gland	am	apical membrane
ap	apices	at	atrium
ax	axon		
b	bursa copulatrix	BM	basement membrane
br	brain	bs	blood sinus
bv	blood vessel	bw	body wall
C	carrefour	Ca	calcium cell
cc	cell cluster	CD	common duct
cg	carrefour gland	cil	cilated cells
cl	clear vesicles	Cm	circular muscle
co	core vesicles	coll	collagen
CT	connective tissue	cy	cytoplasm
d	desmosome	div	carrefour diverticulum

dl	descending limb of carrefour loop	du	ductule
ec	cone of epiphallus	ed	electron-dense granules
Ep	epithelium	epi	epiphallus
F	fibroblast	f	lateral foot
Fd	finger-like diverticulum	fo	focus of multiplication
foll	follicle		
g	granular connective tissue cells	gl	gland
Gly	glycogen	gr	granules
hd	hemidesmosome		
iv	intercellular vacuole	IV	intracellular vacuole
j	jelly layer		
L	duct lumen	LA	lower atrium
LM	longitudinal muscle	Ly	lysosome
M	mitochondria	mc	muscle
mf	microfibrils	mt	microtubules
mu	mucocytes	mv	microvilli

MVB	multivesicular body		
N	nucleus	Ne	neuron
nt	neurotransmitter granules	nu	nucleolus
Nv	nerve		
O	oviducal gland of common duct	oo	oocyte
Ov	oviduct		
P	polysome	pap	papilla
pb	polar body	Pd	pouched diverticulum
ph	posterior, slender region of hermaphrodite	pig	pigment
PM	penial mass	po	pore cell
pr	prostate gland	Ps	penial sac
Psp	phagocytosed sperm	pvf	perivitelline fluid
r	ciliary rootlet	rER	rough endoplasmic reticulum
S	sarcobellum	sc	secretory cells
sd	septate desmosomes	sER	smooth endoplasmic reticulum
Sg	sarcobellum gland cells	Sh	shell
sn	secretion	Sp	sperm

Sph	spermatophore	SR	sarcoplasmic reticulum
SV	seminal vesicle	Syn	synapse
t	tubule	ta	trifid appendage
tER	transitional endoplasmic reticulum		
UA	upper atrium	uncil	unciliated cells
V	vacuoles	Vd	vas deferens
za	zonula adhaerens		
♀	female duct	♂	male duct
I	type I secretory cell	II	type II secretory cell

Fig. 1 External appearance of adult *D.reticulatum* (a) and *A.hortensis* (b).

a

b

Fig. 1

Fig. 2 Diagrams of the reproductive tracts of *D.reticulatum* (a) and *A.hortensis* (b).

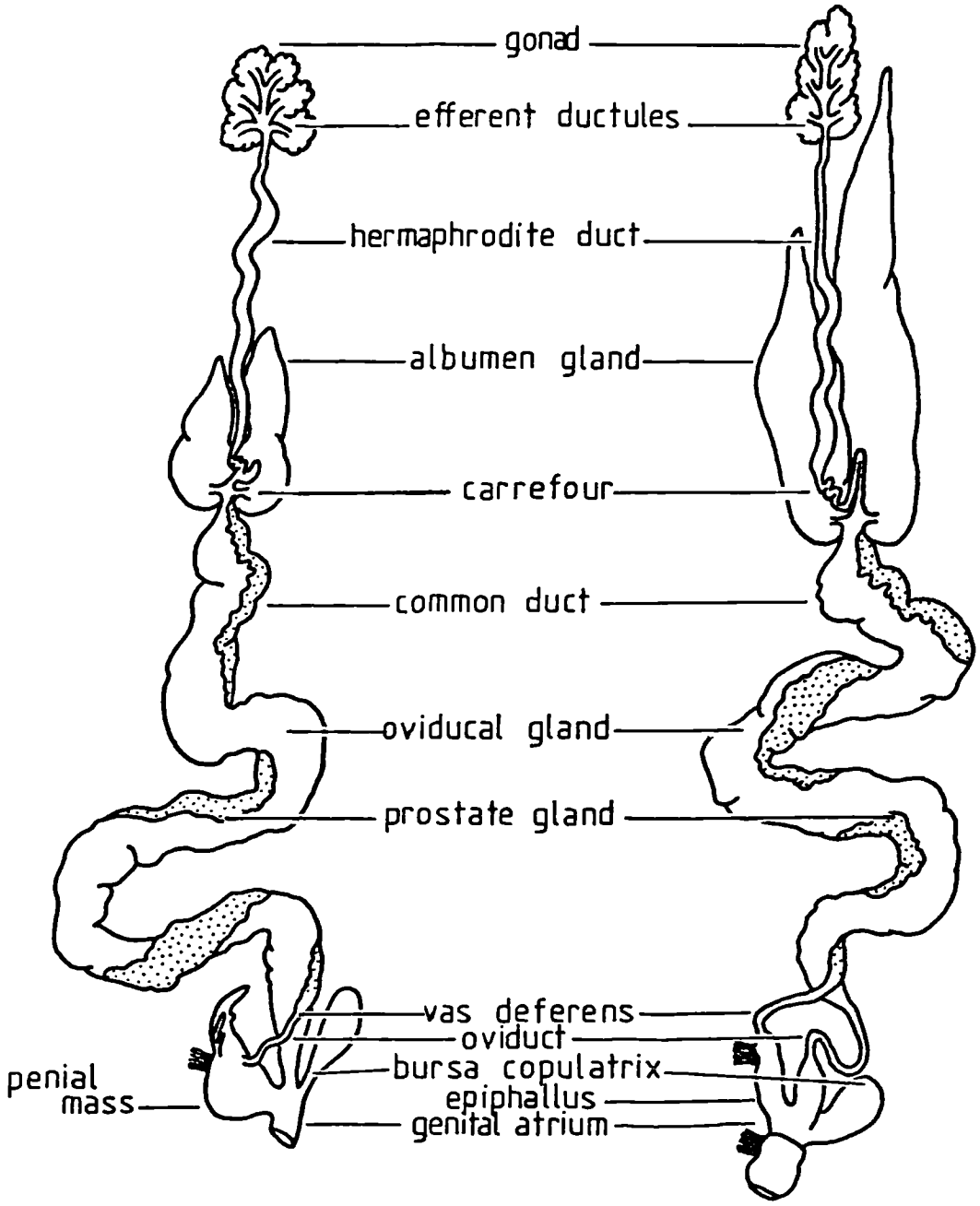

a) D. reticulatum b) A. hortensis

Fig. 2

Fig. 3 Interpretatiion of cell activity.

Key: rER rough endoplasmic reticulum

tER transitional endoplasmic reticulum

MVB multivesicular body

PV phagocytotic vacuole

CV condensing vacuole

2^{y} secondary lysosome

● primary lysosome

◉ primary lysosome with clathrin coat

◎ clathrin-coated vesicles

○ uncoated vesicles

⟶ flow demonstrated

----→ possible flow

(a) to (s) see text

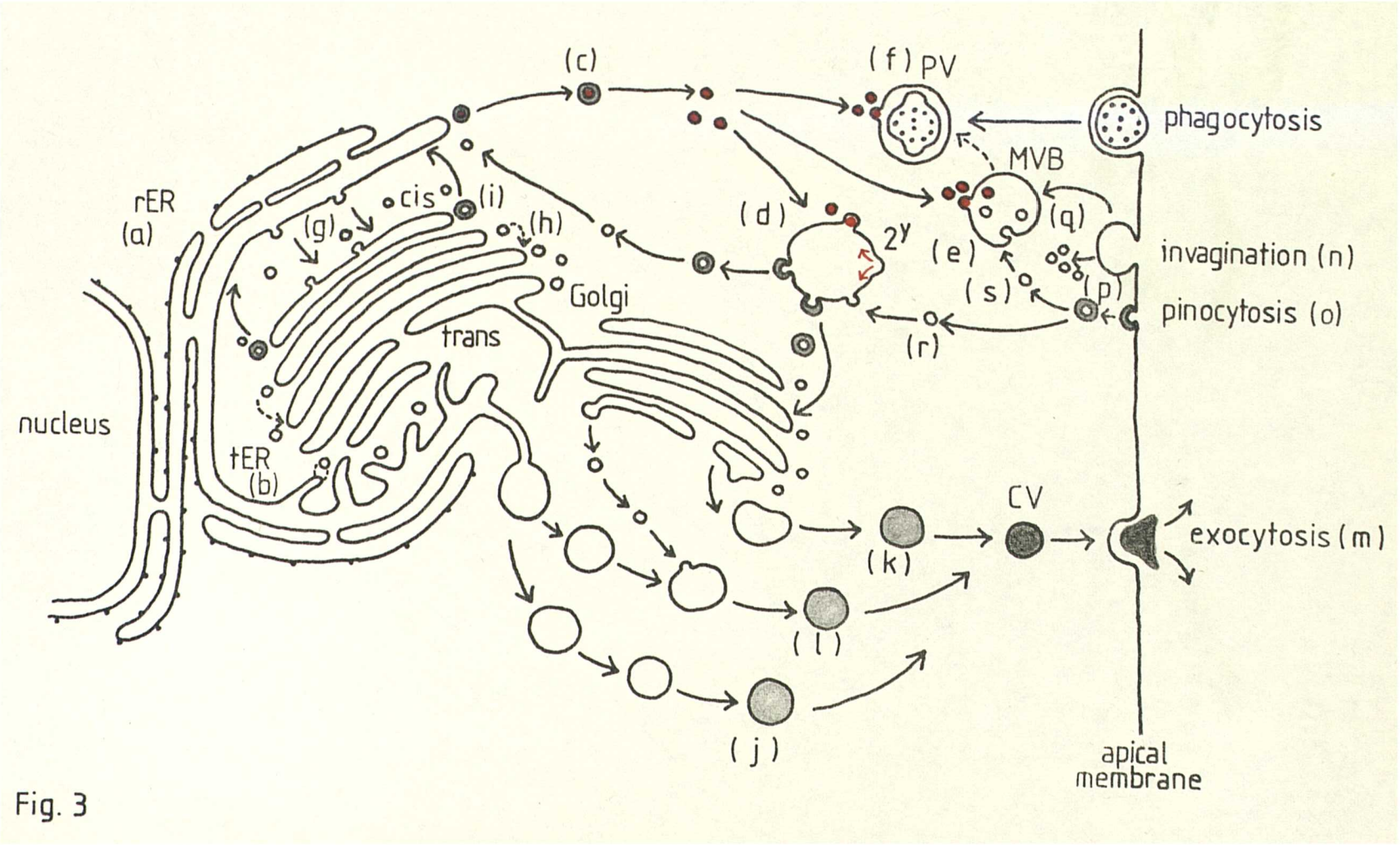
(c)
(f) PV
phagocytosis
MVB
rER
(a)
cis
(i)
(g)
(h)
(d)
2y
(e)
(q)
invagination (n)
(s)
(p)
pinocytosis (o)
Golgi
trans
(r)
nucleus
tER
(b)
CV
exocytosis (m)
(k)
(l)
(j)
apical
membrane

Fig. 3

Fig. 4 Diagram of the morphology of the mature hermaphrodite duct.

Fig. 5 T.S. through the seminal vesicle and posterior slender region of the hermaphrodite duct in D.reticulatum (x 150). The arrows indicate the transition from ciliated to unciliated cells.

Fig. 6 T.S. through the seminal vesicle in A. hortensis (x300). The arrows indicate the transition from ciliated to unciliated cells.

Fig. 7 T.S. through the anterior slender region of the hermaphrodite duct in D.reticulatum (x250).

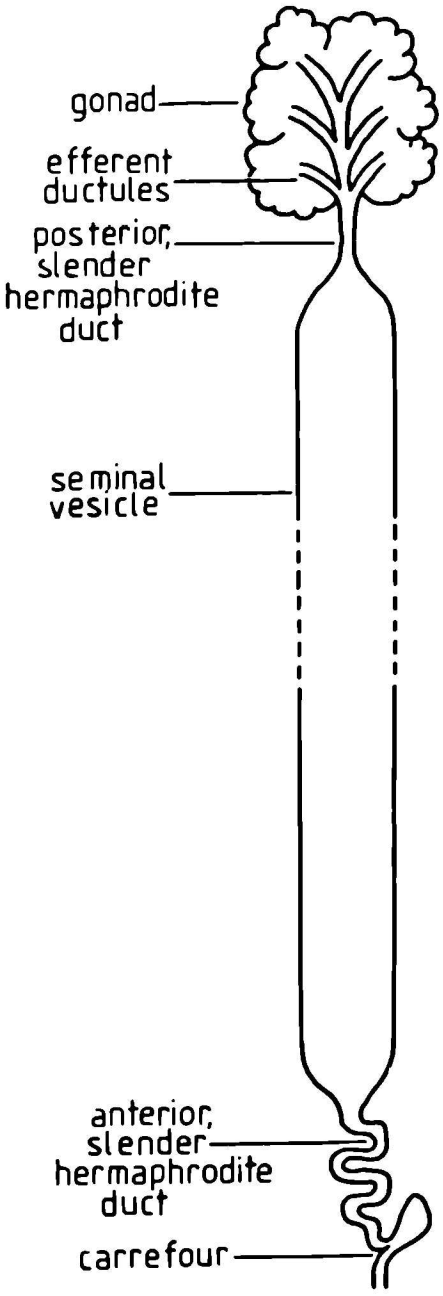
gonad
efferent ductules
posterior, slender hermaphrodite duct
seminal vesicle
anterior, slender hermaphrodite duct
carrefour

Fig. 4

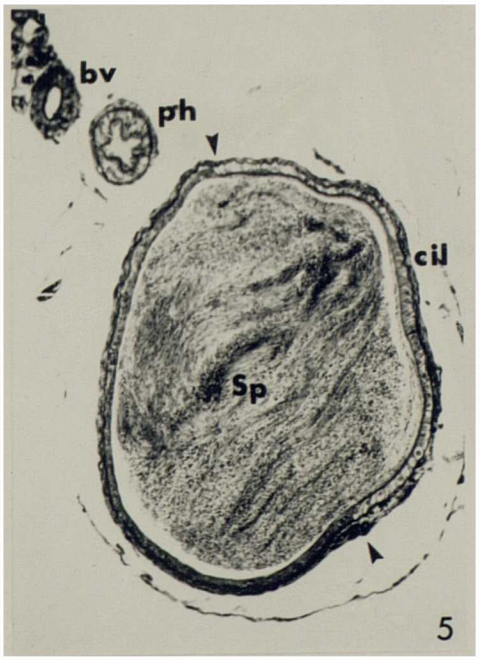
bv
ph
cil
Sp
5

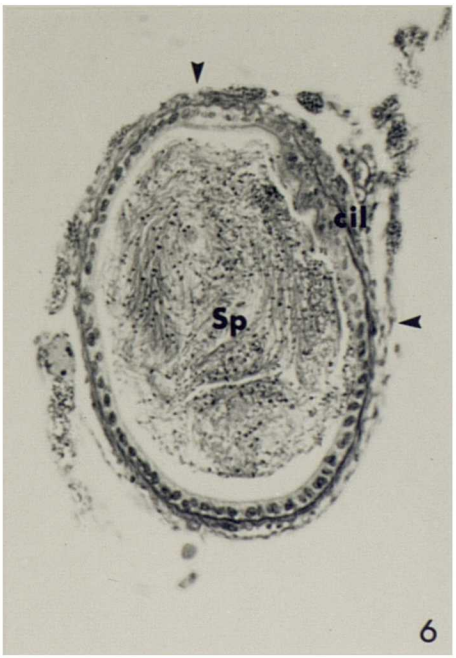
cil
Sp
6


bv
ah
7

Fig. 8 Diagram of the carrefour region in *D. reticulatum* (a) and *A.hortensis* (b).

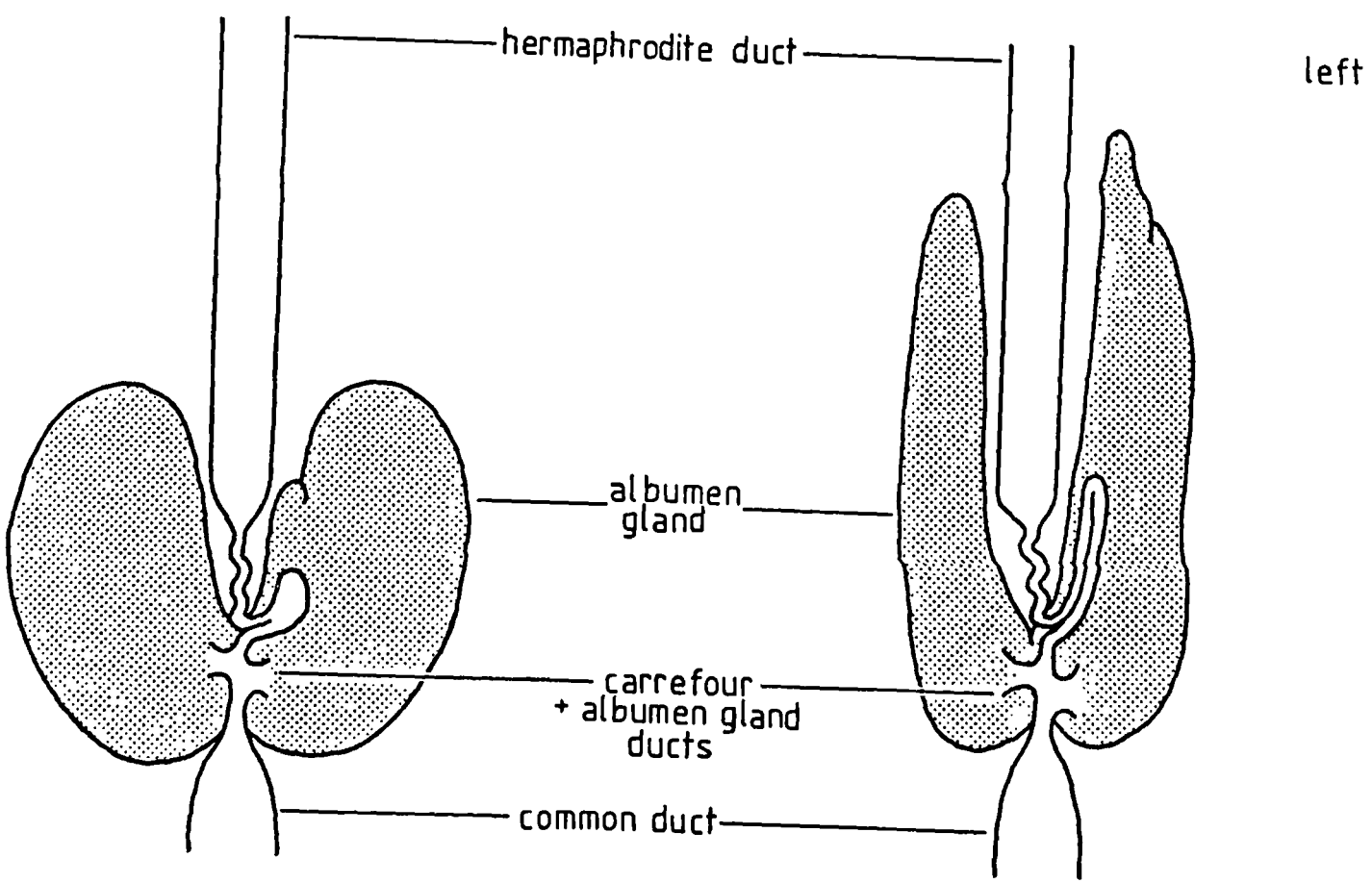
right
hermaphrodite duct
left
albumen gland
carrefour + albumen gland ducts
common duct
a. D.reticulatum
b. A.hortensis
1mm.

Fig. 8

Fig. 9 Diagram of the mature carrefour of D.reticulatum, front and rear views. Sections through this structure are illustrated in the following figures.

A-A Fig. 10

B-B Fig. 11

C-C Fig. 12

D-D Fig. 14

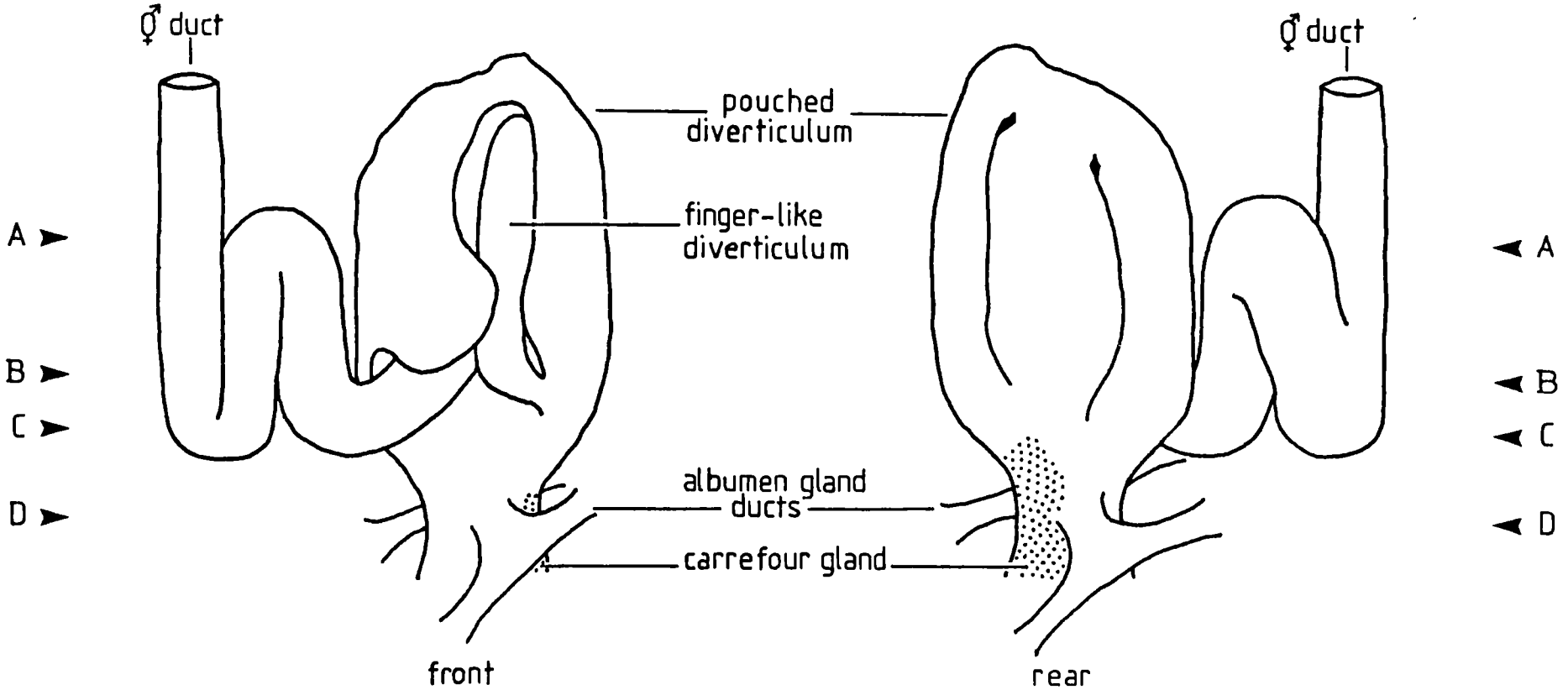
♀♂ duct
♀♂ duct
pouched diverticulum
finger-like diverticulum
albumen gland ducts
carrefour gland
A
B
C
D
A
B
C
D
front
rear
100µm

Fig. 9

Figs. 10-14 Transverse sections at different levels (see Fig. 9) through the mature carrefour of *D. reticulatum* (x180).

Fig. 15 T.S. through the posterior region of the common duct (x60).

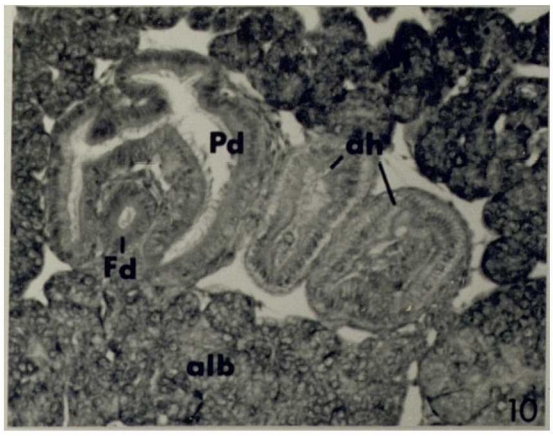
Pd
dh
Fd
alb
10

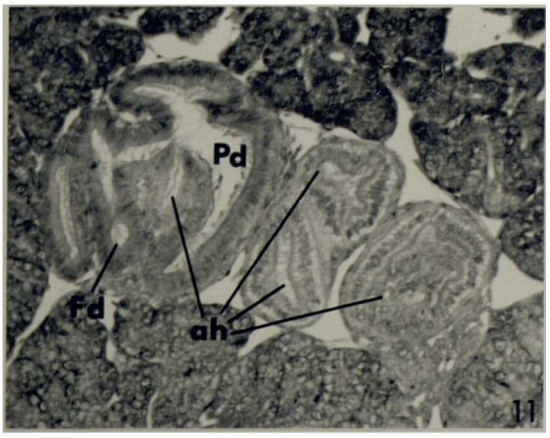
Pd
Fd
ah
11

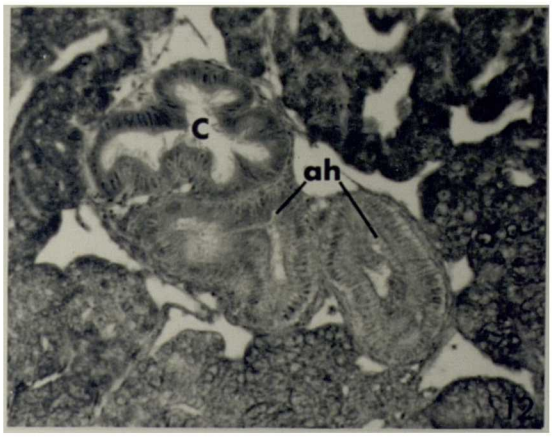
C
ah
12

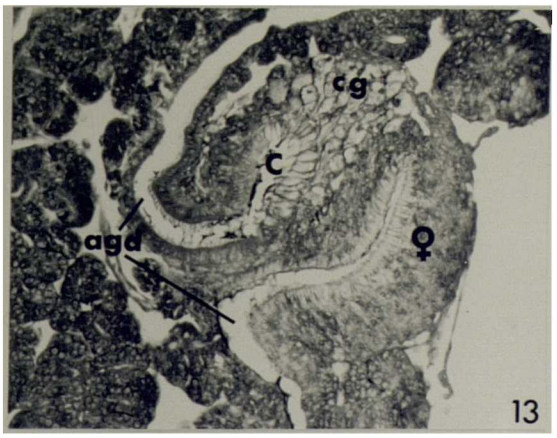
cg
C
agd
♀
13

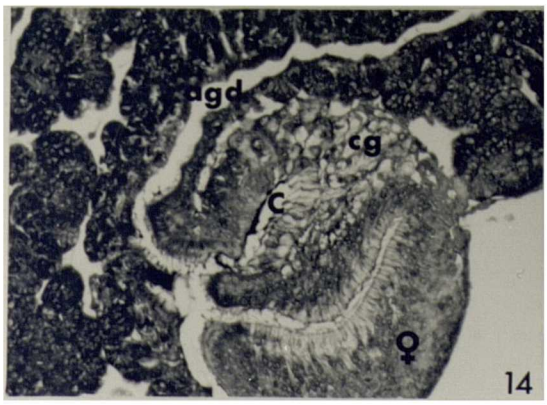
agd
cg
C
♀
14

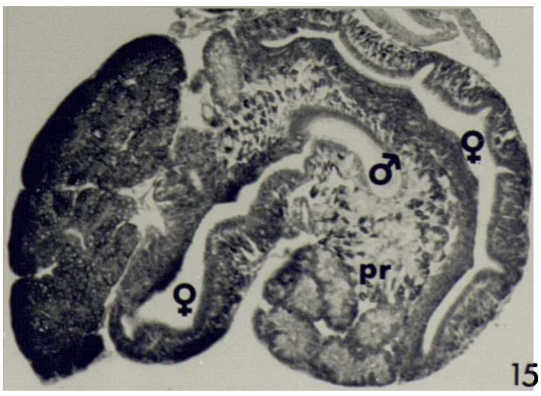
♀
♂
pr
♀
15

Fig. 16 Vascularization of the carrefour and albumen gland of D.reticulatum. Drawn from dissection. Blood vessels injected with Indian ink by A. Duval.

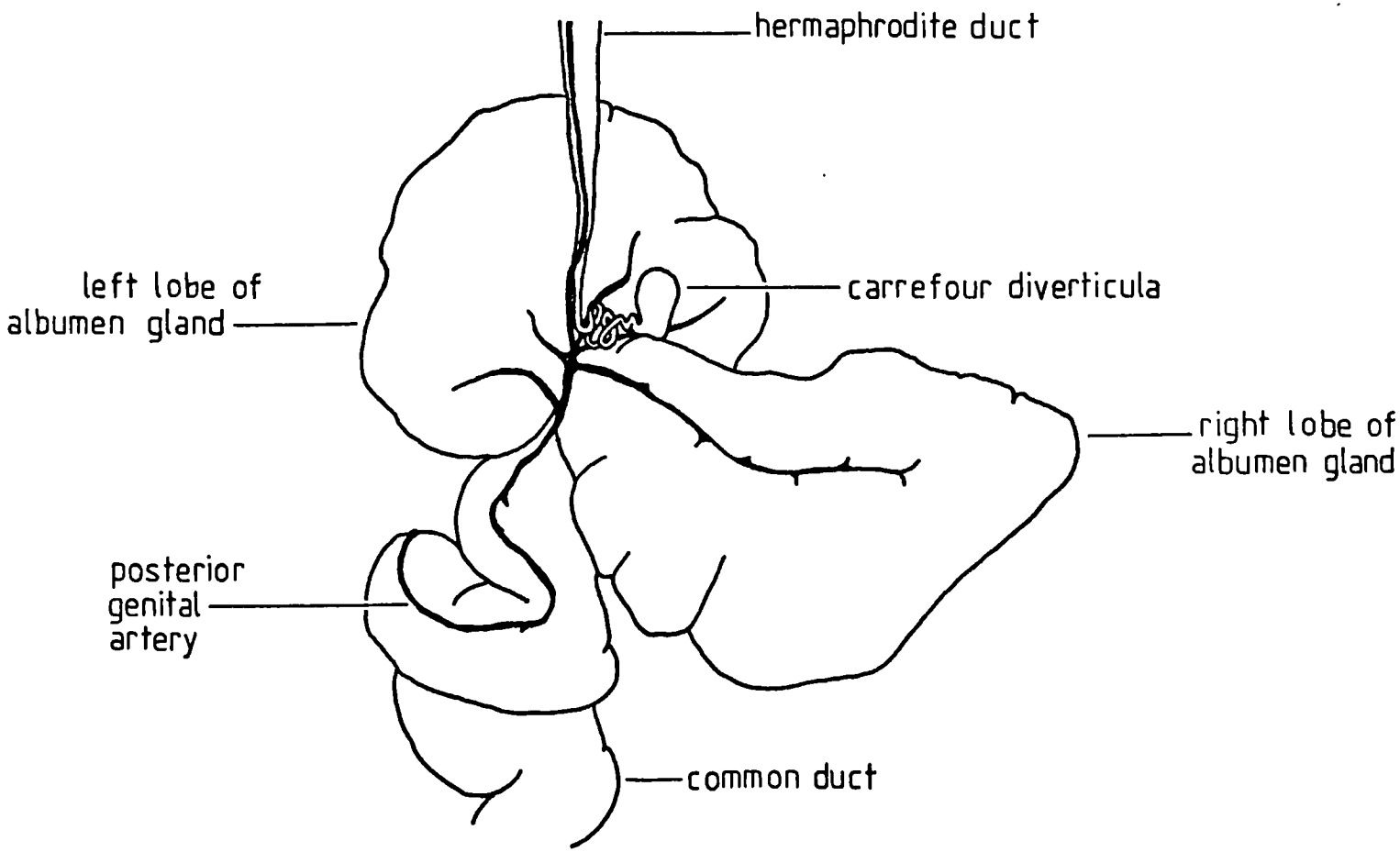
hermaphrodite duct
left lobe of albumen gland
carrefour diverticula
right lobe of albumen gland
posterior genital artery
common duct

Fig. 16

Fig. 17 Diagram of the mature carrefour of A.hortensis, front and rear views. Sections through this structure are illustrated in the following figures.

A-A Fig. 18

B-B Fig. 19

C-C Fig. 20

D-D Fig. 21

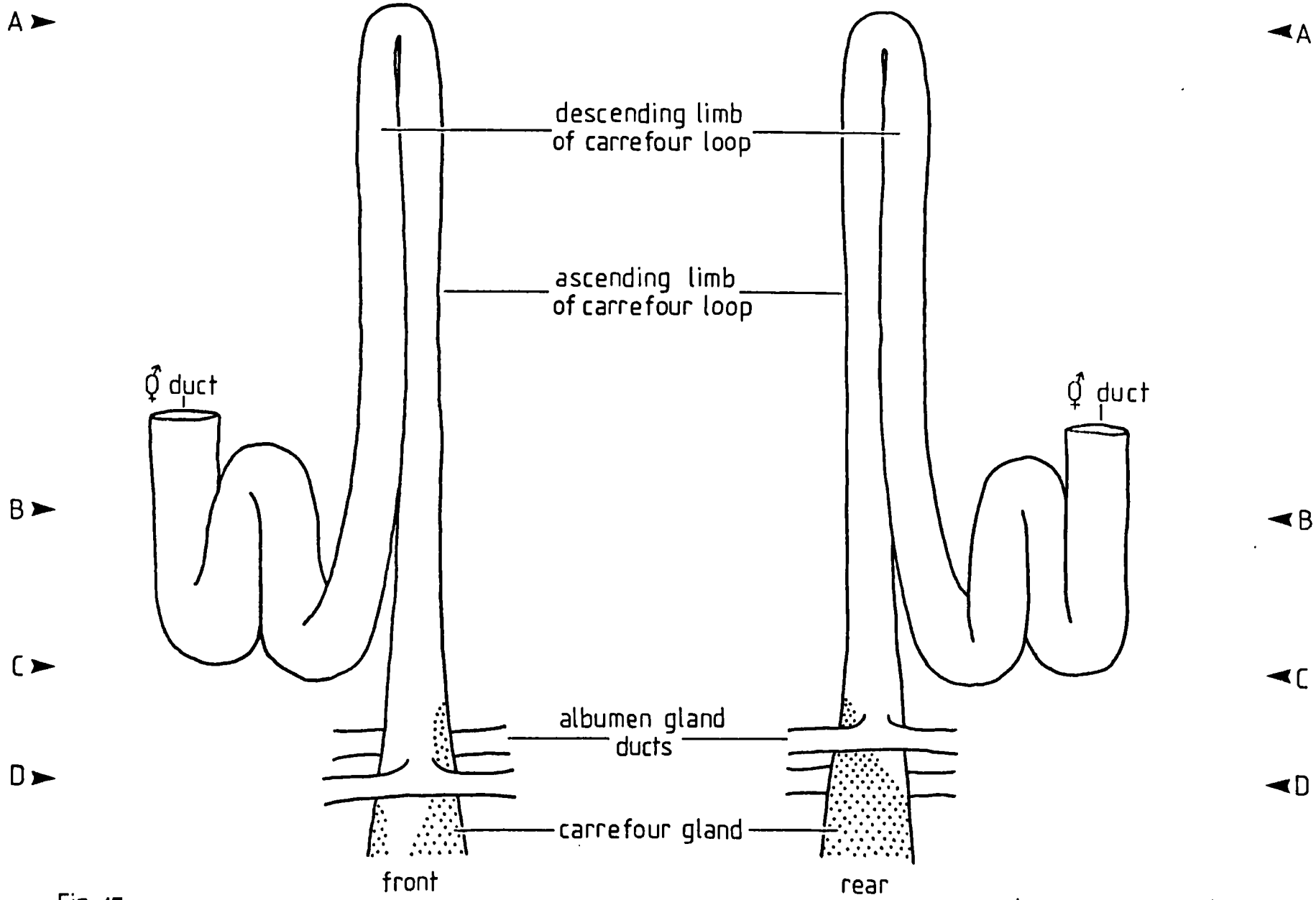
A
A
descending limb
of carrefour loop
ascending limb
of carrefour loop
♀♂ duct
♀♂ duct
B
B
C
C
albumen gland
ducts
D
D
carrefour gland
front
rear
0·5mm.

Fig. 17

Figs. 18-22 Transverse sections at different levels (see Fig. 17) through the mature carrefour of *A. hortensis* (x160).

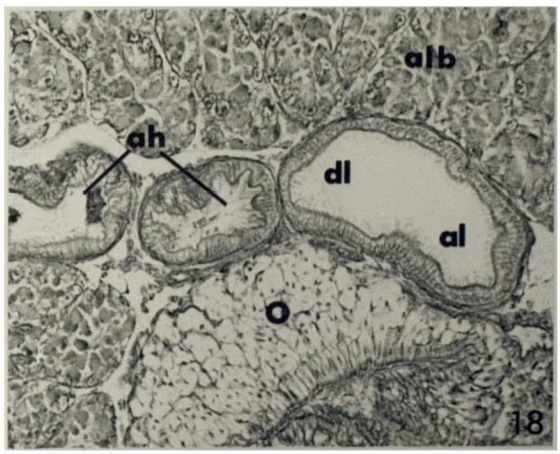
alb
ah
dl
al
O
18

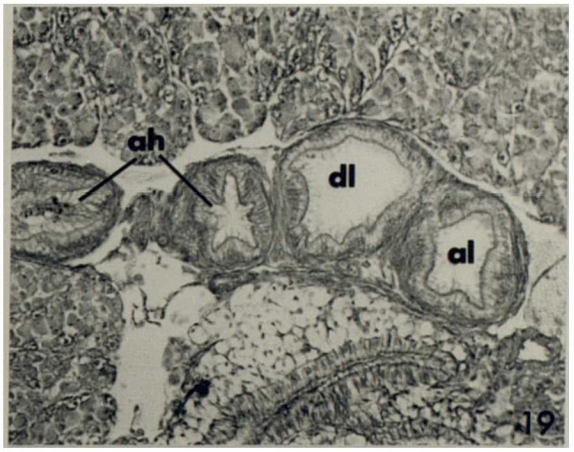
ah
dl
al
19

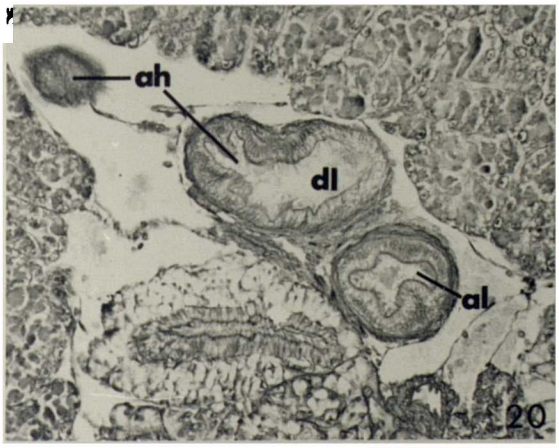
ah
dl
al
20

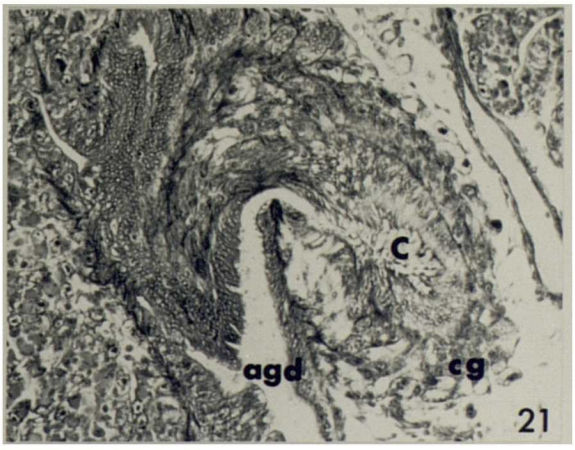
C
agd
cg
21

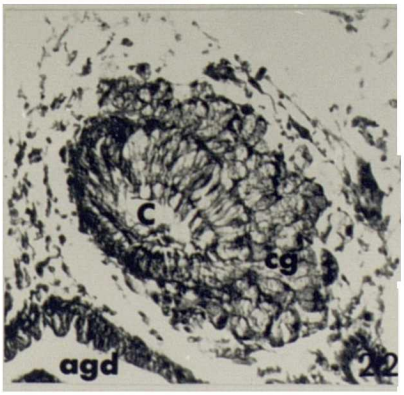
C
cg
agd
22

Fig. 23 Vascularization of the carrefour and albumen gland of A.hortensis. Drawn from dissection. Blood vessels injected with Indian ink by A. Duval.

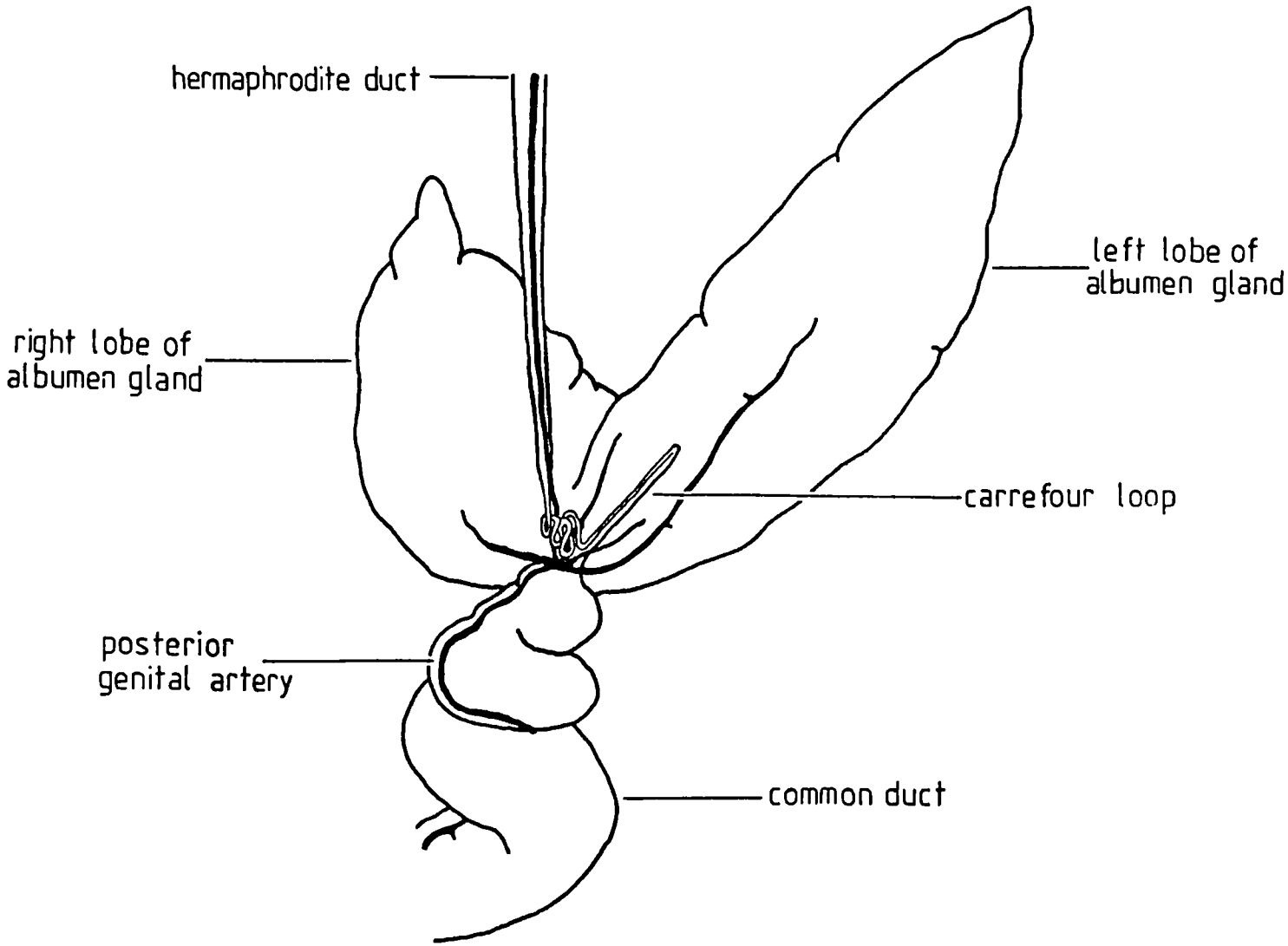
hermaphrodite duct
left lobe of albumen gland
right lobe of albumen gland
carrefour loop
posterior genital artery
common duct

Fig. 23

D.reticulatum, T.S. through the reproductive tract in the region of the carrefour.

Fig. 24 Early A-stage (x500).

Fig. 25 Late A-stage (x800).


24

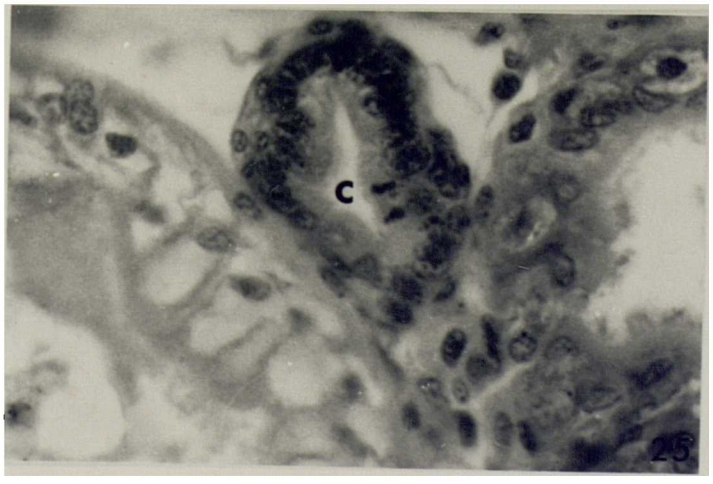
C
25

Fig. 26 Diagrams of immature carrefours in D.reticulatum, front and rear views.

(a) Early B-stage.
Sections through this structure are illustrated in the following figures.

A-A Fig. 27
B-B Fig. 28
C-C Fig. 29
D-D Fig. 30

(b) Late B-stage.
Sections through this structure are illustrated in the following figures.

A-A Fig. 32
B-B Fig. 33
C-C Fig. 34

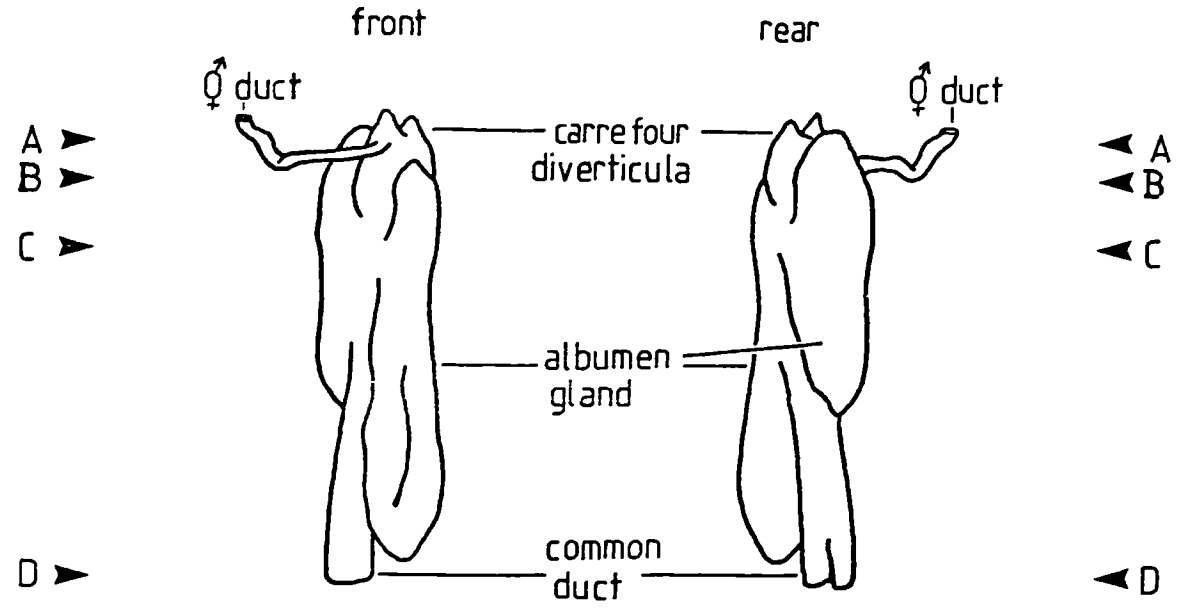

a. Early B

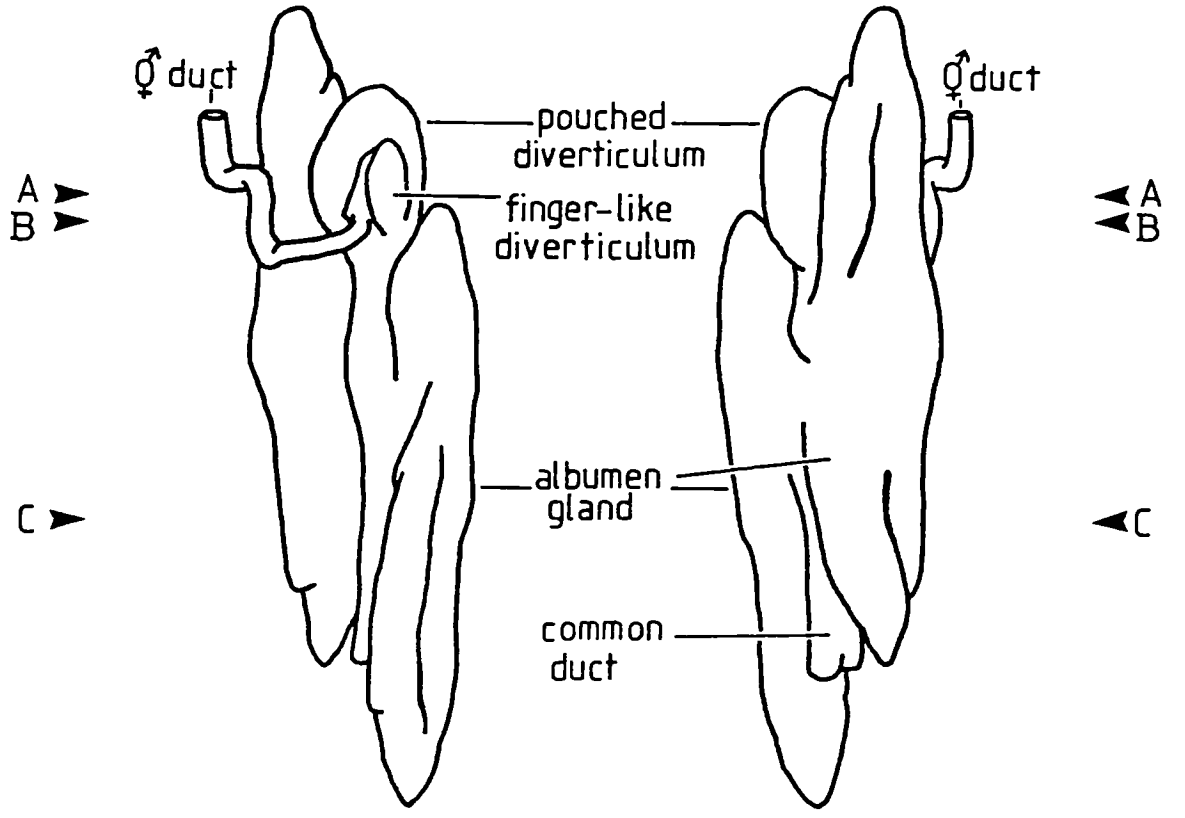

b. Late B

Fig. 26

50μm

Figs. 27-30 D.reticulatum, transverse sections at different levels (see Fig. 26a) through an early B-Stage carrefour (x310).

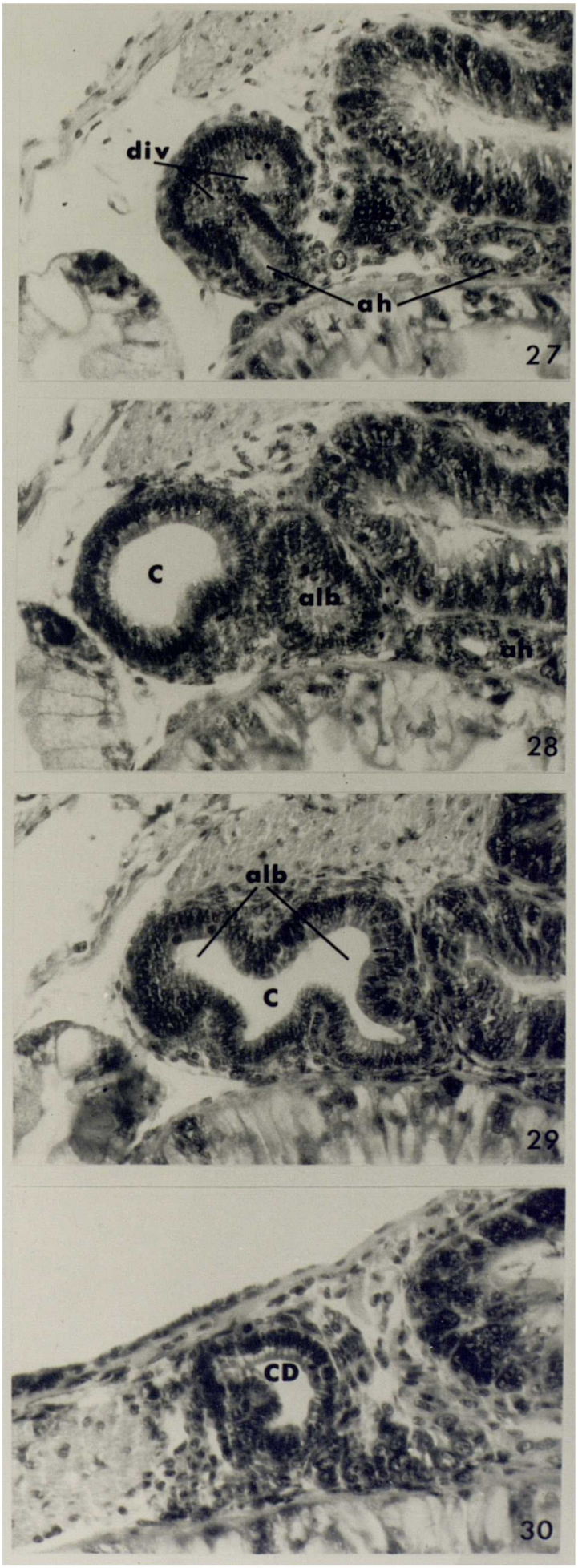
div
ah
27
C
alb
ah
28
alb
C
29
CD
30

Fig. 31 D.reticulatum, T.S. through the hermaphrodite duct of a late B-stage animal (x310).

Figs 32-34 D.reticulatum, transverse sections at different levels (see Fig. 26b) through a late B-stage carrefour (x310).

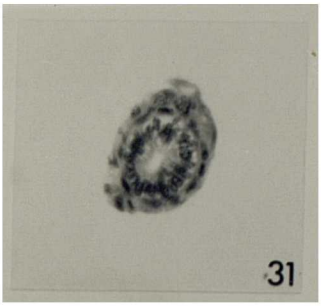
31

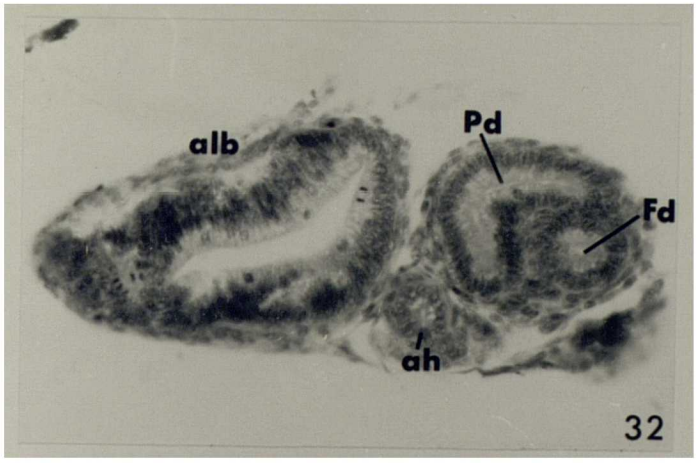
alb
Pd
Fd
ah
32

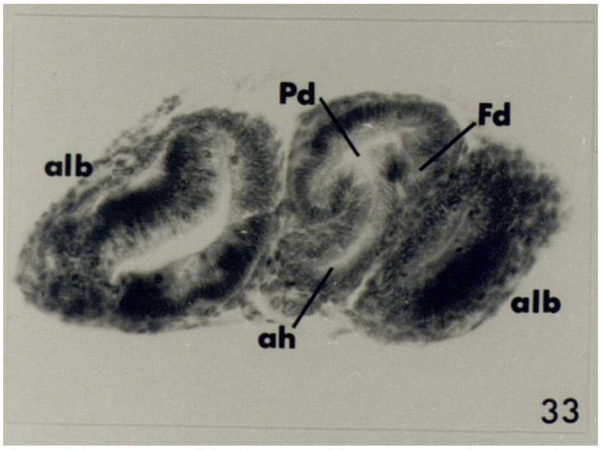
Pd
Fd
alb
alb
ah
33

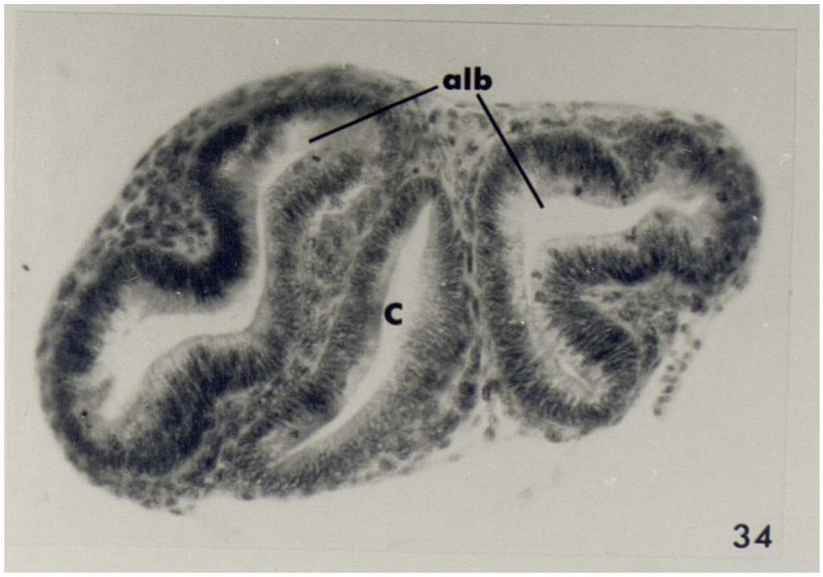
alb
C
34

A.hortensis, T.S. through the reproductive tract in the region of the carrefour.

Fig. 35 Early A-stage (x560).

Fig. 36 Late A-stage (x400).

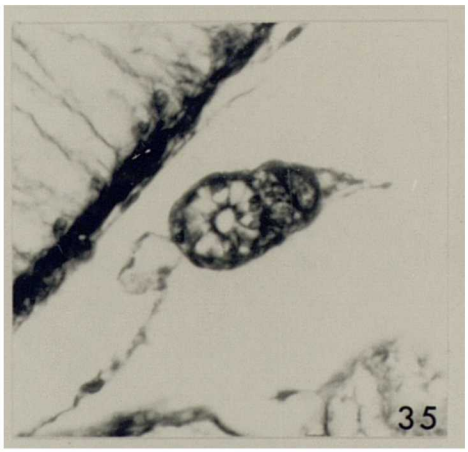
35

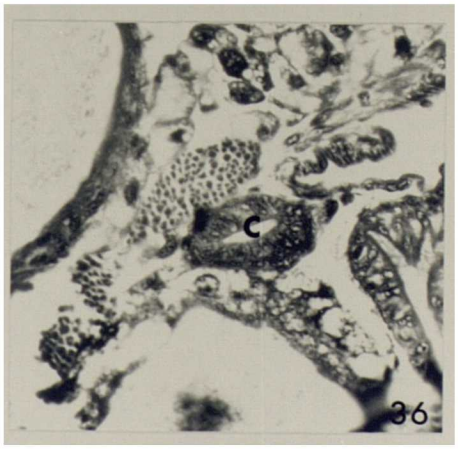
C
36

Fig. 37 Diagrams of immature carrefours in A.hortensis, front and rear views.

(a) Early B-stage.

Sections through this structure are illustrated in the following figures.

A-A Fig. 38

B-B Fig. 39

C-C Fig. 40

D-D Fig. 41

(b) Late B-stage.

Sections through this structure are illustrated in the following figures.

A-A Fig. 42

B-B Fig. 43

C-C Fig. 44

D-D Fig. 45

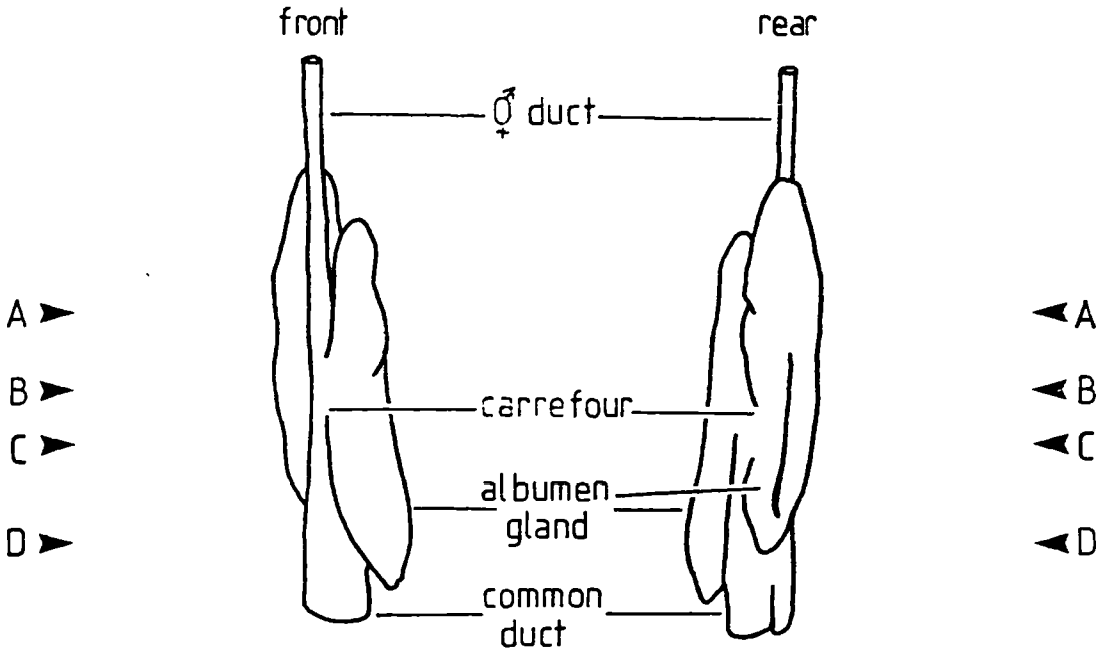

a. Early B

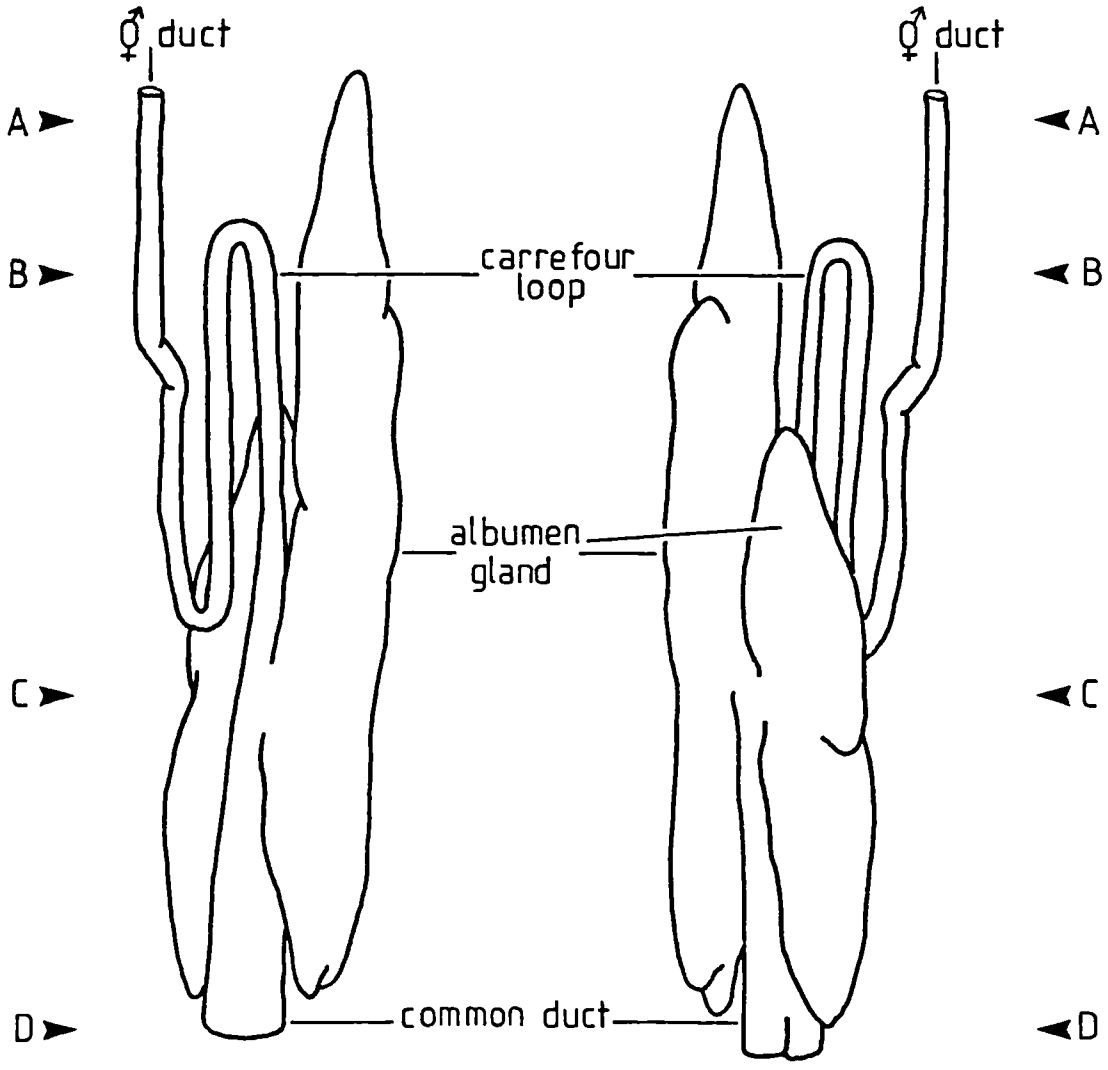

b. Late B

Fig. 37

50µm

Figs. 38-41 A.hortensis, transverse sections at different levels (see Fig. 37a) through an early B-stage carrefour (x250).

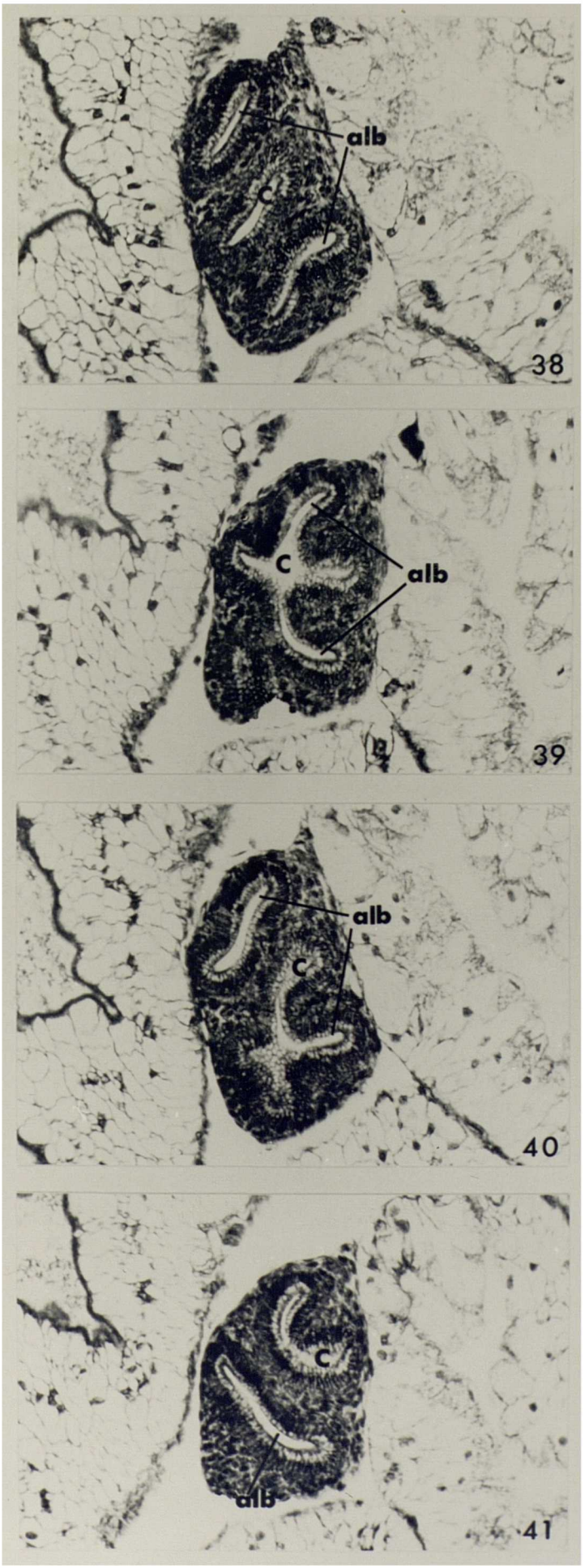
alb
C
38
C
alb
39
alb
C
40
C
alb
41

Figs. 42-45 A.hortensis, transverse sections at different levels (see Fig. 37b) through a late B-stage carrefour (x250).


dl
al
ah
alb
42
C
alb
43
ah
alb
44
CD
45

D.reticulatum, reproductive tract of a newly-hatched animal.

Fig. 46 Transverse section (x1K).

Fig. 47 Longitudinal section (x1.5K).

Fig. 48 Transverse section (x6K).

46

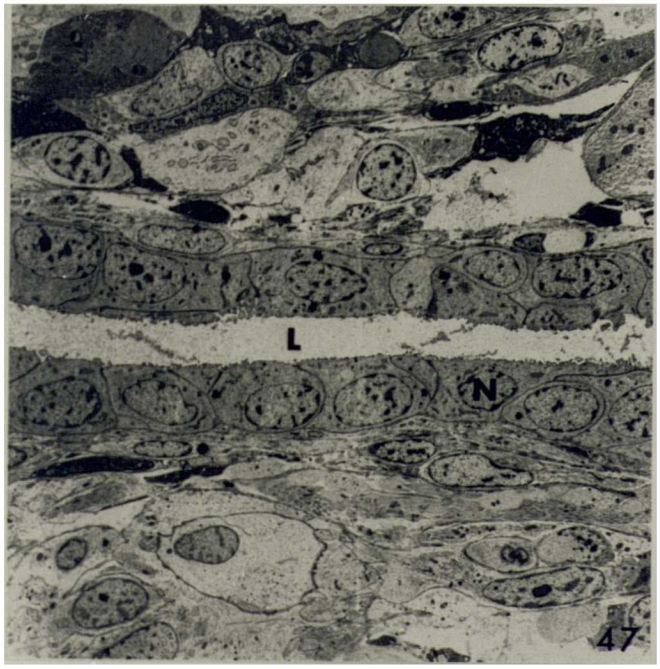

47

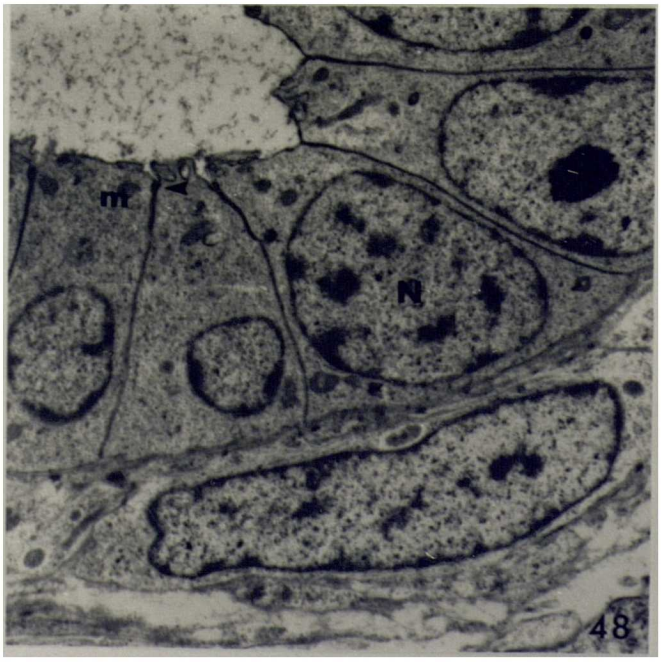

48

D.reticulatum, hermaphrodite duct, epithelial cells lining the seminal vesicle.

Fig. 49 Transition between the ciliated and unciliated cells (*arrowed*) (x250).

Fig. 50 General view of the ciliated cells (x3.5K). The arrow indicates the position of a Golgi body.

Fig. 51 Detail of the Golgi region in the ciliated cells (x37.5K).

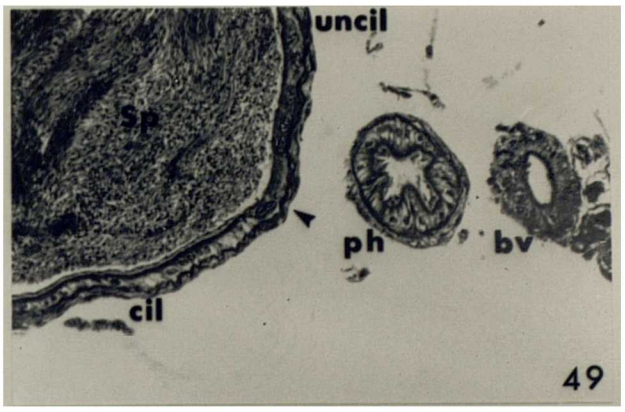
uncil
Sp
ph
bv
cil
49


Sp
Gly
50

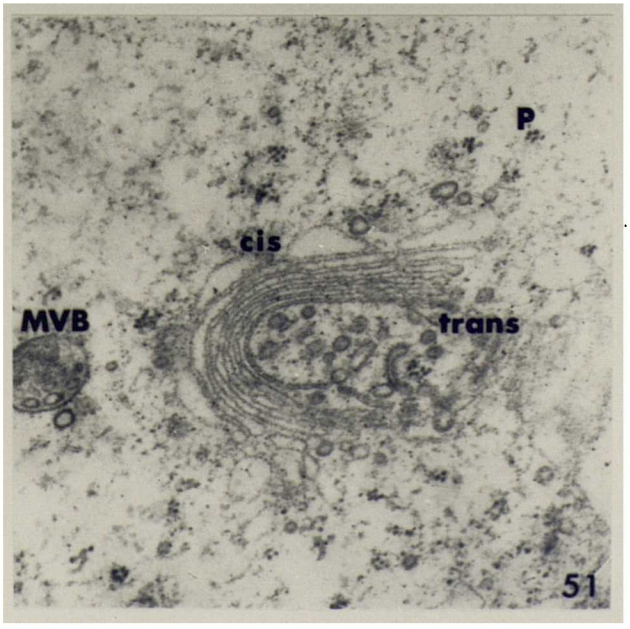
P
cis
MVB
trans
51

D.reticulatum, hermaphrodite duct, ciliated epithelial cells lining the seminal vesicle.

Fig. 52 Detail of the apices (x15K). Arrows indicate the position of desmosomes.

Fig. 53 Detail of the sub-apical region (x15K).

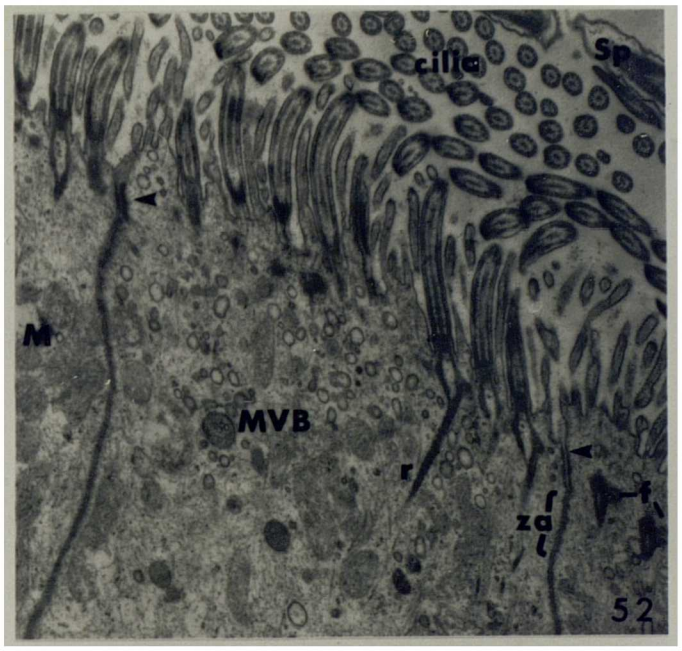
cilia
Sp
M
MVB
r
za
f
52

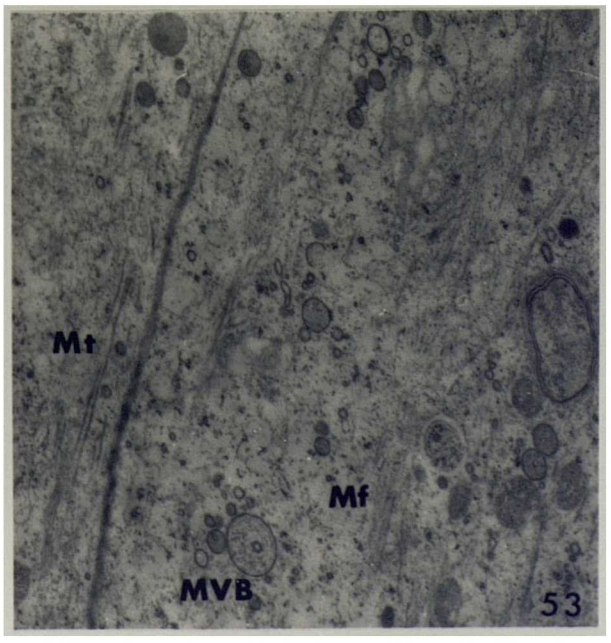
Mt
Mf
MVB
53

D.reticulatum, hermaphrodite duct, unciliated epithelial cells lining the seminal vesicle.

Fig. 54 Columnar epithelial cells (x3.5K).

Fig. 55 Squamous epithelial cells (x3.5K).

Fig. 56. Detail of the Golgi region (x27.5K). Arrows indicate coated vesicles.

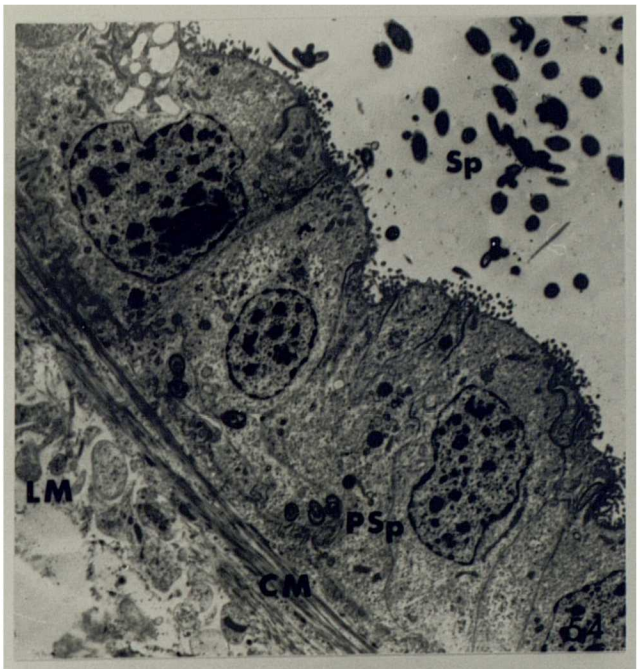
Sp
LM
PSp
CM
54

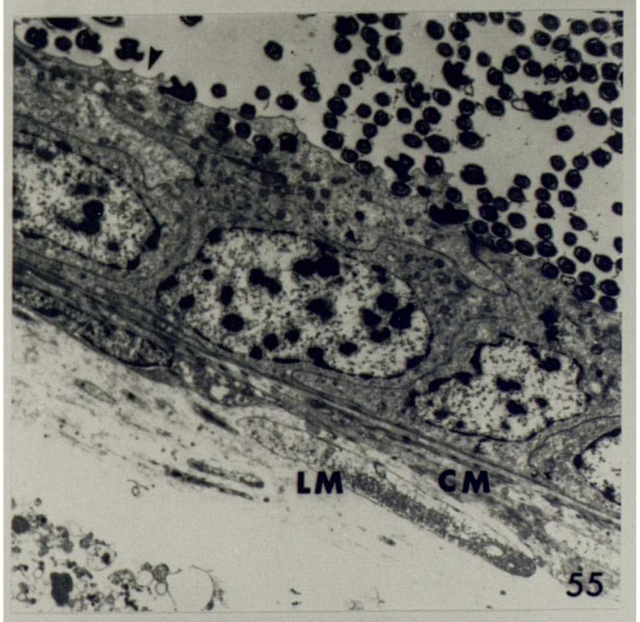
LM
CM
55

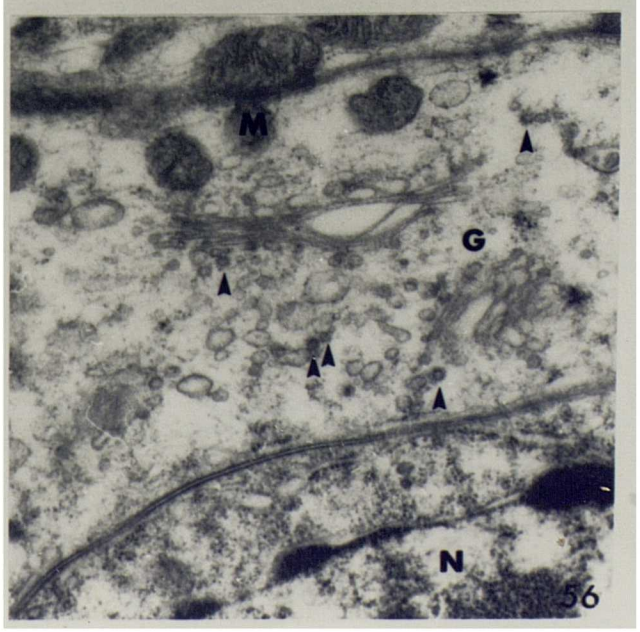
M
G
N
56

D.reticulatum, hermaphrodite duct, unciliated epithelial cells lining the seminal vesicle.

Fig. 57 Detail of the cell apex (x22.5K). Arrows indicate desmosomal junctions.

Fig. 58 Detail of the phagocytosed sperm (x21K).

Fig. 59 Epithelium with intercellular vacuoles (x8.5K). Large arrows indicate MVBs, small arrows indicate pinocytotic vesicles.


MVB
zo
M
57

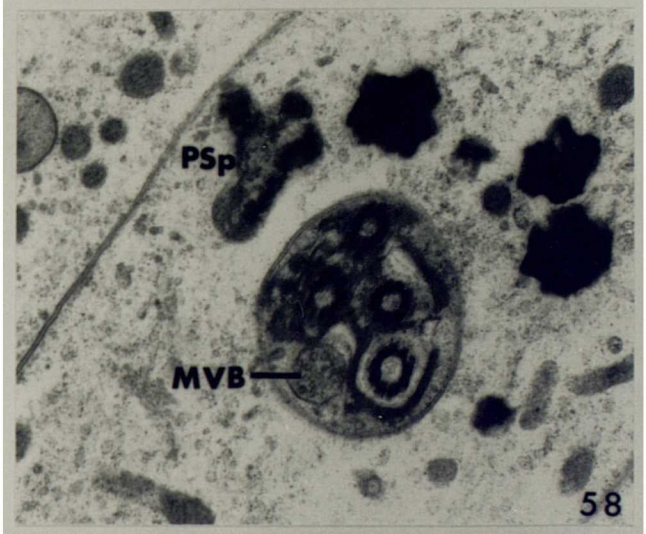
PSp
MVB
58

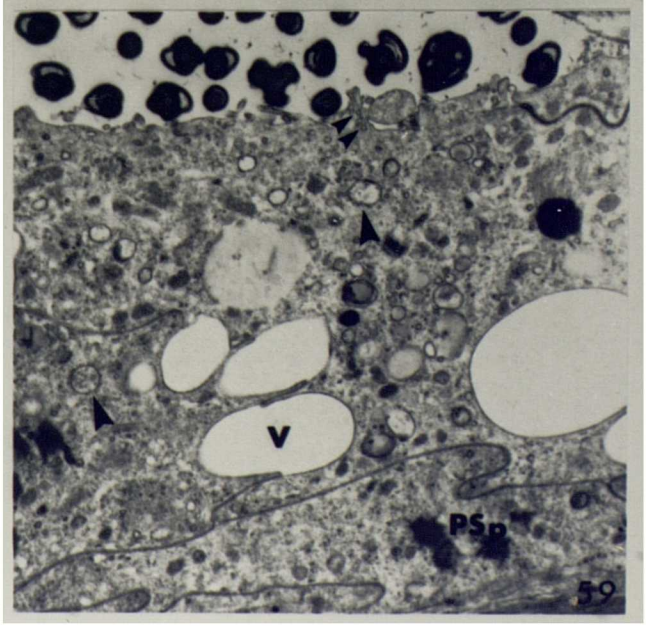
V
PSp
59

D.reticulatum, hermaphrodite duct.

Fig. 60 The connective tissue underlying the epithelium of the seminal vesicle (x19.5K).

Fig. 61 Muscular and nervous components of the connective tissue sheath (x6K).

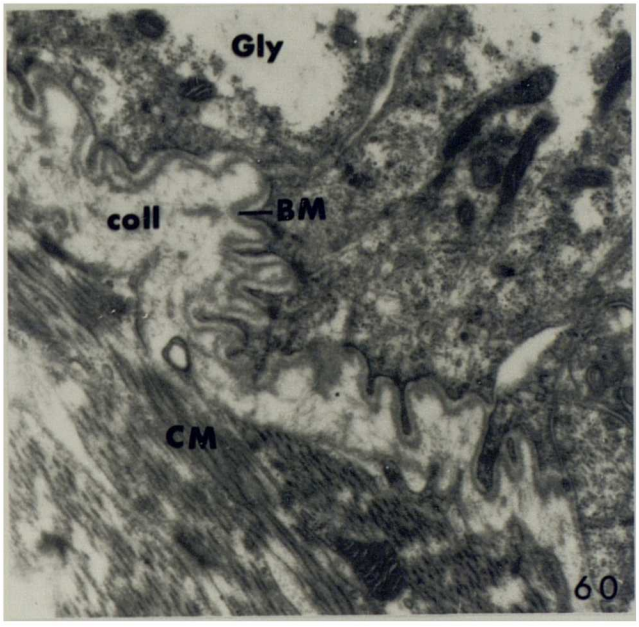
Gly
coll
BM
CM
60

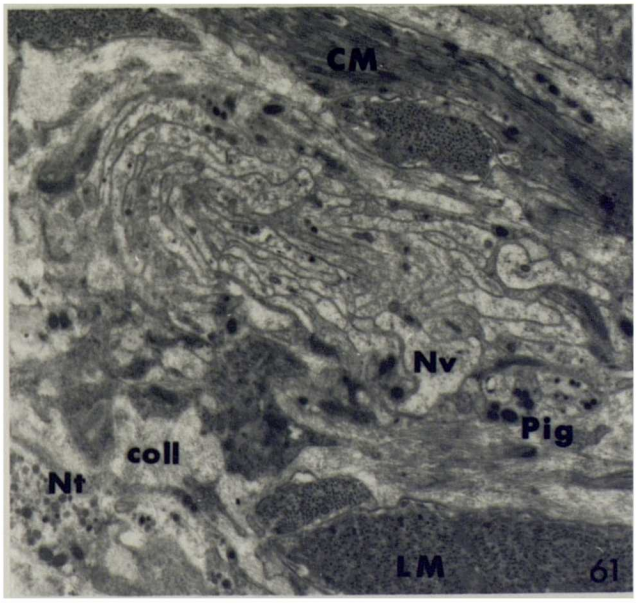
CM
Nv
Pig
coll
Nt
LM
61

D.reticulatum, epithelial cells lining the anterior, slender region of the hermaphrodite duct.

Fig. 62 General view of the epithelium (x3.75K).

Fig. 63 Detail of the cell apices (x9K).

Fig. 64 General view of the epithelium near the carrefour (x3.75K).

(arrows indicate Golgi bodies)

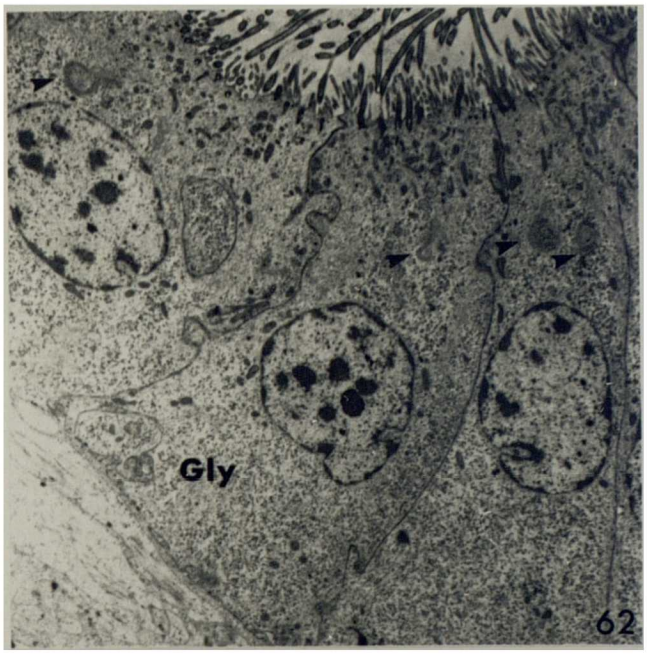
Gly
62

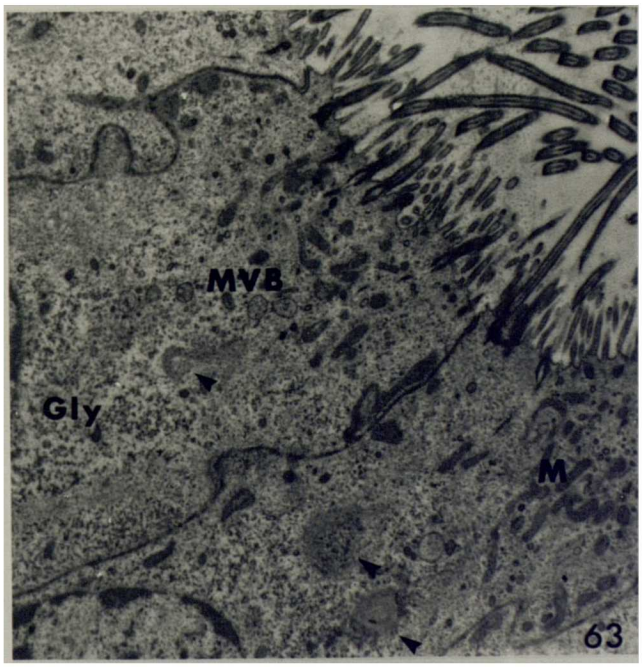
MVB
Gly
M
63

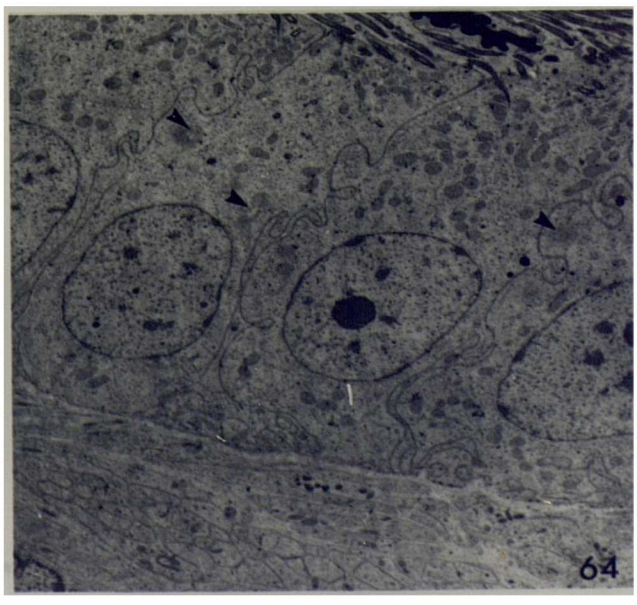
64

D.reticulatum, hermaphrodite duct.

Fig. 65 The epithelial cells lining the anterior, slender region of the hermaphrodite duct at its junction with the carrefour (x22.5). Large arrows indicate MVBs, small arrow indicates vesicle chain.

Fig. 66 The muscular and nervous components of the connective tissue sheath surrounding the anterior, slender region of the hermaphrodite duct (x9K).

Fig. 68 Axons lying in grooves in the bases of the epithelial cells lining the anterior, slender region of the hermaphrodite duct (x9K).

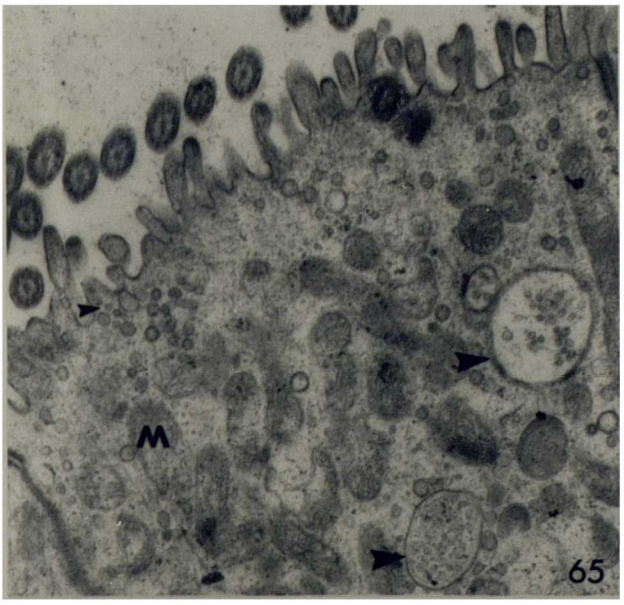
M
65

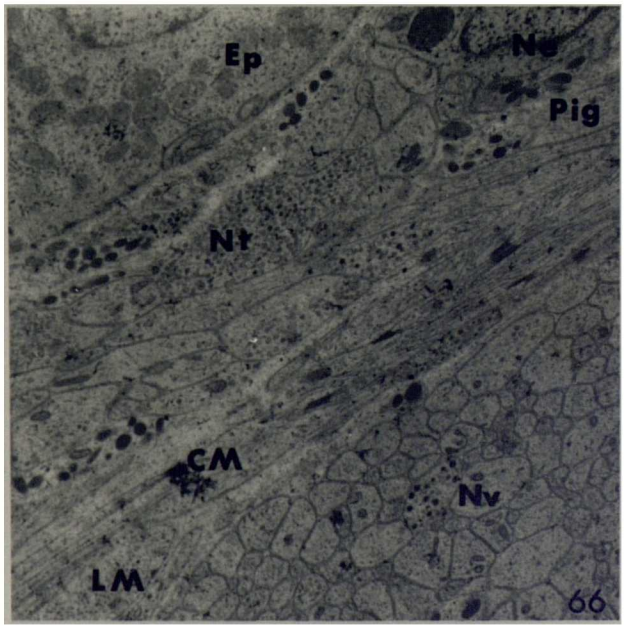
Ep
Pig
Nt
CM
Nv
LM
66

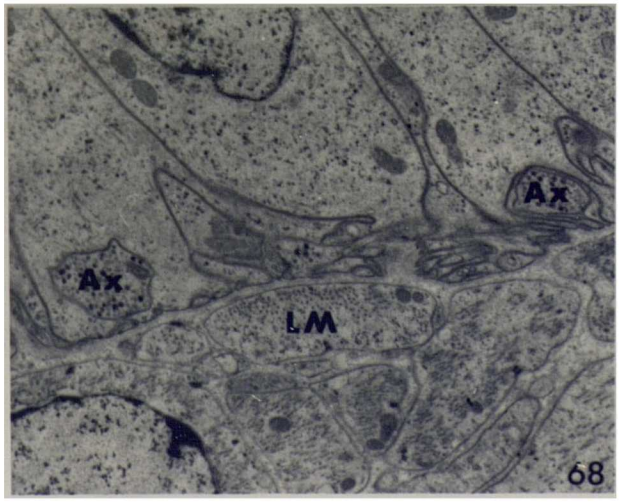
Ax
Ax
LM
68

Fig. 67 Diagram illustrating the distribution of the neurons and nerves observed in a section through the anterior, slender region of the hermaphrodite duct in D.reticulatum.

neurons

nerves

Fig. 67

D.reticulatum, carrefour diverticula.

Fig. 69 The epithelial cells lining the immature carrefour diverticula (x3.75K). Arrows indicate developing cilia.

Fig. 70 The epithelial cells lining the pouched diverticulum in a mature animal (x1.5K).

Fig. 71 Horizontal section through the epithelial cells lining the pouched diverticulum in the region of the Golgi apparatus (x9K). Arrows indicate electron-dense vesicles.

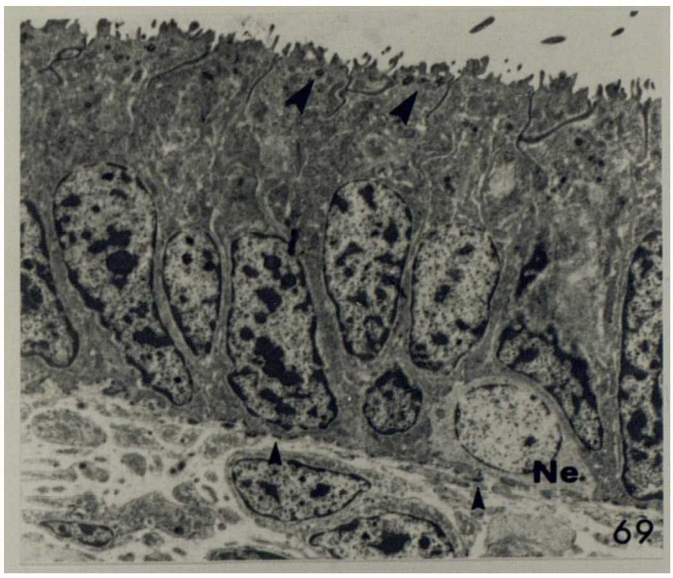
Ne.
69

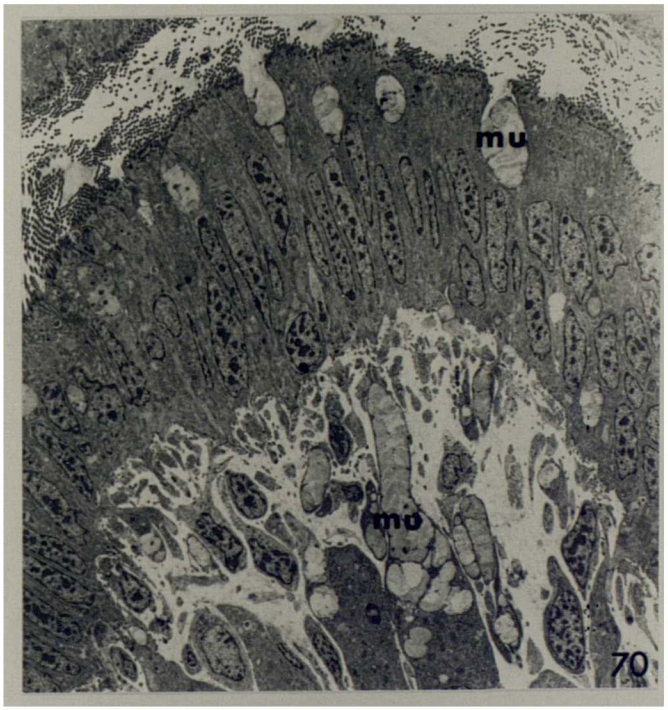
mu
mu
70

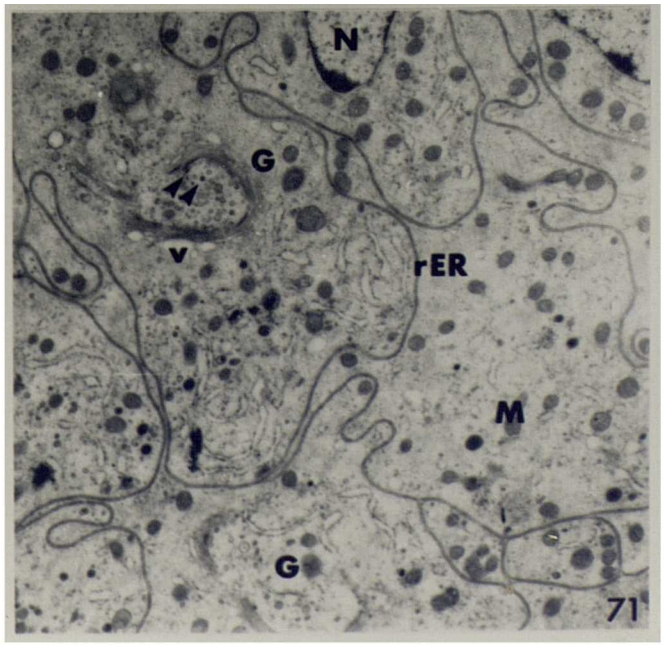
N
G
v
rER
M
G
71

D.reticulatum, epithelial cells lining the pouched diverticulum of the carrefour.

Fig. 72 Detail of the Golgi region (x22.5K). Arrows indicate microtubules.

Fig. 73 Detail of the cell apices (x15K).

Fig. 74 (inset) Detail of an omega body in the apical membrane (x56.25K).

Fig. 75 Detail of the unciliated epithelial cells along the lateral edges of the pouch (x15K). Arrows indicate vesicle chains.

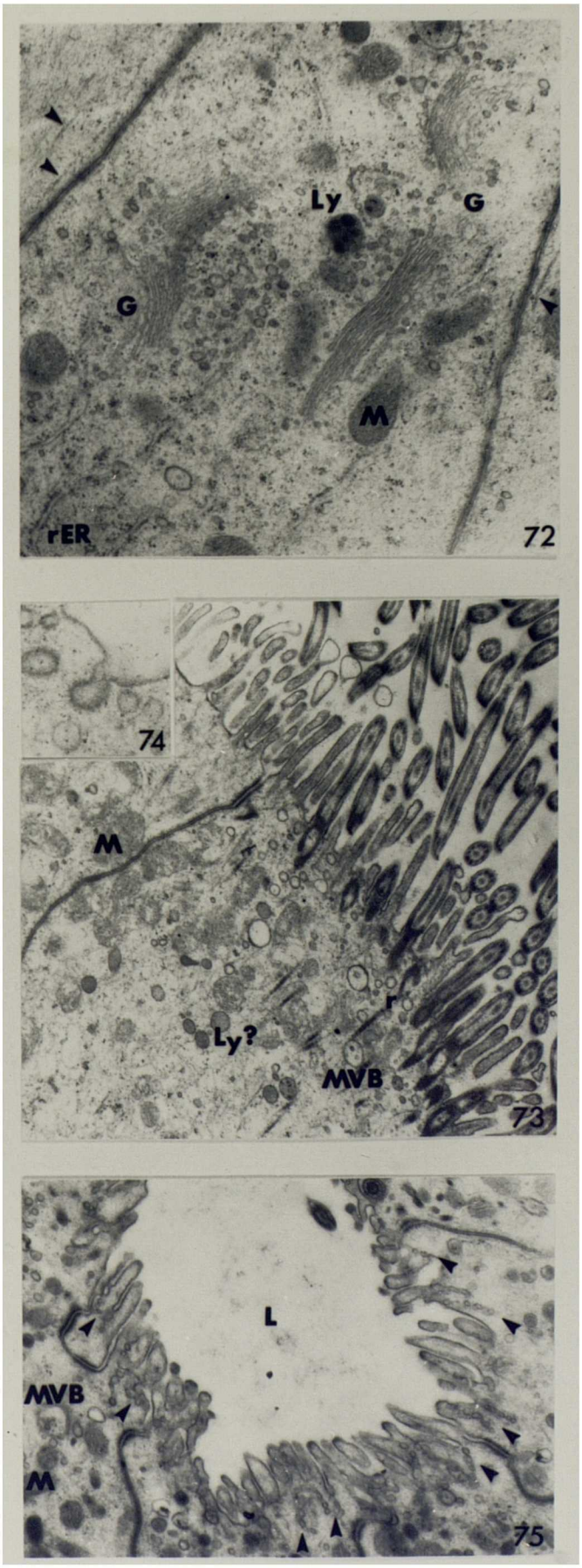
Ly
G
G
M
rER
72
74
M
r
Ly?
MVB
73
L
MVB
M
75

D.reticulatum, carrefour diverticula.

Fig. 76 Detail of the unciliated epithelial cells at the junction with the hermaphrodite duct (x9K). Arrows indicate vesicle chains.

Fig. 77 Detail of the highly folded basal membranes of the epithelial cells lining the pouched diverticulum (x9K). Arrows indicate hemidesmosomes.

Fig. 78 The epithelial cells lining the finger-like diverticulum (x3.75K).

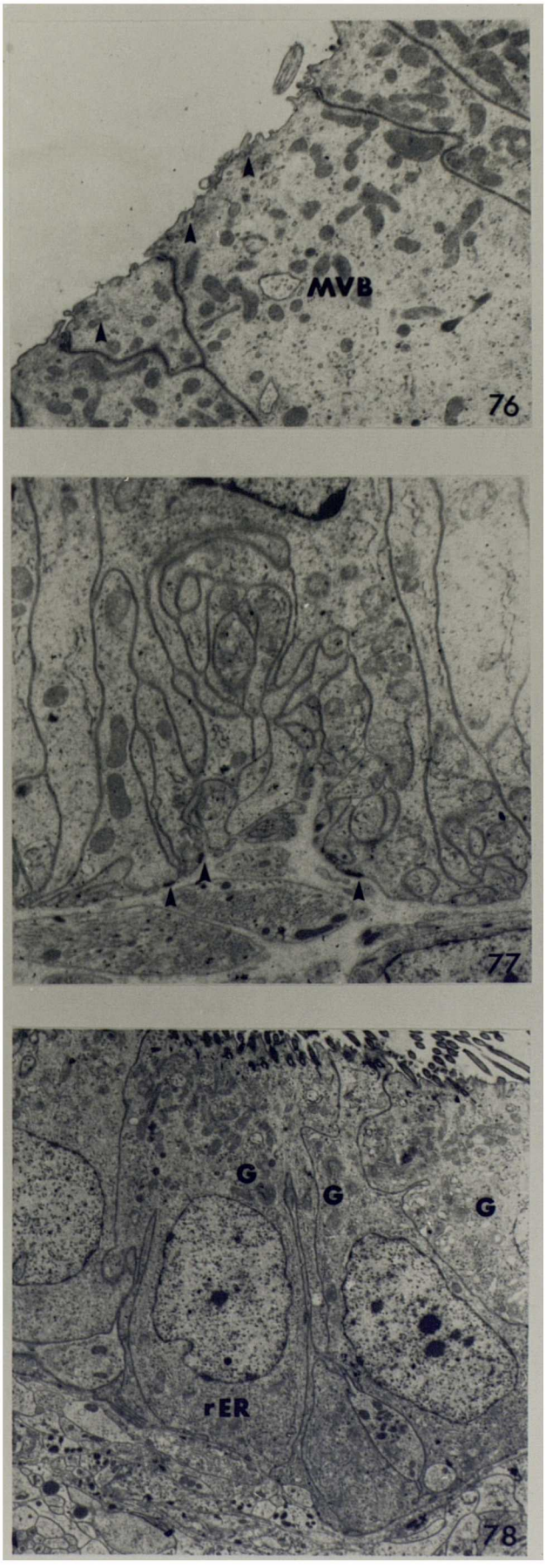
MVB
76
77
G
G
G
rER
78

D.reticulatum, connective tissue surrounding the carrefour diverticula in an immature animal.

Fig. 79 The connective tissue at the outer surface of the pouched diverticulum (x2.1K). The arrow indicates a cell in the later stages of cell division.

Fig. 81 The connective tissue at the inner surface of the pouched diverticulum (x1.8K). The arrow indicates the neuron seen in Fig. 82.


Ne
F
Mc
Ep
79

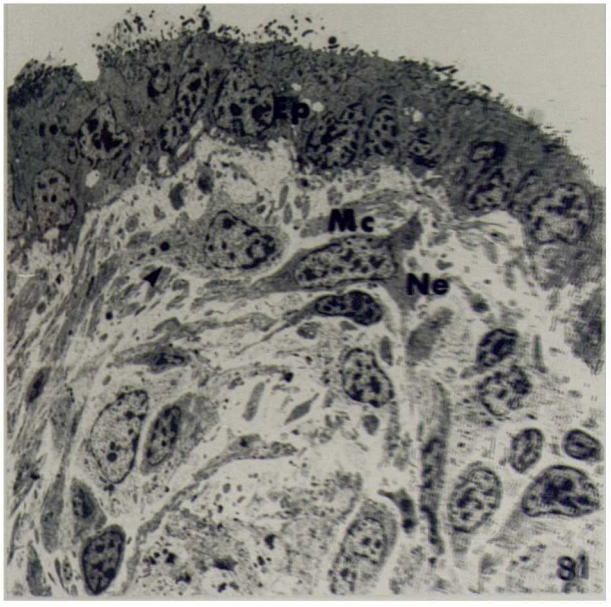
Ep
Mc
Ne
81

Fig. 80 Diagram illustrating the distribution of the neurons and nerves observed in a section through the immature pouched diverticulum of D.reticulatum.

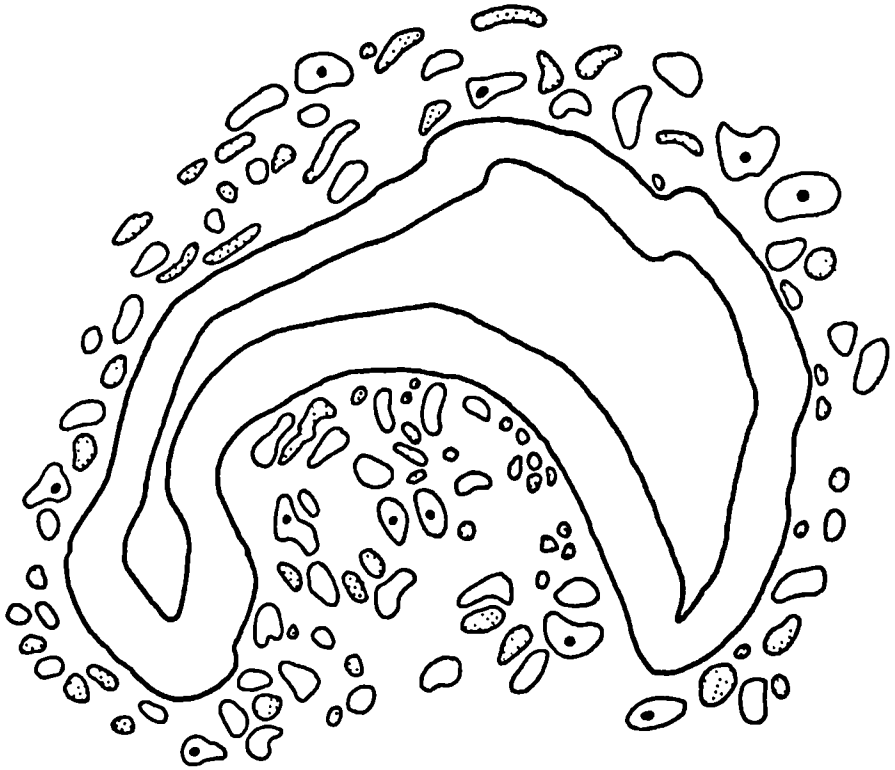

neurons

nerves

Fig. 80

D.reticulatum, connective tissue surrounding the carrefour diverticula in an immature animal.

Fig. 82 Immature neuron seen in Fig. 81 (x9K).

Fig. 83 Immature nerve (x18K).

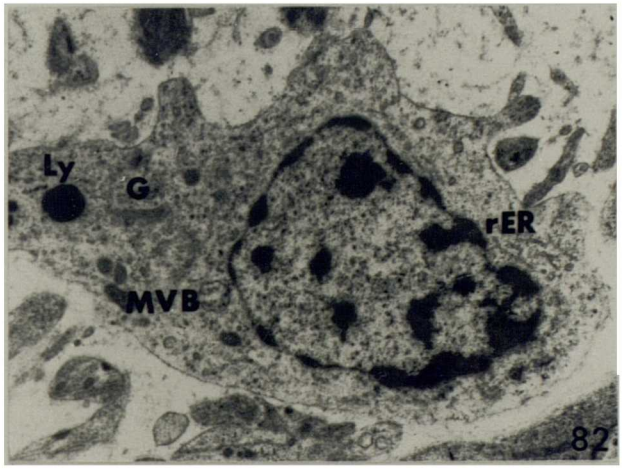
Ly
G
rER
MVB
82

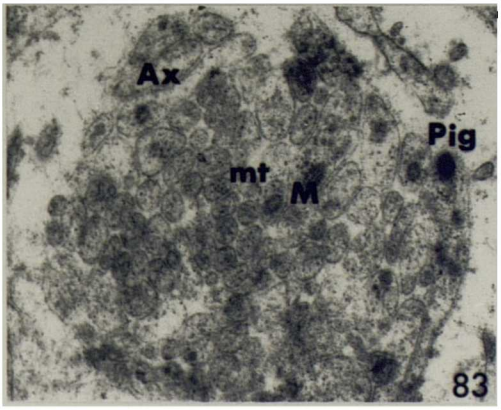
Ax
Pig
mt
M
83

D.reticulatum, connective tissue surrounding the carrefour diverticula in a mature animal.

Fig. 84 The connective tissue at the outer surface of the pouched diverticulum (x3.4K).

Fig. 85 The connective tissue at the inner surface of the pouched diverticulum (x1.5K).

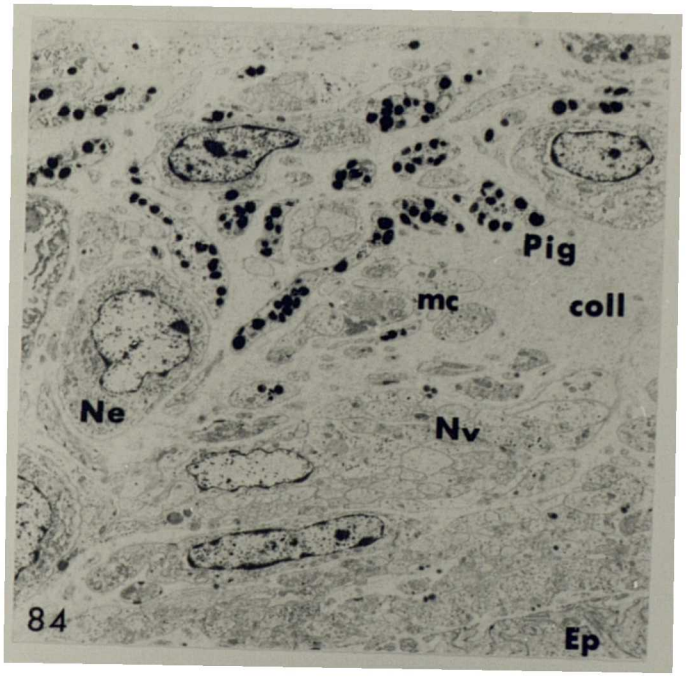
Pig
mc
coll
Ne
Nv
84
Ep

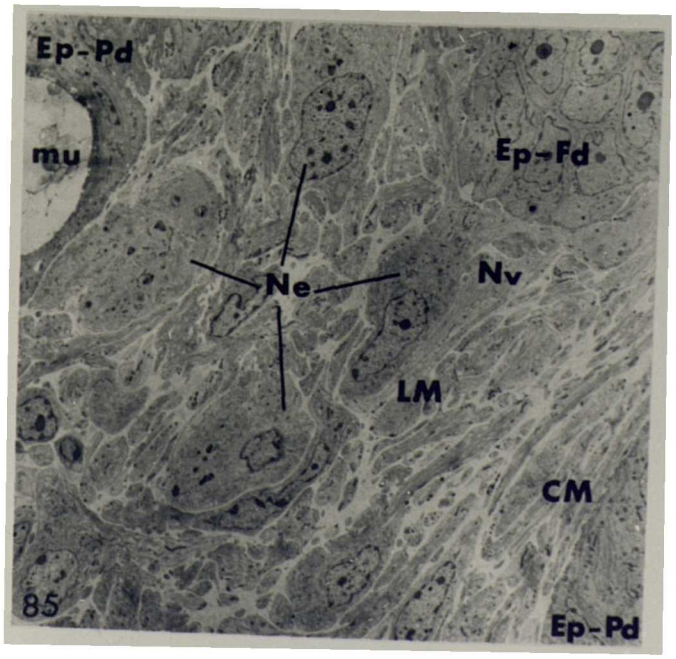
Ep-Pd
mu
Ep-Fd
Ne
Nv
LM
CM
85
Ep-Pd

Fig. 86 Diagram illustrating the distribution of the neurons and nerves observed in a section through the mature pouched diverticulum of D.reticulatum.

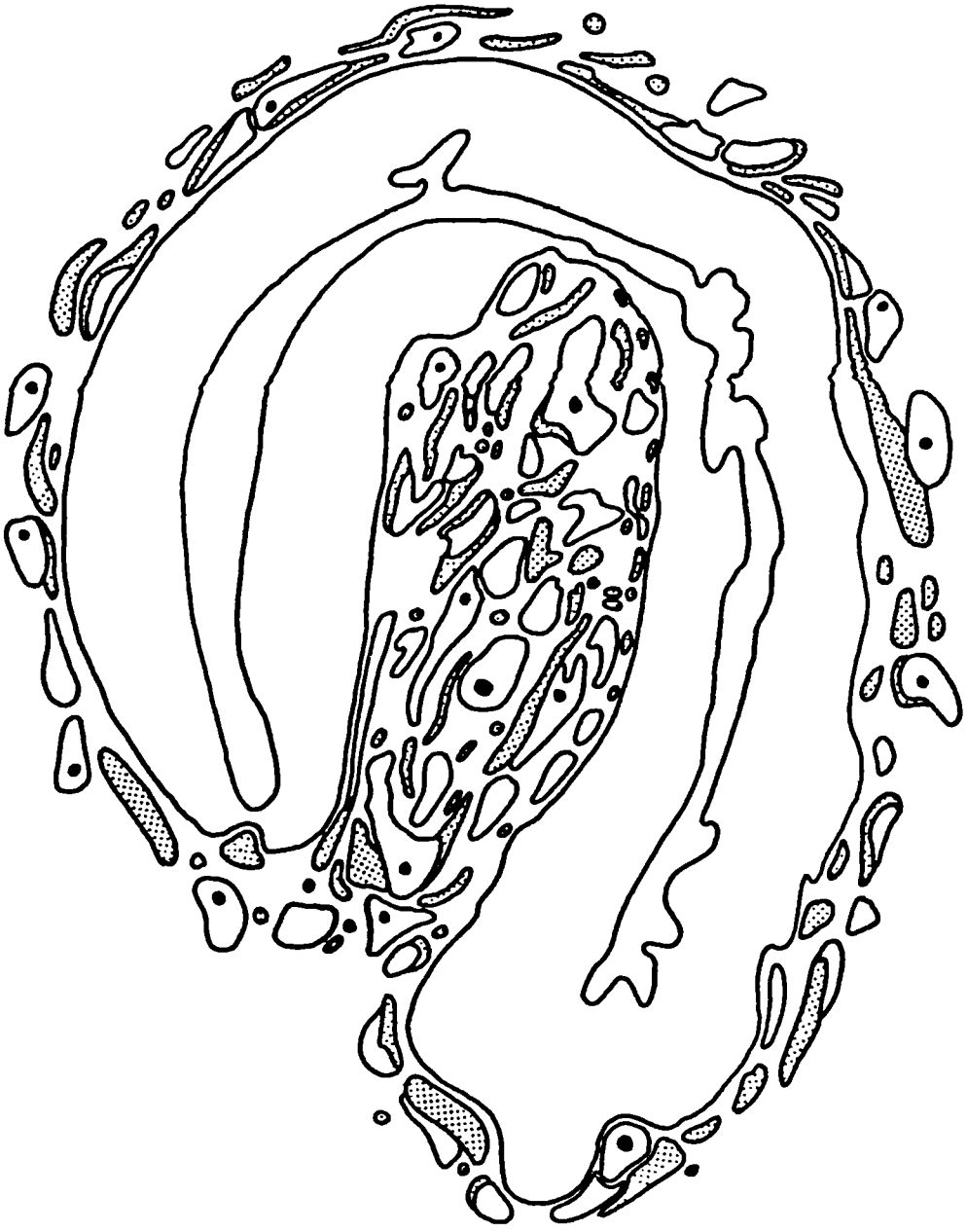

□ neurons

▨ nerves

Fig. 86

Fig. 87 D.reticulatum, neuron with three axonal processes (1, 2 and 3) within the connective tissue surrounding the carrefour diverticula in a mature animal (x9K).

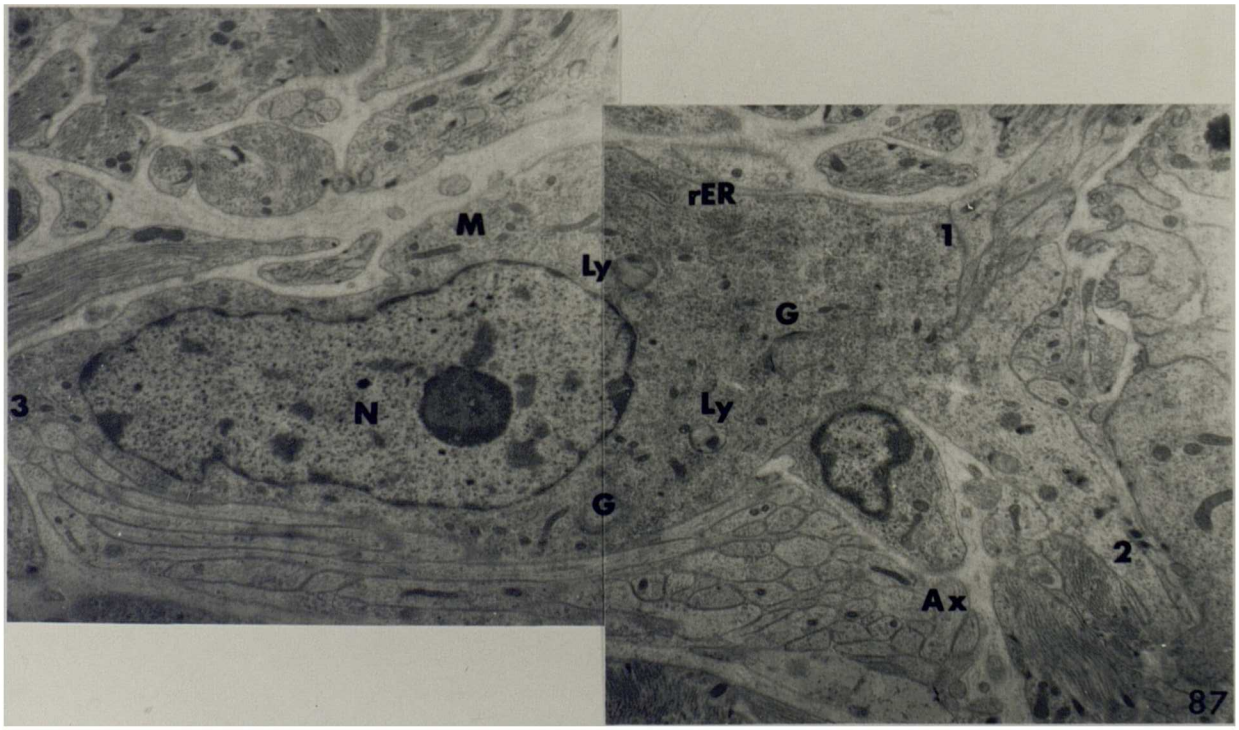
M
Ly
3
N
G
rER
1
G
Ly
2
Ax
87

D.reticulatum, detail of neurons observed in the connective tissue surrounding the carrefour diverticula in a mature animal.

Fig. 88 General view of the cytoplasm in the region of the Golgi apparatus (22.5K). Arrow indicates cored vesicle.

Fig. 89 Accumulation of lysosomes in a neurone from a stage E animal (x22.5K).

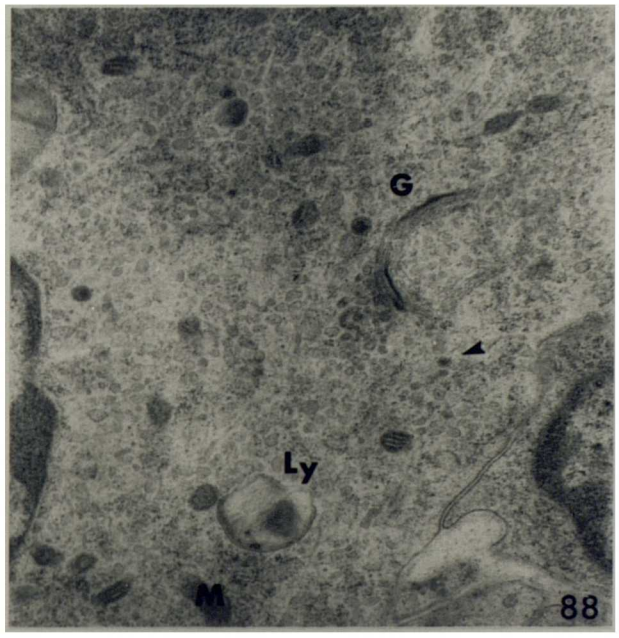
G
Ly
M
88


89

D.reticulatum, connective tissue surrounding the carrefour diverticula in a mature animal.

Fig. 90 Three nerve layers (1, 2 and 3) in the connective tissue sheath (x9K).

Fig. 91 T.S. through axons, showing the variety of cytoplasmic inclusions (x22.5K).

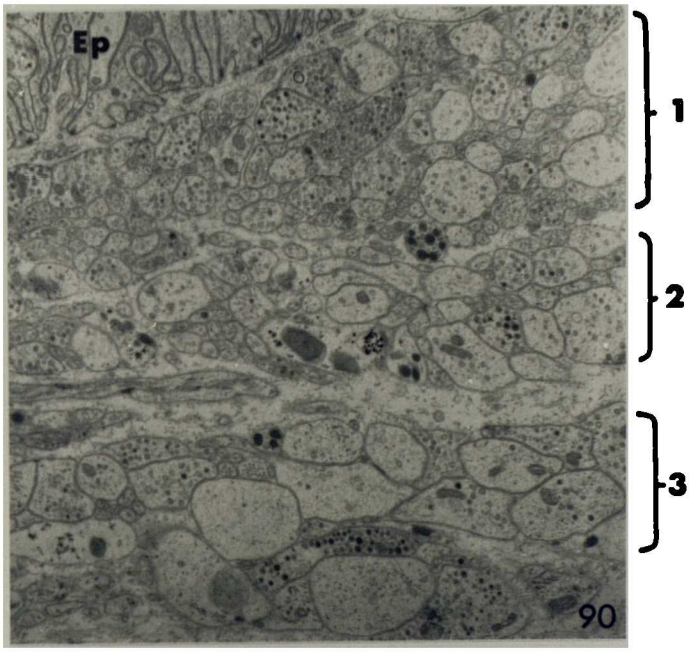
Ep
1
2
3
90

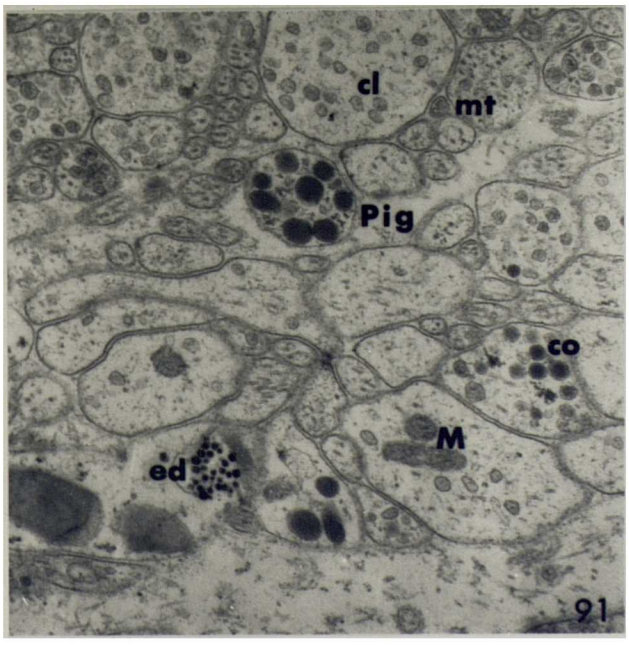
cl
mt
Pig
co
M
ed
91

D.reticulatum, connective tissue surrounding the carrefour diverticula in a mature animal.

Fig. 92 Detail of a probable synapse (x22.5K).

Fig. 93 Detail of possible neuromuscular junctions (x15K). Arrows indicate possible release sites.

Fig. 94 Detail showing the intimate relationship of axons with the epithelial cells lining the pouched diverticulum (x22.5K).

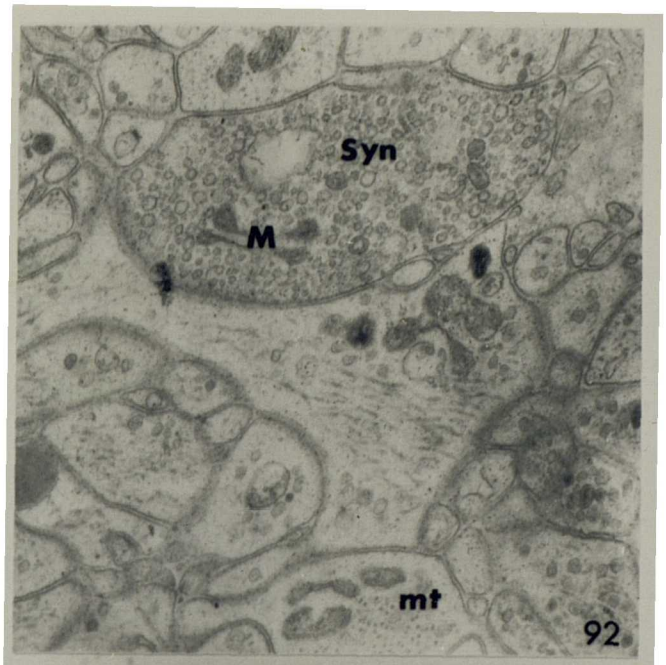
Syn
M
mt
92

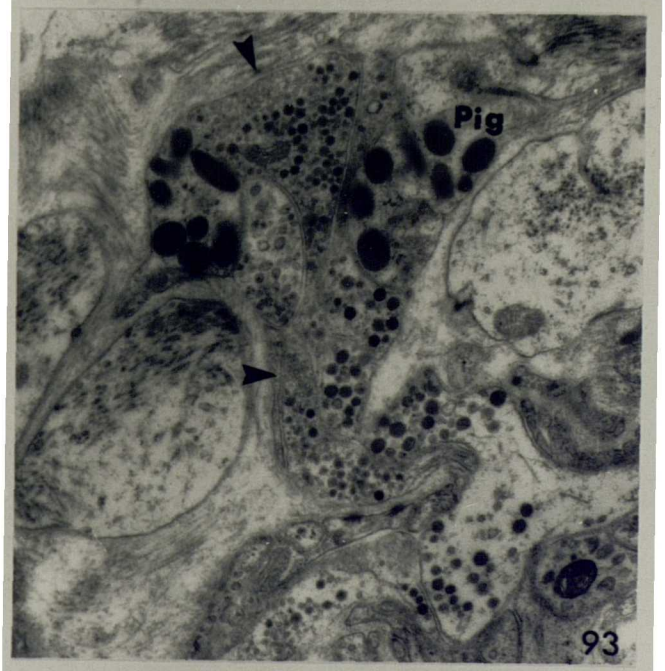
Pig
93

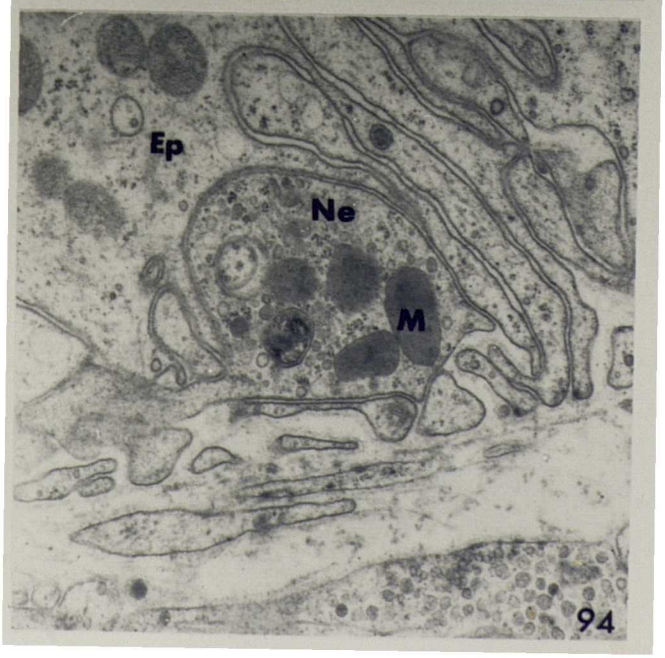
Ep
Ne
M
94

D.reticulatum, connective tissue surrounding the carrefour diverticula in a mature animal.

Fig. 95 Muscle cells (x15K). Arrows indicate intercellular junctions.

Fig. 96 Detail of muscle cells (x37.5K). Small arrow indicates thin filaments, large arrow indicates thick filaments.

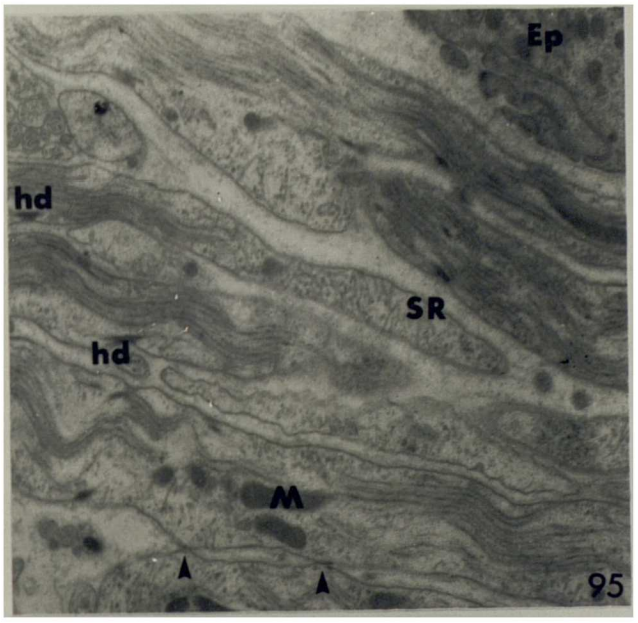
Ep
hd
SR
hd
M
95

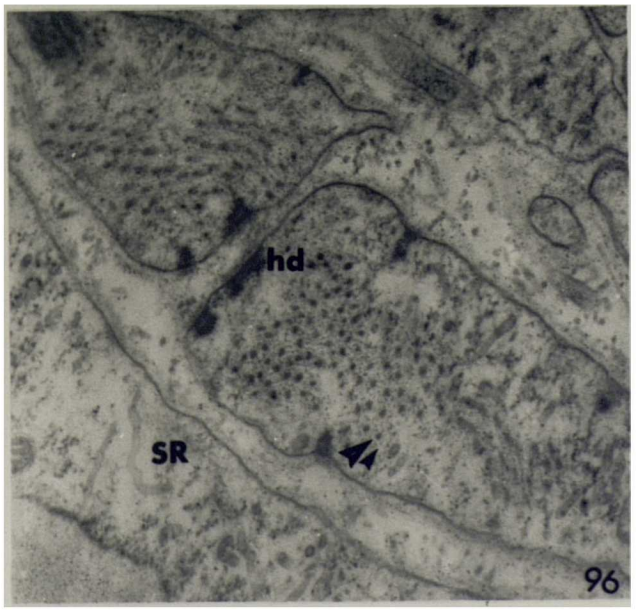
hd
SR
96

D.reticulatum, connective tissue surrounding the carrefour diverticula in a mature animal.

Fig. 97 Pore cell (x3.75K). Arrows indicate pores in the cell membrane.

Fig. 98 Pore cell with large accumulation of lysosomes.

a. Detail of the Golgi region (x10K). Arrow indicates region of cell membrane seen in (b).

b. Detail of the pores (x22.5K).

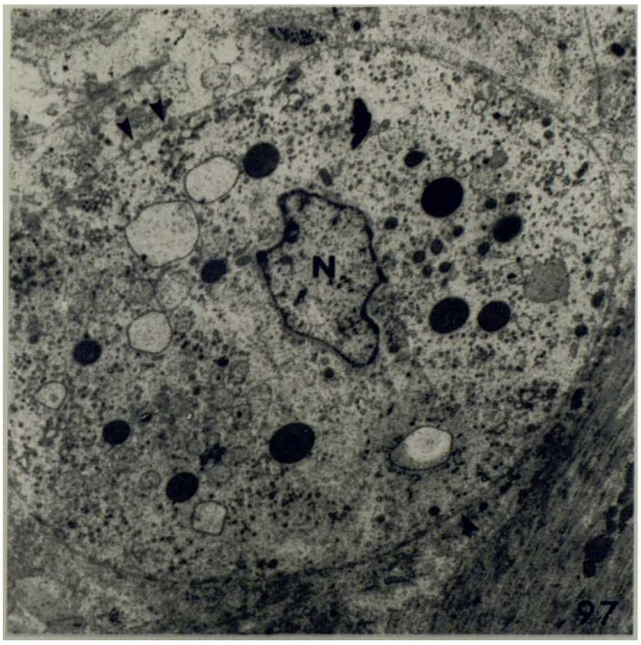
N
97

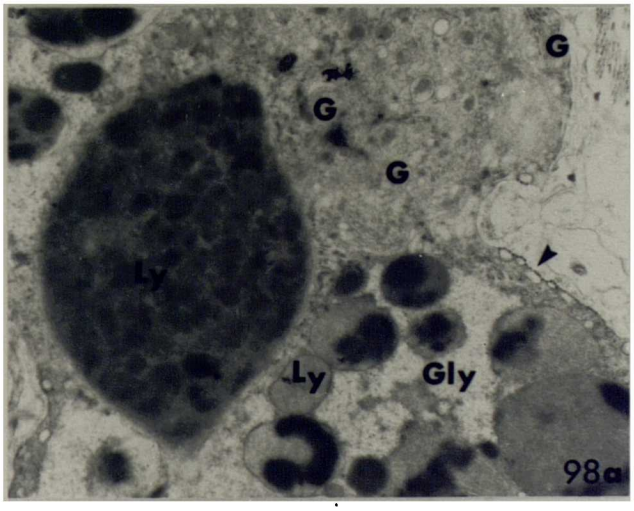
G
G
G
Ly
Ly
Gly
98a

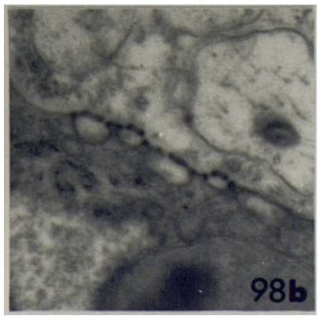
98b

D.reticulatum, carrefour gland.

Fig. 99 Sub-epithelial secretory cells opening into the carrefour (x1.5K).

Fig. 100 T.S. through the base of a typical secretory cell (x2.25K).

Fig. 101 Detail of the rER cisternae containing rod-like granules (x37.5K). Arrows indicate the relationship of granules with ribosomes.

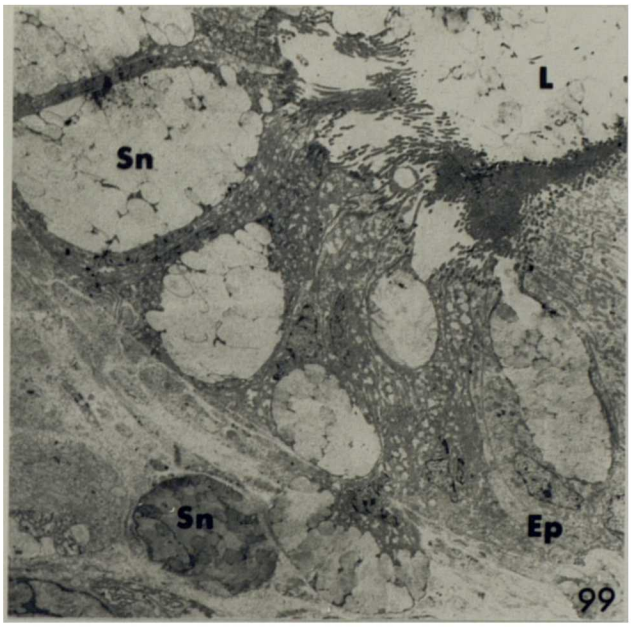
L
Sn
Sn
Ep
99

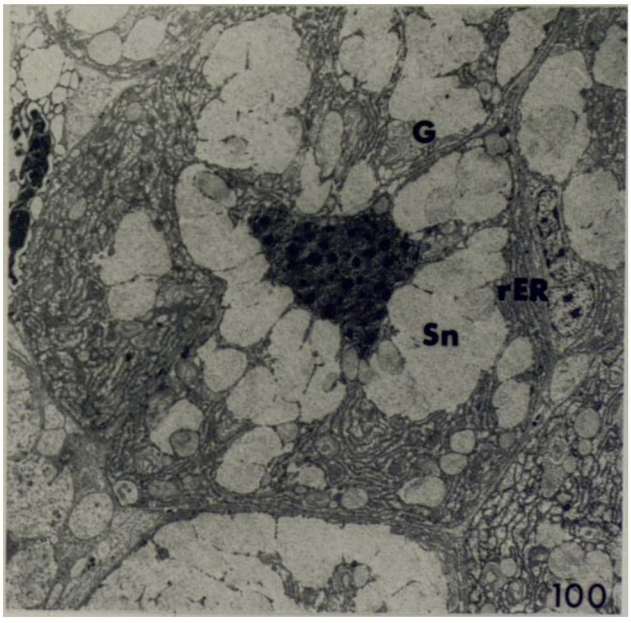
G
rER
Sn
100

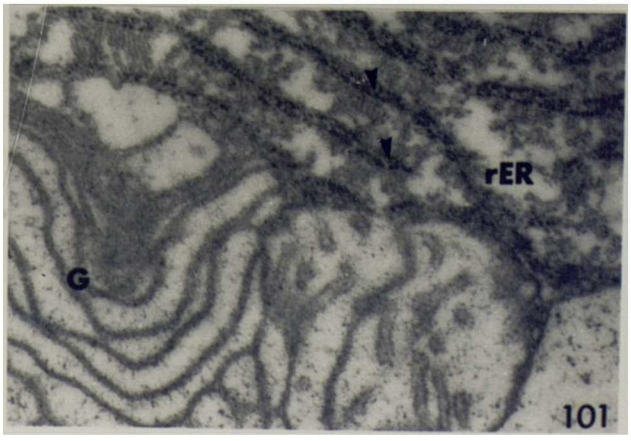
rER
G
101

D.reticulatum, carrefour gland.

Fig. 102 Detail showing the Golgi-rER relationship and the formation of secretion granules (x15K). Arrows indicate confluence of rER cisternae and secretion granules.

Fig. 103 Typical cup-shaped Golgi bodies (x10K).

Fig. 104 Detail showing the relationship between the tubules of the transitional ER and the Golgi cisternae (x36K).

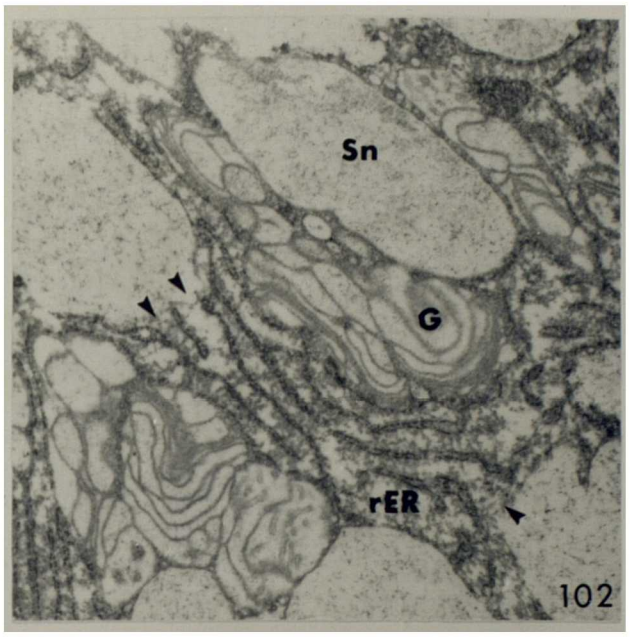
Sn
G
rER
102

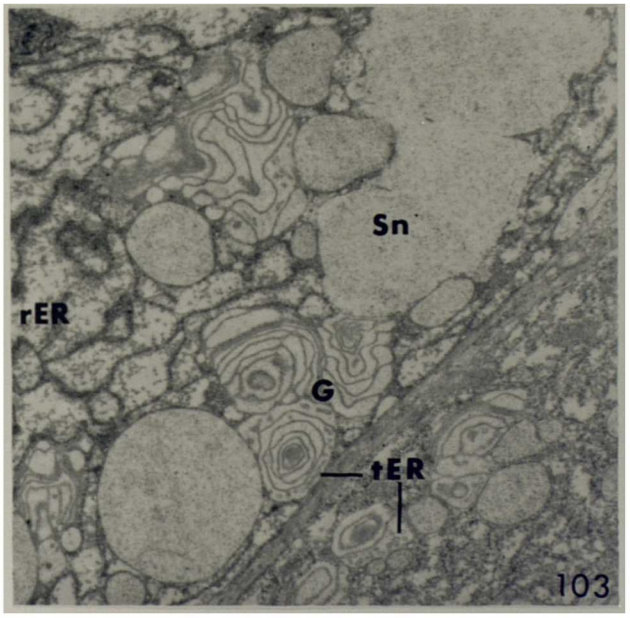
Sn
rER
G
tER
103

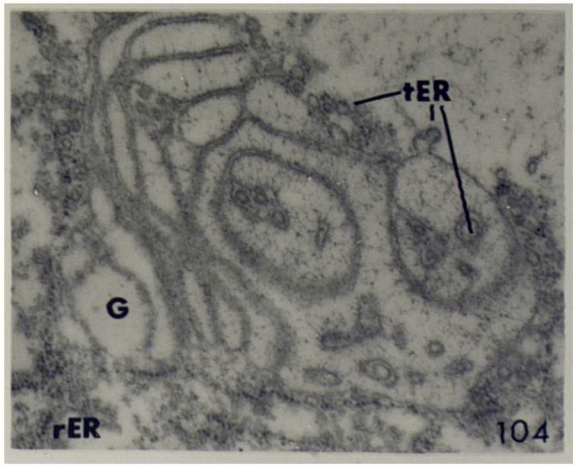
tER
G
rER
104

Fig. 105 Diagram showing the different phases of albumen gland development in D.reticulatum.

a. undifferentiated epithelium.

b. proliferation phase.

c. accumulation phase (developing gland cells shaded).

d. secretory phase.

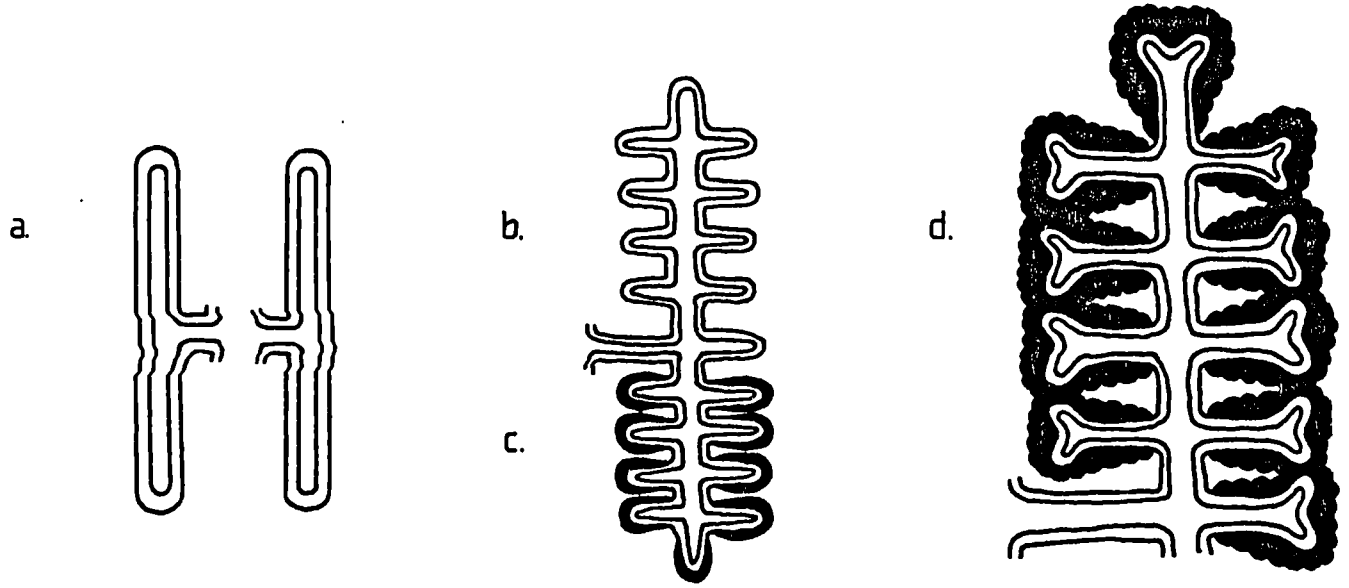

Fig. 105

D.reticulatum, albumen gland.

Fig. 106 Undifferentiated epithelial cells (x6K).

Fig. 107 Proliferation phase (x280).

Fig. 108 Accumulation phase (x280).

Fig. 109 Secretory phase (x280).

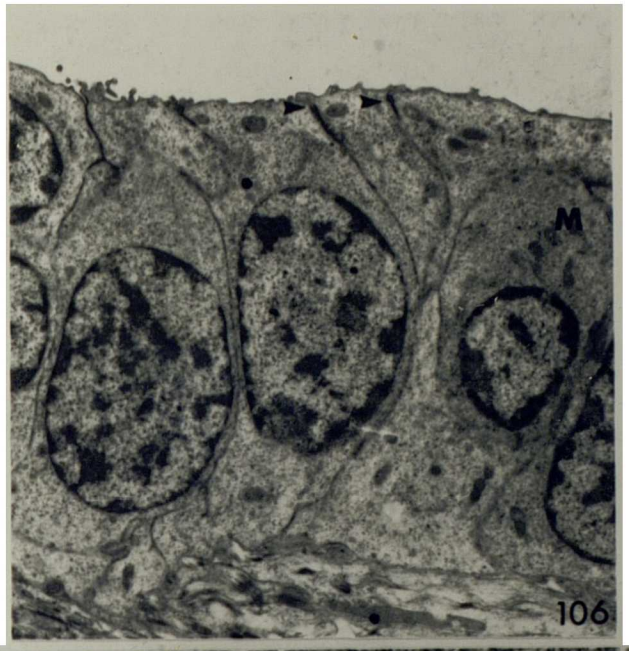
M
106

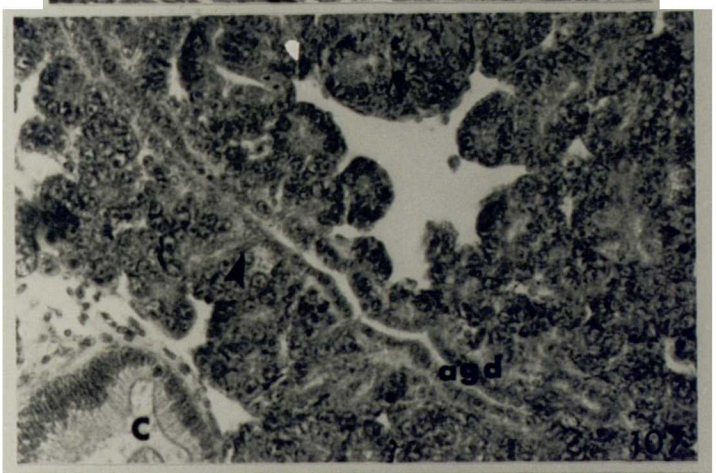
agd
C
107

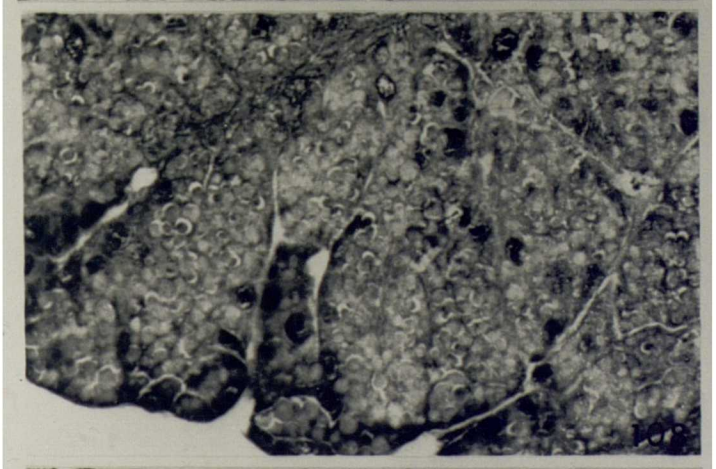


agd
109

D.reticulatum, albumen gland, proliferation phase.

Fig. 110 Section through tubule and main collecting duct (x1.5K).

Fig. 111 T.S. through tubules (x1.5K). The arrow indicates a cell undergoing mitosis.

Fig. 112 Formation of sub-epithelial cell clusters around a tubule (x1.5K).

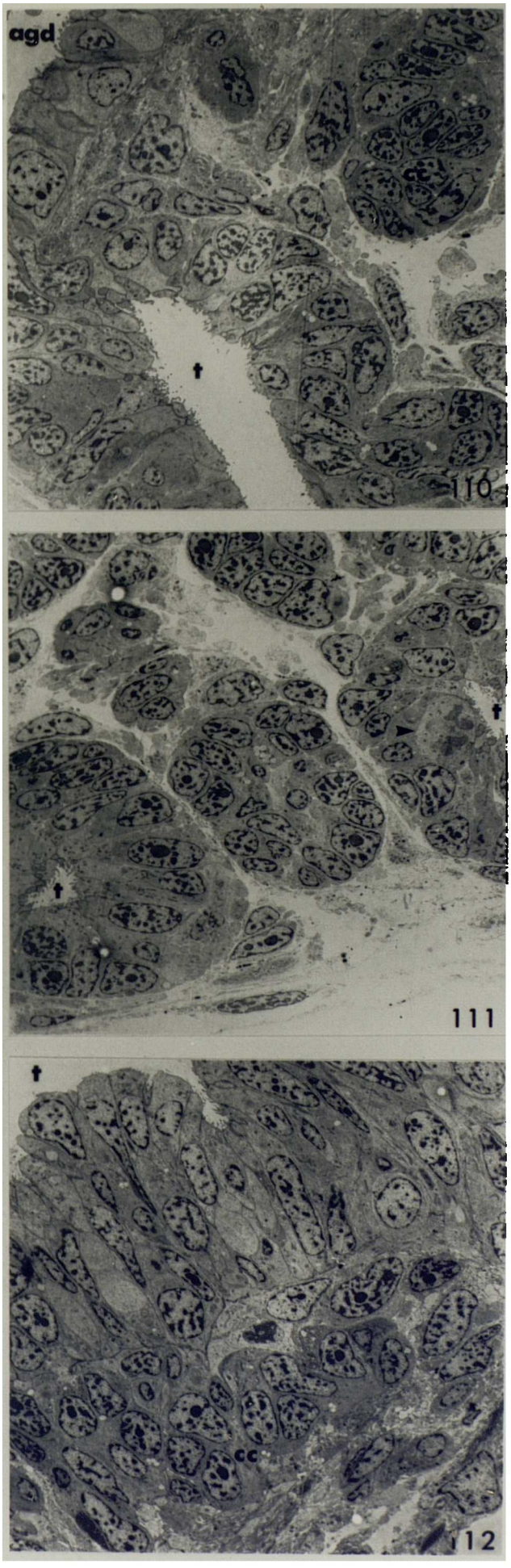
agd
t
110
t
t
111
t
cc
112

D.reticulatum, albumen gland, proliferation phase.

Fig. 113 Detail of sub-epithelial cell at the completion of cell division (x3.75). The arrow indicates the cell plate.

Fig. 114 a. T.S. through a tubule showing the accumulation of glycogen in the apices of the secretory cells (x1.5K).

b. Detail of cell cluster (x3.75K).

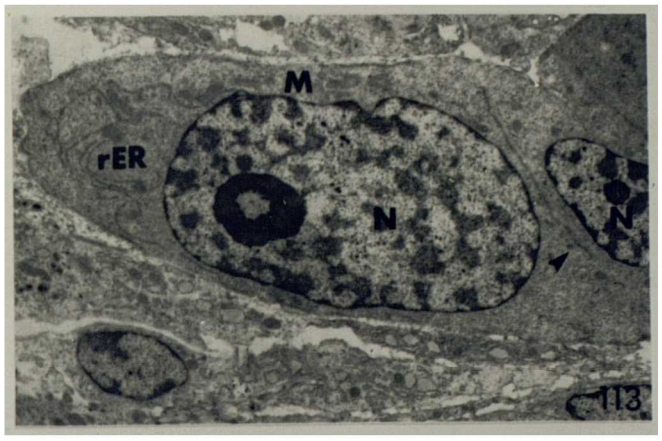

113

114a

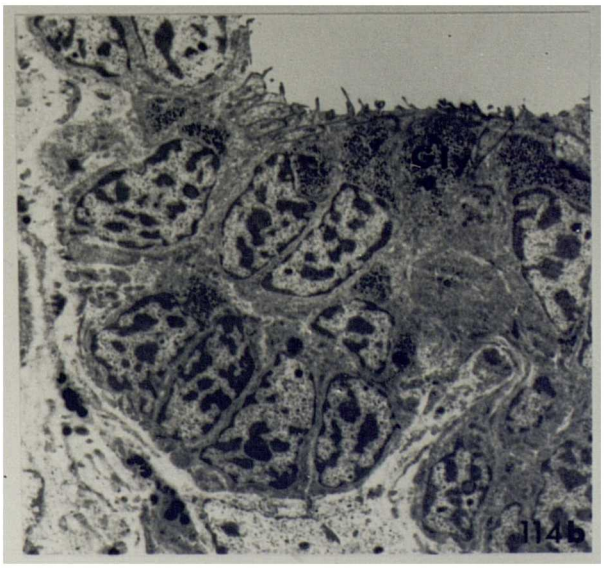

114b

D.reticulatum, albumen gland, accumulation phase.

Fig. 115 Secretory cell opening into the lumen of the tubule (x3.9K).

Fig. 116 Detail of the Golgi apparatus and early secretion granules (x15K).

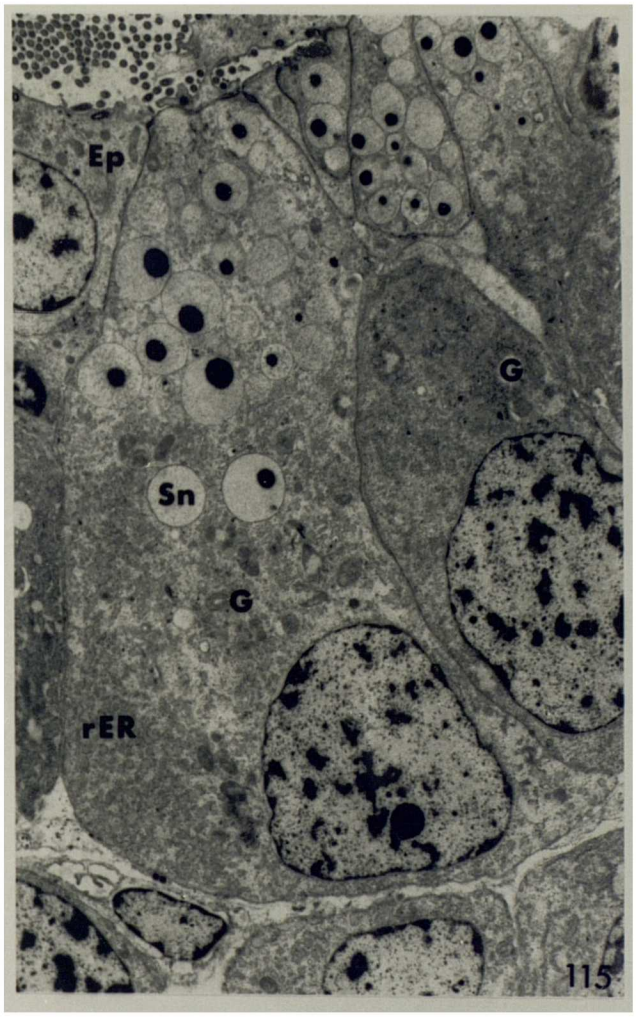
Ep
G
Sn
G
rER
115

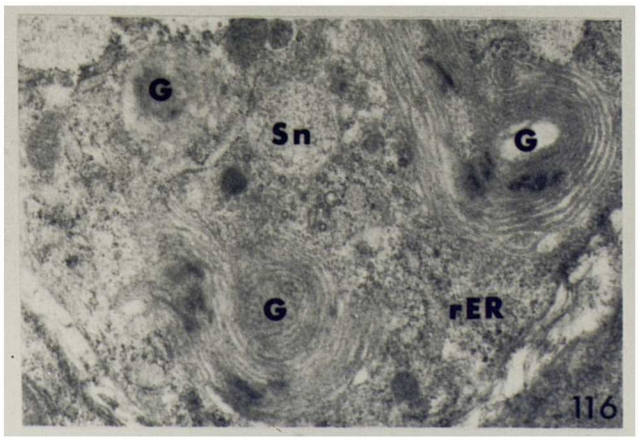
G
Sn
G
G
rER
116

D.reticulatum, albumen gland, accumulation phase.

Fig. 117 Detail of a secretion granule with electron-dense core (x37.5K).

Fig. 118 Detail of the cell apex of a secretory cell (x22.5K).

Fig. 119 Detail of the junctional complexes along the longitudinal membrane (x11K). Arrows indicate zonulae adhaerentes.

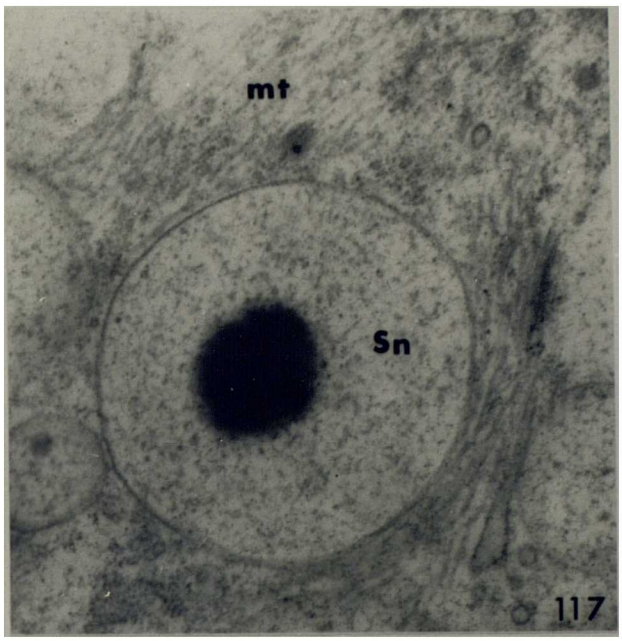
mt
Sn
117

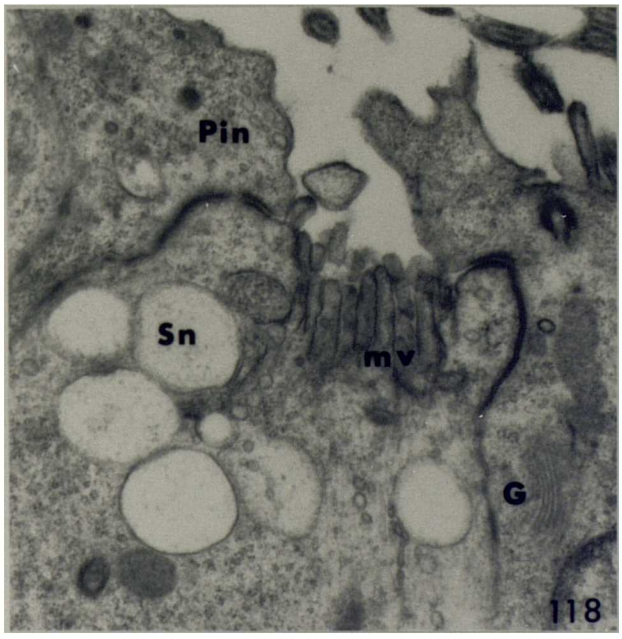
Pin
Sn
mv
G
118

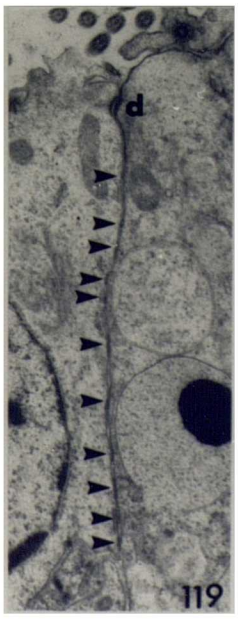
d
119

D.reticulatum, albumen gland, secretory phase.

Fig. 120 Detail of the rough endoplasmic reticulum at the periphery of a secretory cell (x22.5K).

Fig. 121 Detail showing the Golgi-rER relationship and the formation of secretion granules (x37.5K). Arrows indicate vesicles budding from rER.

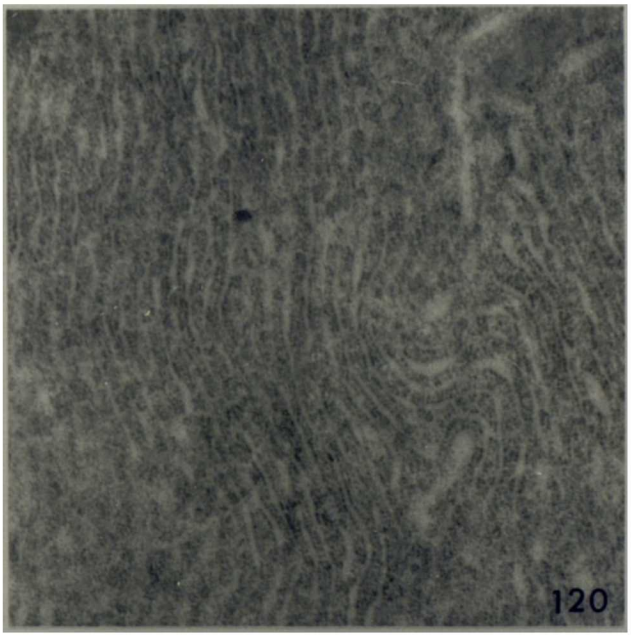
120

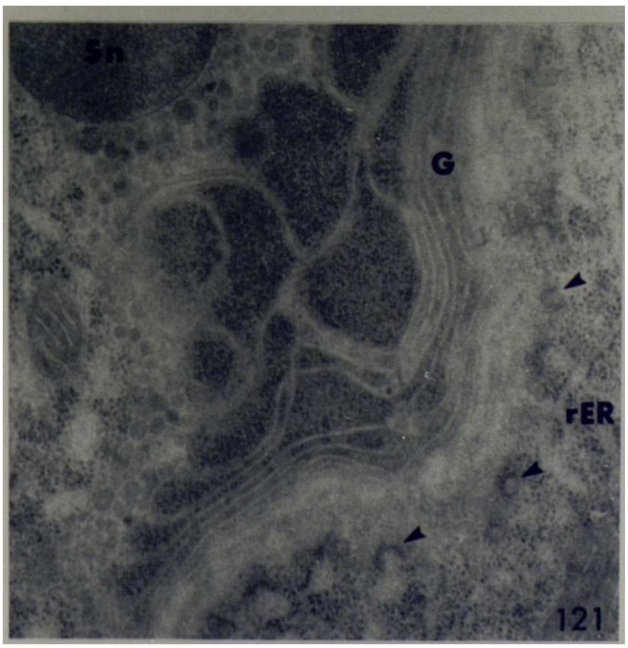
Sn
G
rER
121

D.reticulatum, albumen gland, secretory phase.

Fig. 122 Secretory cell opening into a tubule (x2.25K). Arrow indicates electron-dense spot.

Fig. 123 T.S. through a tubule filled with secretion (x1.8K).

Fig. 124 Detail of the cell apex of a secretory cell (x22.5K). Small arrows indicate zonulae adhaerentes, large arrow indicates vesicle chain.

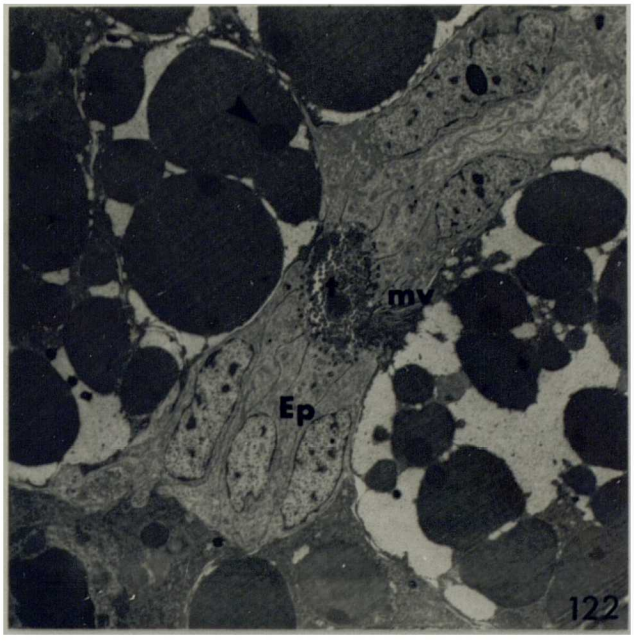
mv
Ep
122

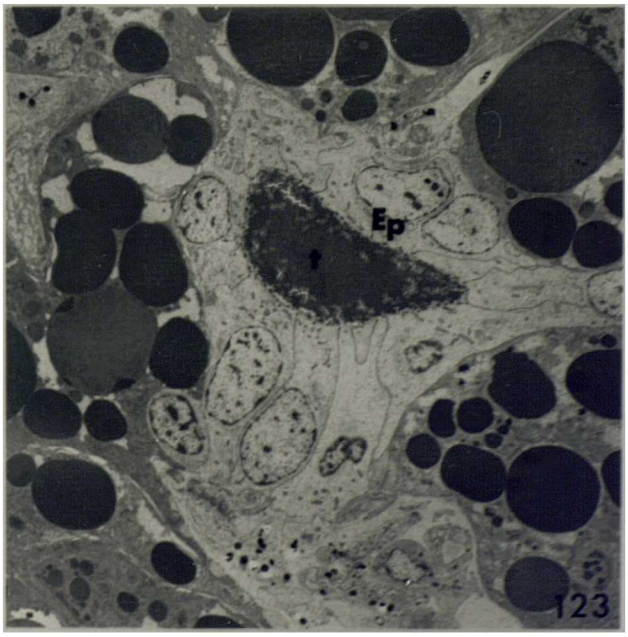
Ep
123

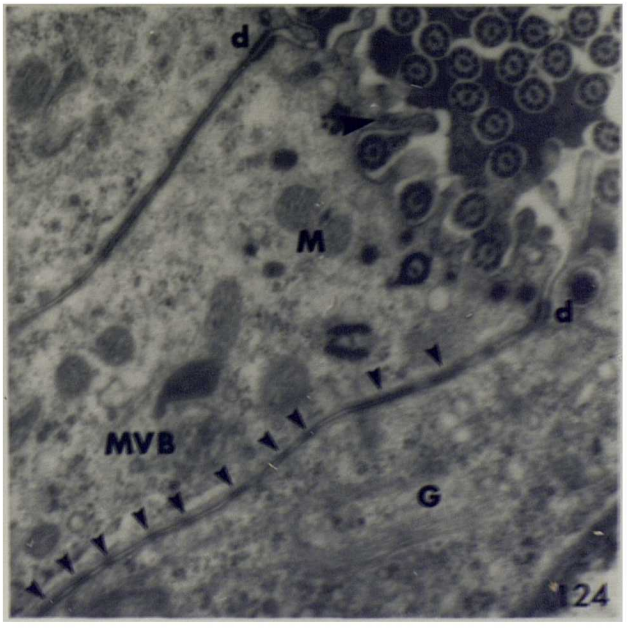
d
M
d
MVB
G
124

D.reticulatum, albumen gland, secretory phase.

Fig. 125 Main collecting duct filled with secretion (x2.2K).

Fig. 126 The apex of an epithelial cell lining the main collecting duct (x22.5K).

Fig. 127 Detail of the junctional complex at the apex of epithelial cells (x45K).


agd
Ep
125

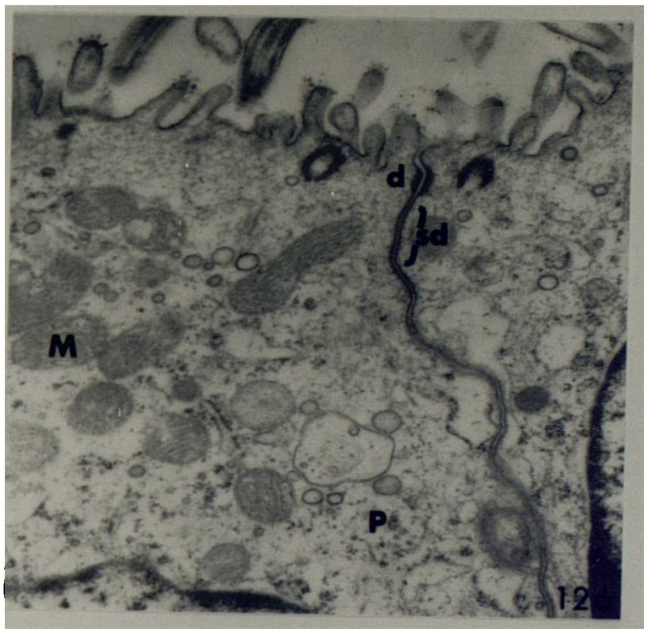
d
sd
M
P
12

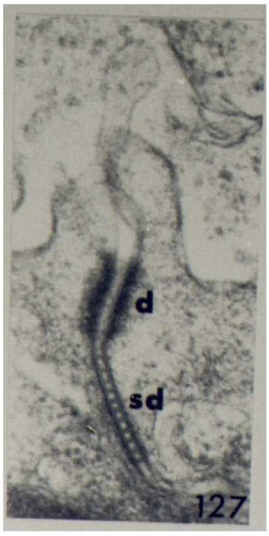
d
sd
127

D.reticulatum,albumen gland, secretory phase.

Fig. 128 Section through the bases of mature secretory cells showing the thin connective tissue sheath which surrounds each acinus (x1.5K).

Fig. 129 Nerve and muscle found near the base of the tubule epithelium (x9K). Detail of Fig. 122.


Pig
Pig
128

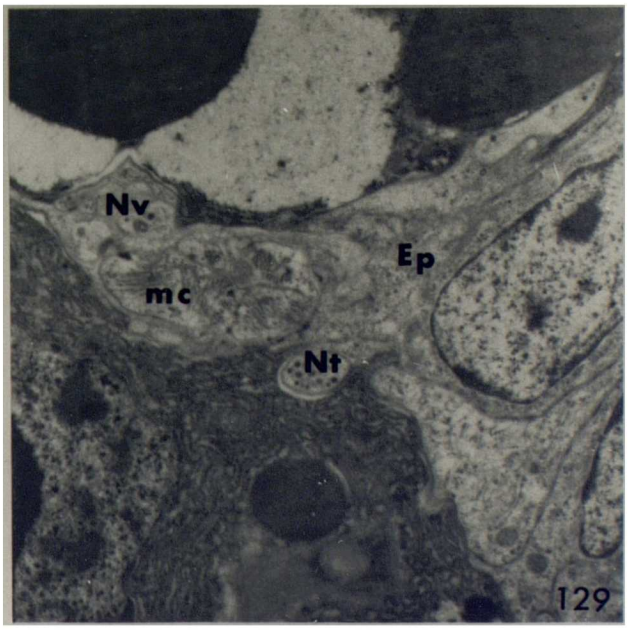
Nv
Ep
mc
Nt
129

A.hortensis, hermaphrodite duct, epithelial cells lining the seminal vesicle.

Fig. 130 Transition between ciliated and unciliated cells (x2.25K).

Fig. 131 The ciliated cells (x3.75K).

Fig. 132 Detail of the apices of the ciliated cells (x15K).

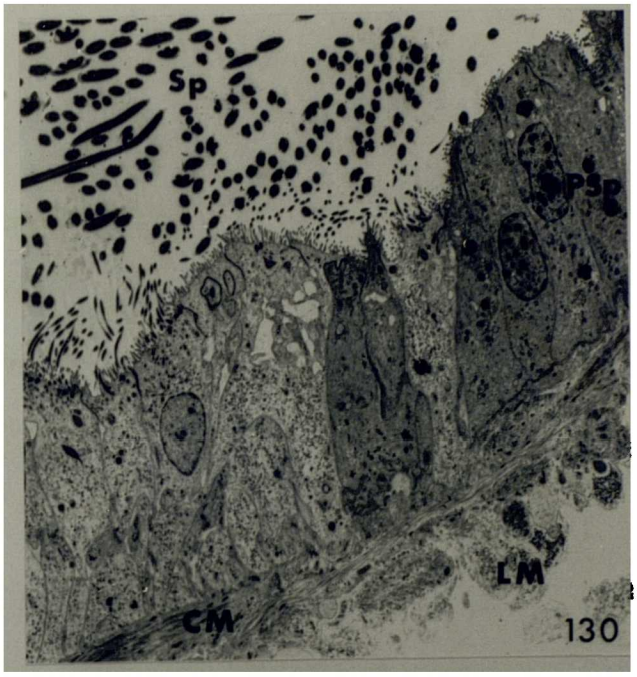
Sp
PSp
LM
CM
130

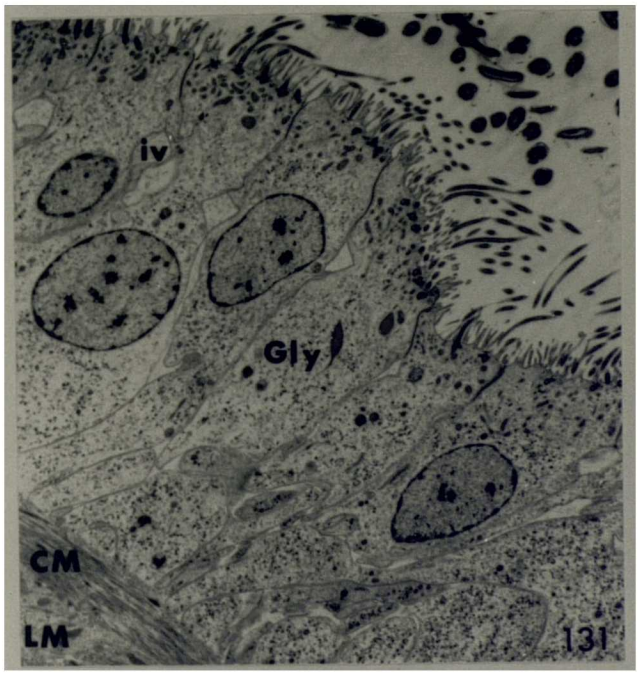
iv
Gly
CM
LM
131

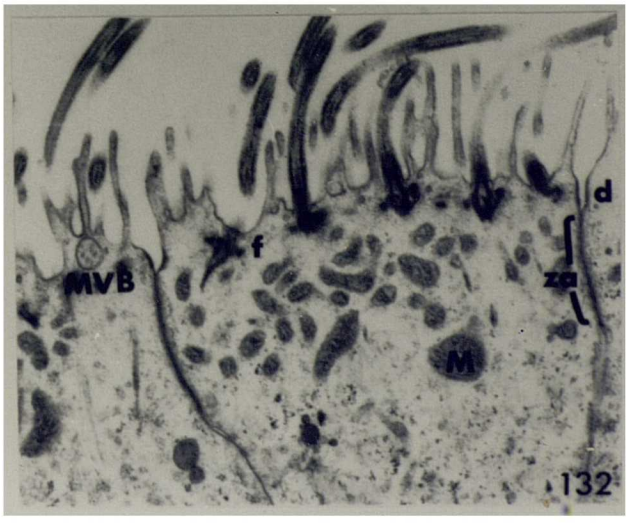
d
f
MVB
za
M
132

A.hortensis, hermaphrodite duct, epithelial cells lining the seminal vesicle.

Fig. 133 The unciliated cells (x3.75K). N.B. the cells are columnar.

Fig. 134 The unciliated cells (x3.75K). N.B. the cells are cuboidal.

Fig. 135 Detail of the apices of the unciliated cells (x15K). Arrows indicate vesicle chains.

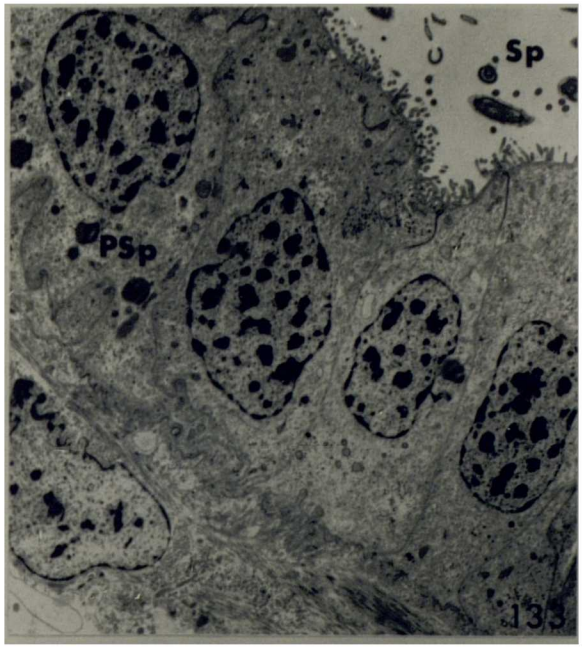
Sp
PSp
133

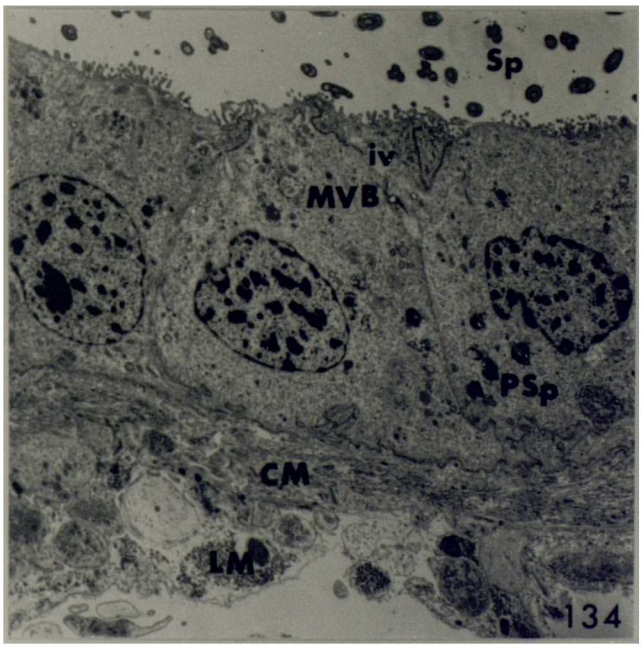
Sp
iv
MVB
PSp
CM
LM
134

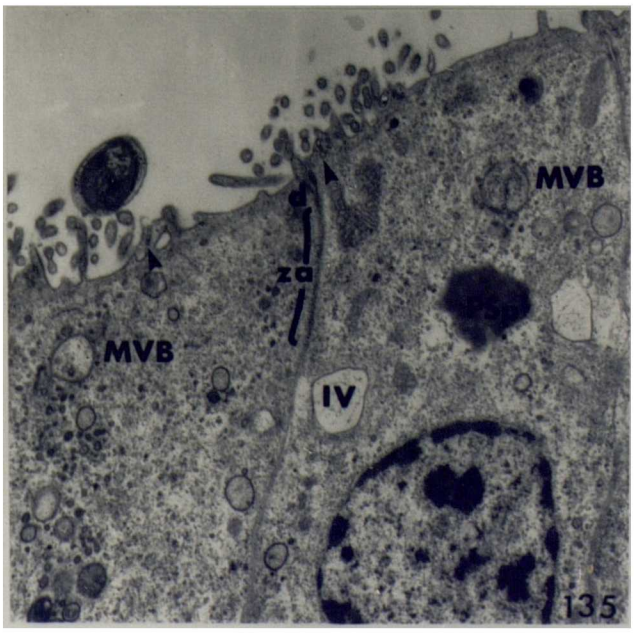
MVB
za
MVB
IV
135

A.hortensis, hermaphrodite duct, epithelial cells.

Fig. 136 Detail of phagocytosed sperm (x25.5K).

Fig. 137 Detail of cell bases (x22.5K).

Fig. 138 The ciliated cells lining the anterior, slender region of the hermaphrodite duct (xl.8K).

136

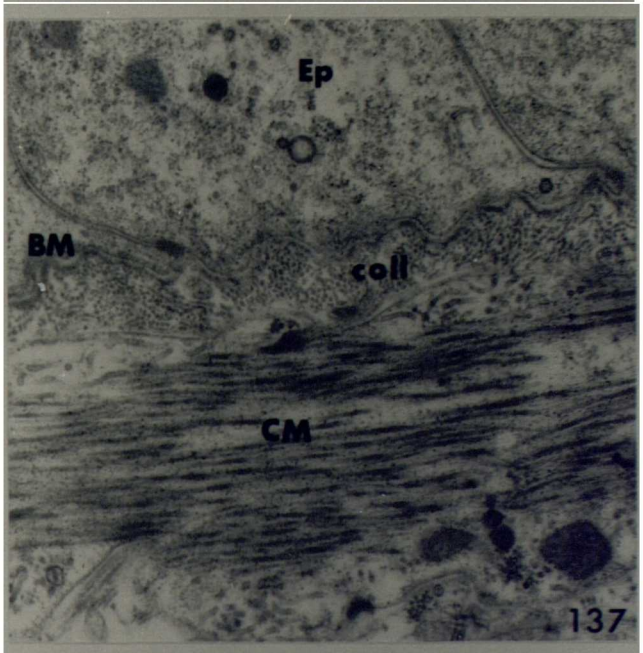

137

138

A.hortensis, carrefour loop, epithelial cells.

Fig. 139 General view (x2.4K).

Fig. 140 Detail of a Golgi body (x37.5K).

Fig. 141 Detail of a cell apex (x15K).

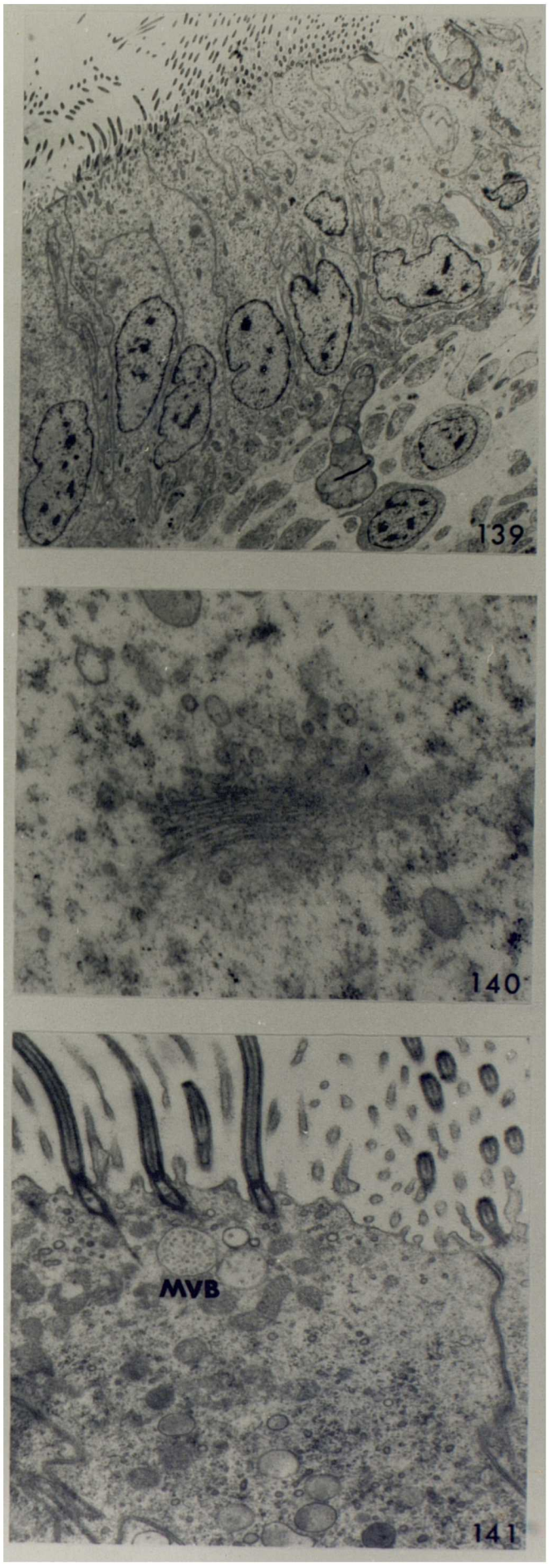
139
140
MVB
141

A.hortensis, carrefour loop, epithelial cells.

Fig. 142 Detail of the sub-apical region (x9K). Stage E.

Fig. 143 Detail showing the relationship of axons with the epithelial cells (x15K).

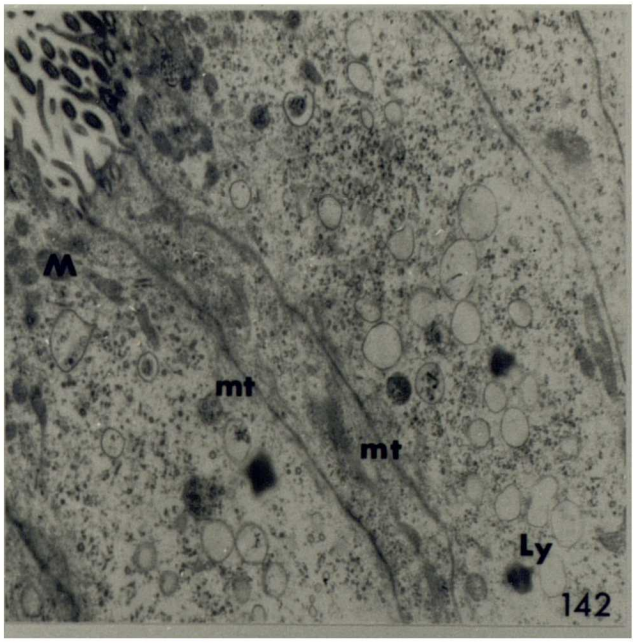
M
mt
mt
Ly
142

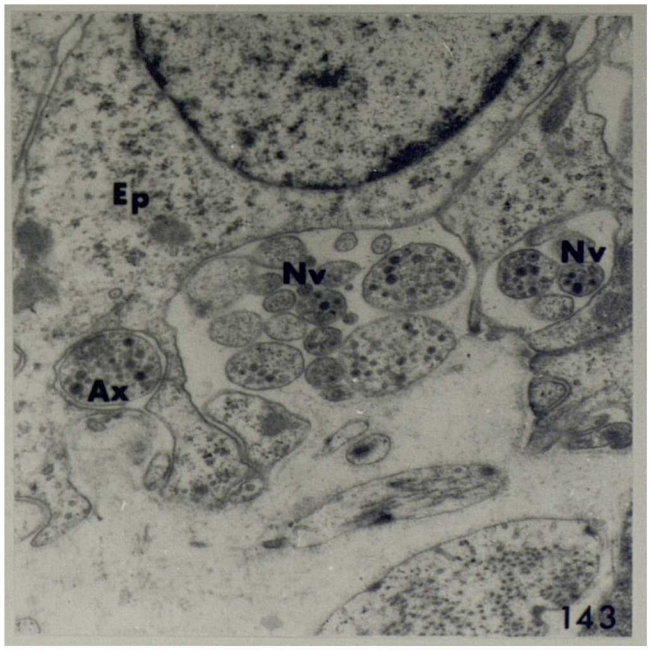
Ep
Nv
Nv
Ax
143

A.hortensis, carrefour gland.

Fig. 144 Sub-epithelial secretory cells (x1.5K).

Fig. 145 The bases of secretory cells (x6K).

Fig. 146 Detail showing the Golgi-rER relationship and the formation of secretion granules (x16K).

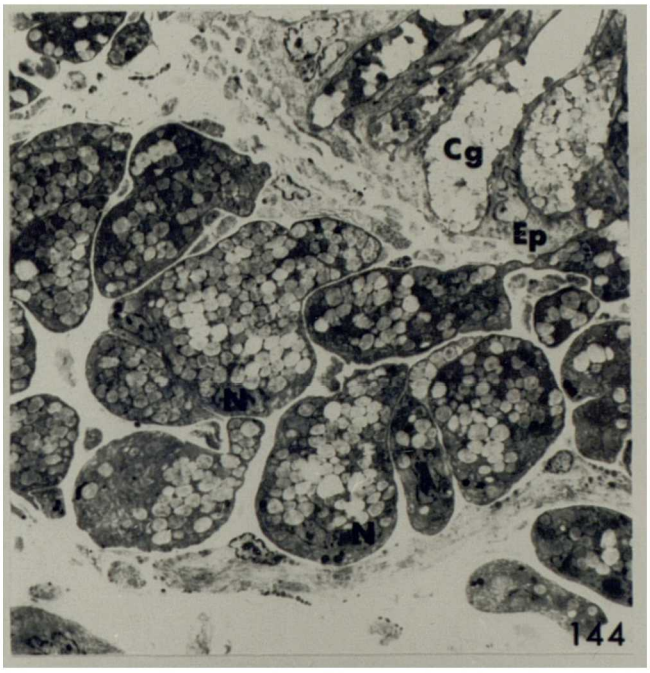
Cg
Ep
N
N
144

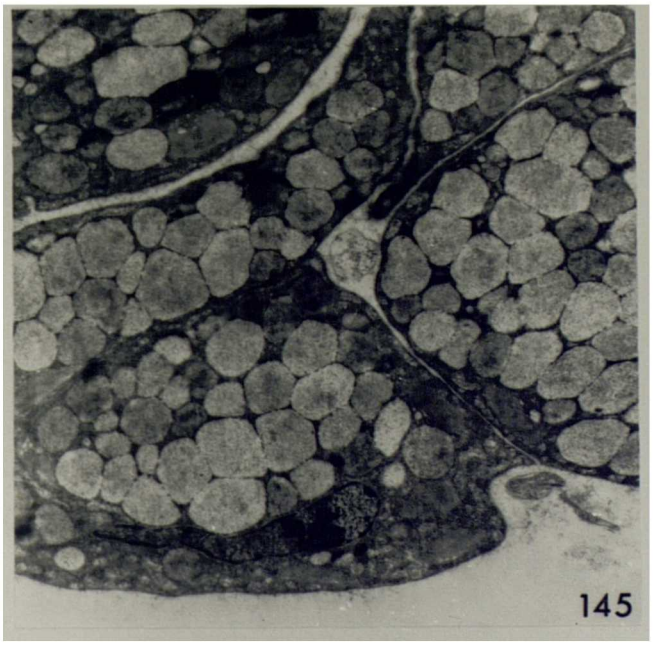
145

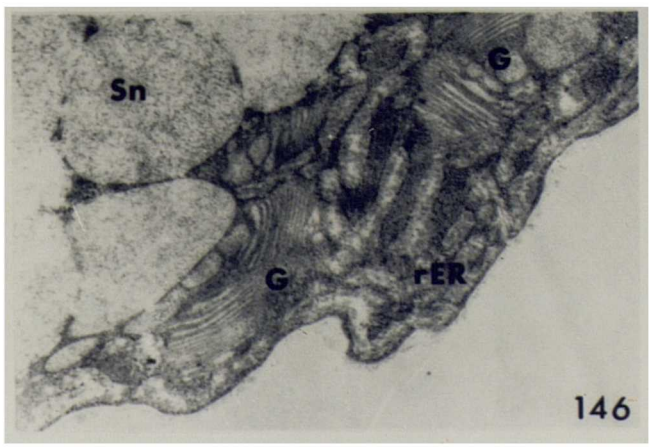
Sn
G
G
rER
146

A.hortensis, carrefour gland.

Fig. 147 Secretory cell opening into the carrefour (x3.4K).

Fig. 148 Apical detail of a secretory cell (x14K).

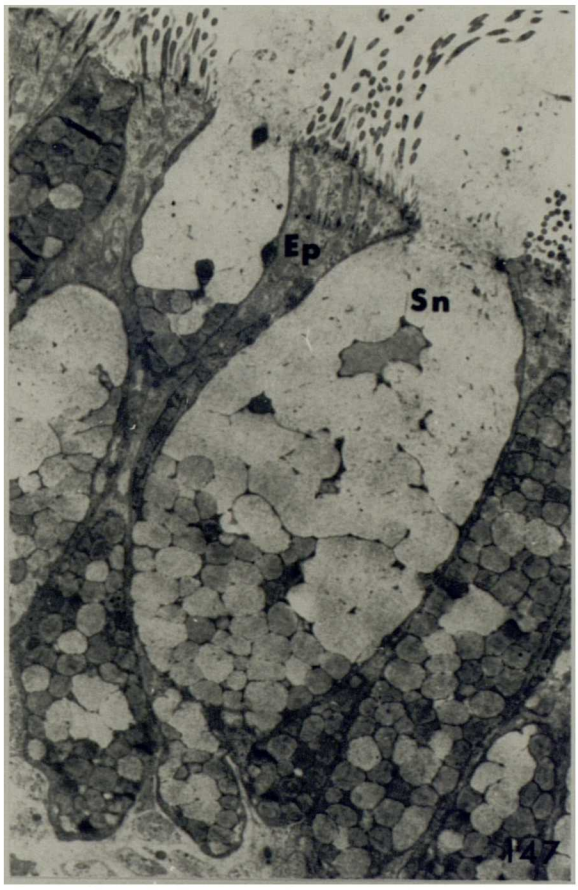
Ep
Sn
147

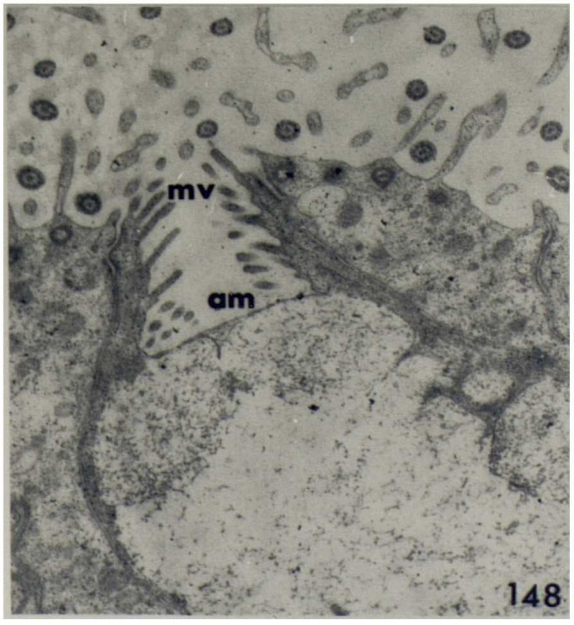
mv
am
148

A.hortensis, carrefour at the junction of the albumen gland ducts and the common duct.

Fig. 149 General view of lining epithelium (x2K). Stars indicate the position of neurons.

Fig. 150 Detail of epithelial cell bases (x6K).


iv
149

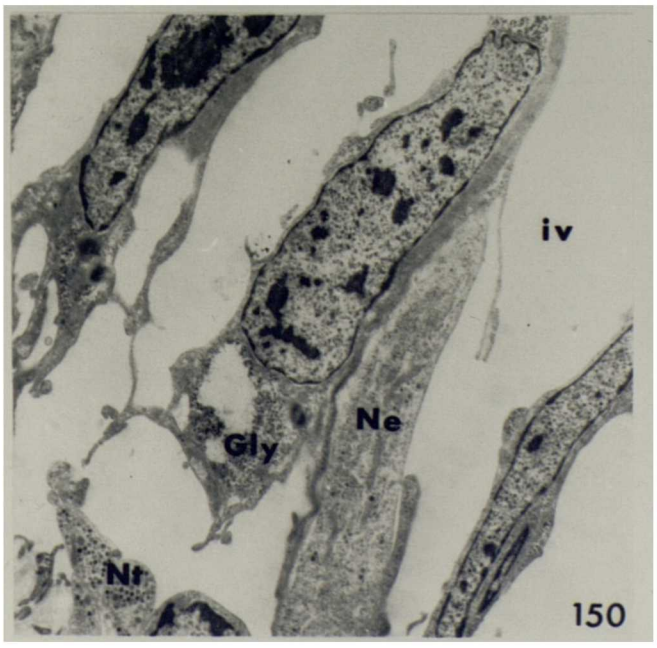
iv
Ne
Gly
Nf
150

A.hortensis, carrefour at the junction of the albumen gland ducts and the common duct.

Fig. 151 Detail of epithelial cell apices (x15K).

Fig. 152 Sensory neuron in epithelium (x10K).

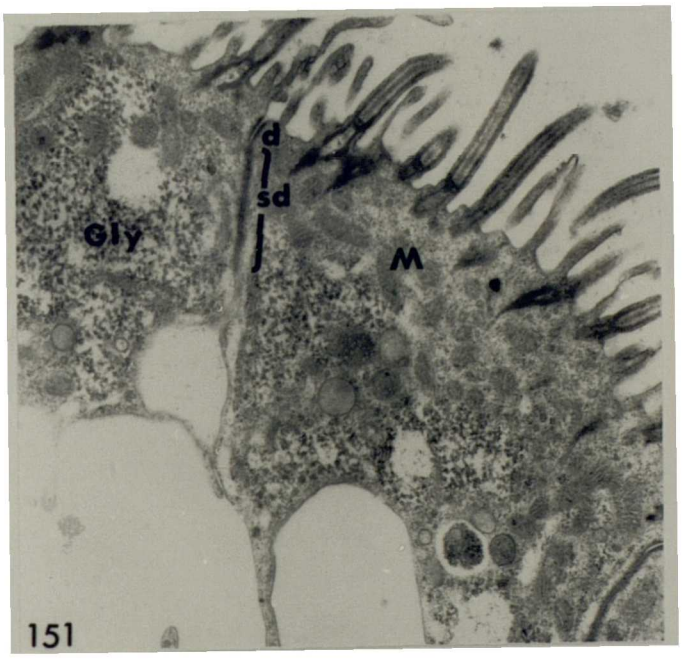

151

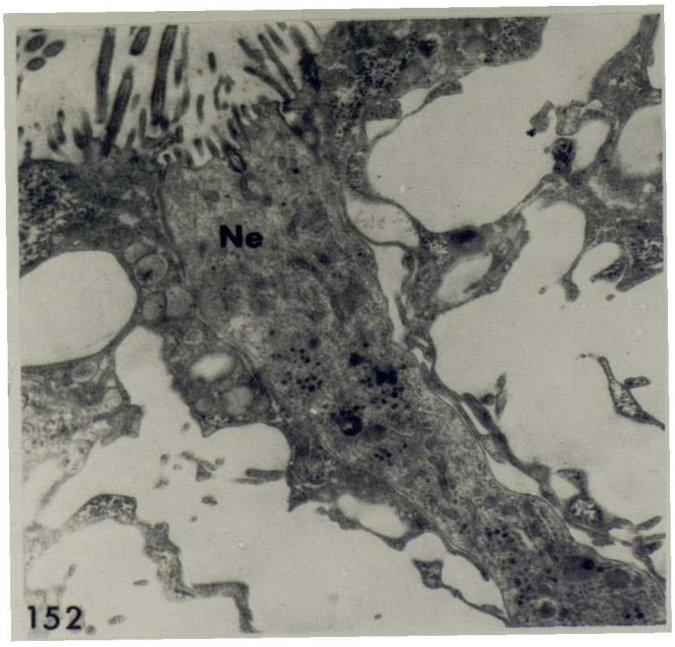

152

A.hortensis, albumen gland.

Fig. 153 Epithelial cells lining the collecting duct (x7K).

Fig. 154 T.S. through a tubule (x3.75K).

153

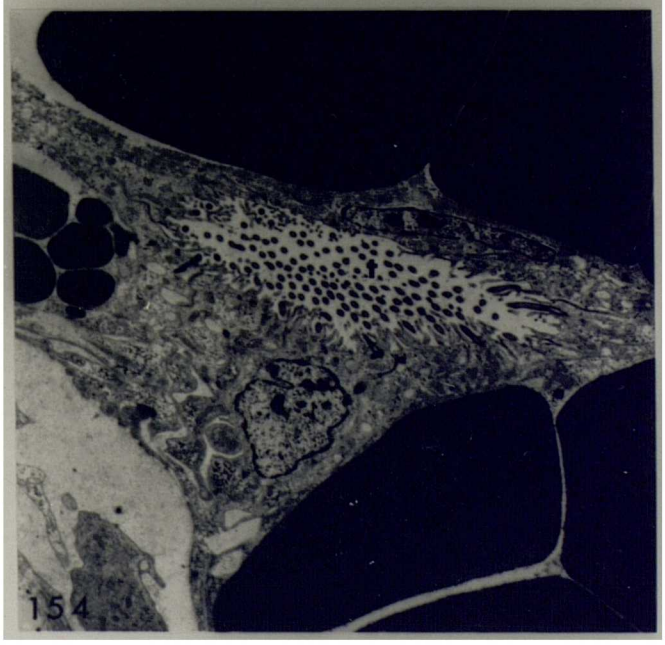
154

Fig. 155 A.hortensis, pore cell in the connective tissue surrounding the hermaphrodite duct (x5K). Arrow indicates region of cell membrane detailed in Fig. 156.

Fig. 156 Detail of Fig. 155 (x25K).

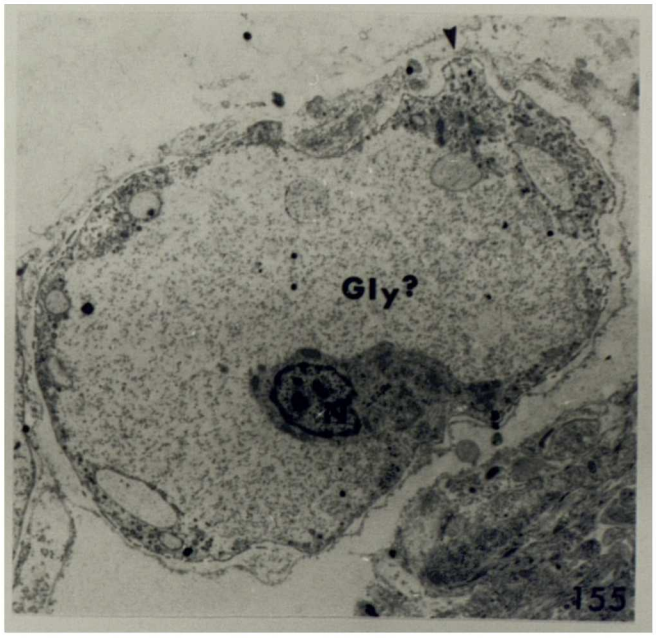
Gly?
155

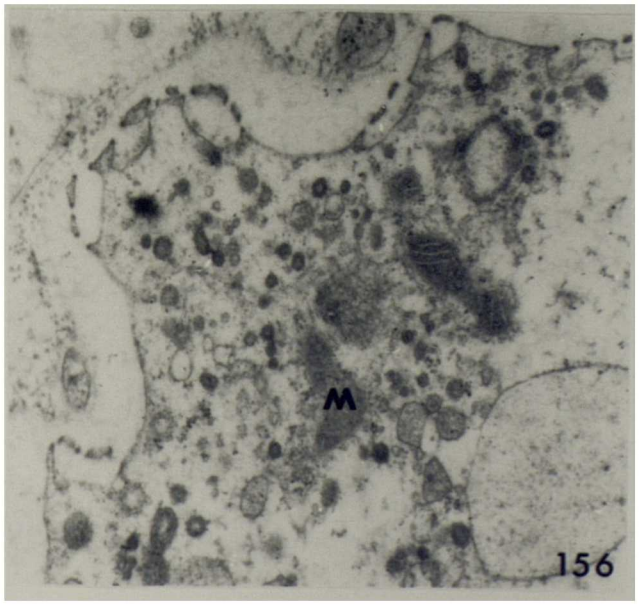
M
156

Fig. 157 Diagram illustrating the distribution of the neurons and nerves observed in a section through the mature carrefour loop of A. hortensis.

a. descending limb.
b. ascending limb.
c. ascending limb in the region of the carrefour gland.

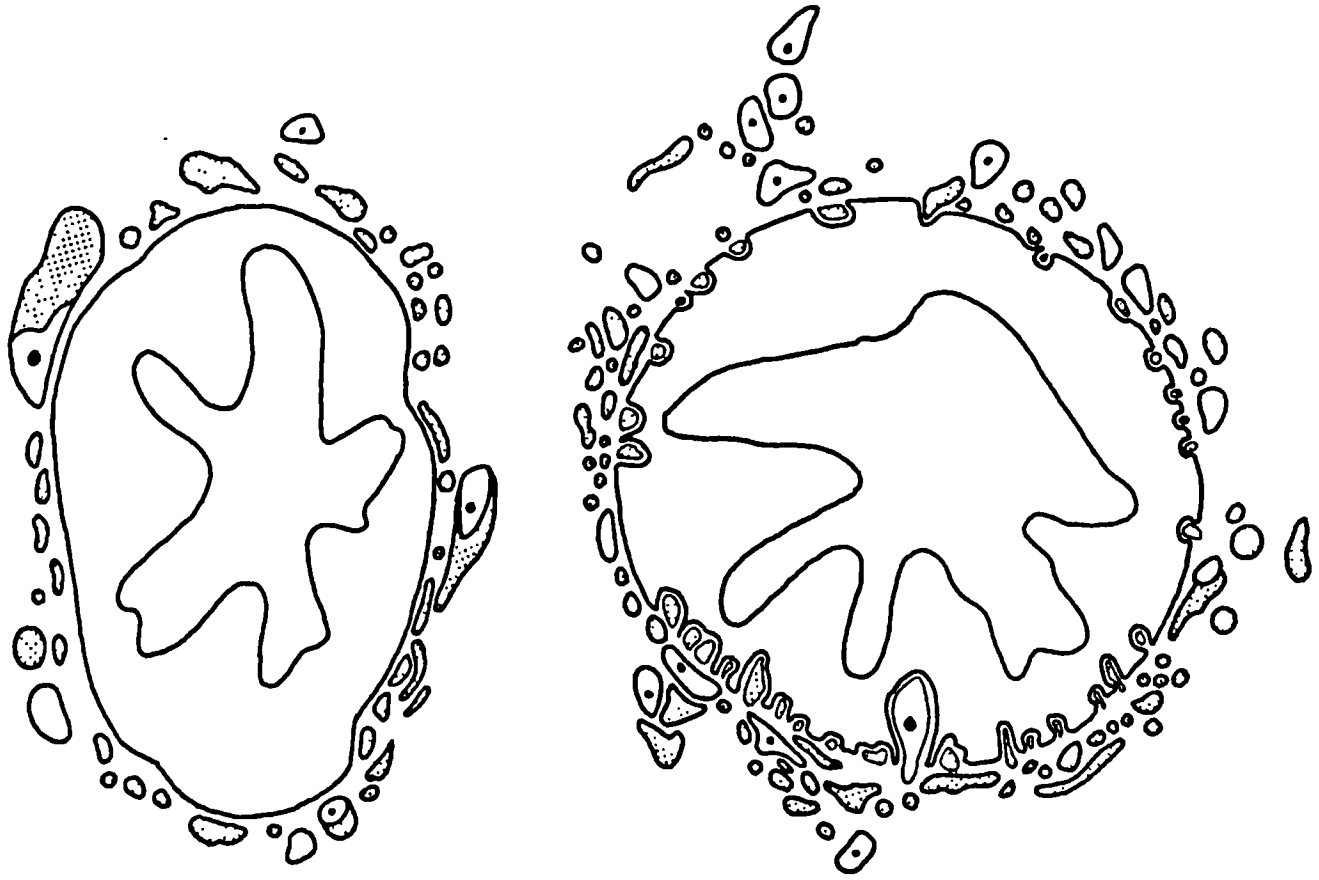

□ neurons

▨ nerves

Fig. 157 a b

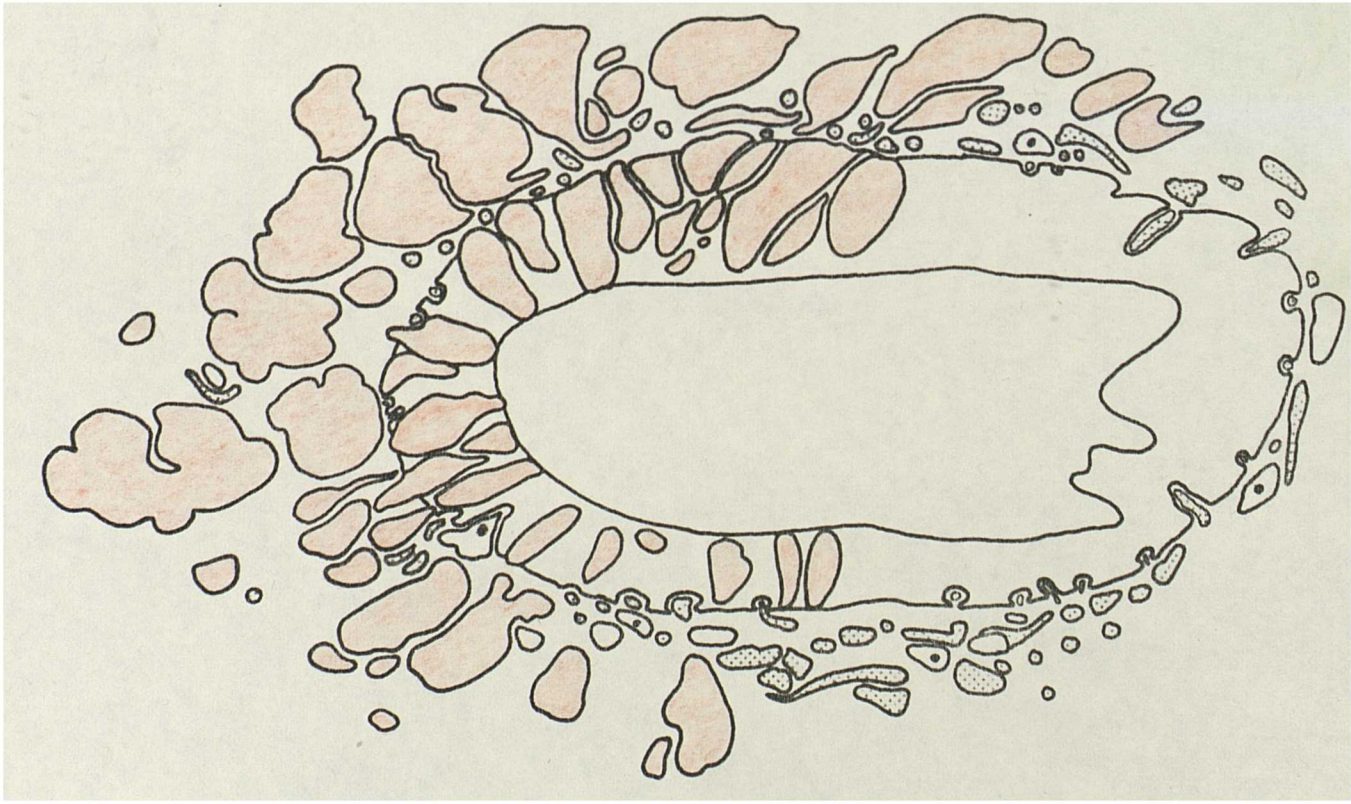

neurons

nerves

carrefour gland cells

Fig. 157c

A.hortensis, connective tissue surrounding the carrefour loop.

Fig. 158 Arrangement of muscle and nervous tissue in the connective tissue surrounding the descending limb (x10K).

Fig. 159 Arrangement of muscle and nervous tissue in the connective tissue surrounding the ascending limb (x10K).

Fig. 160 Detail showing the intimate relationship of nerves with the epithelial cells lining the ascending limb (x15K).

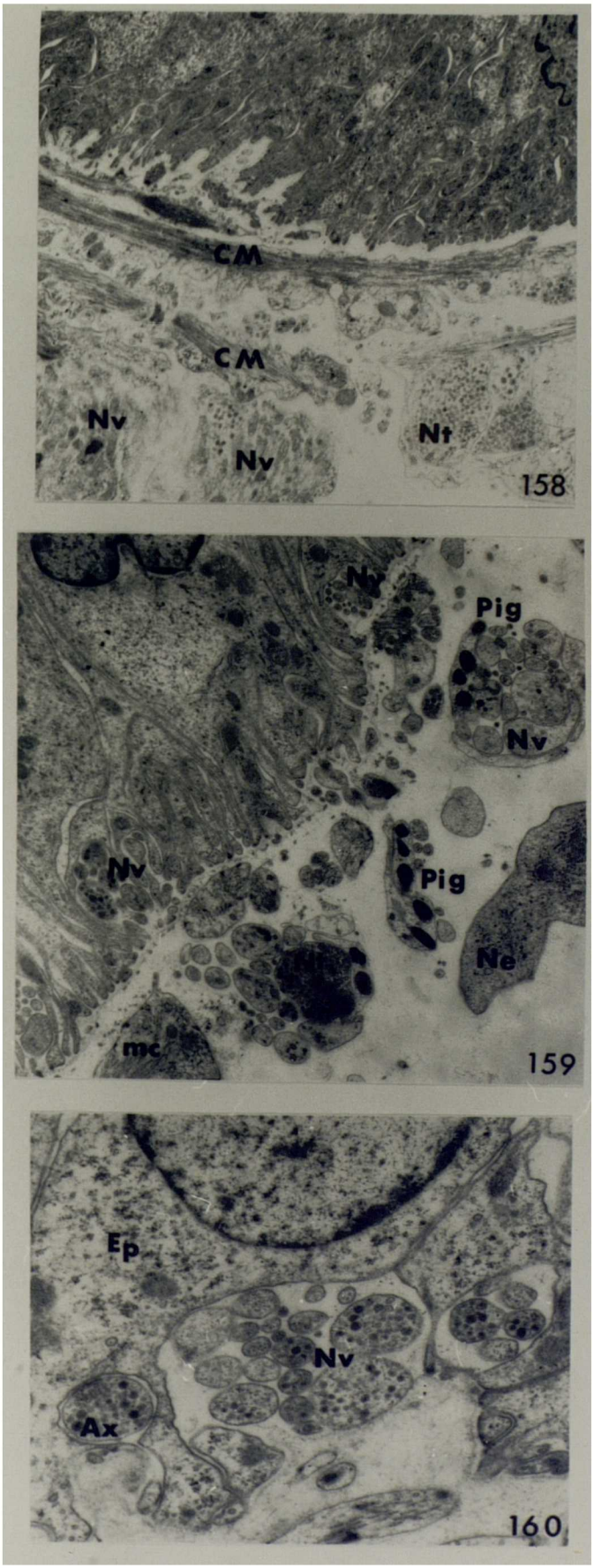
CM
CM
Nv
Nv
Nt
158
Nv
Pig
Nv
Nv
Pig
Ne
mc
159
Ep
Nv
Ax
160

A.hortensis, connective tissue surrounding the carrefour gland.

Fig. 161 Arrangement of muscle and nervous tissue (x2.8K).

Fig. 162 Detail showing the intimate relationship of nerves with the epithelial cells (x4K).

Fig. 163 Detail of the nerve ring surrounding the neck of a secretory cell (x16K).

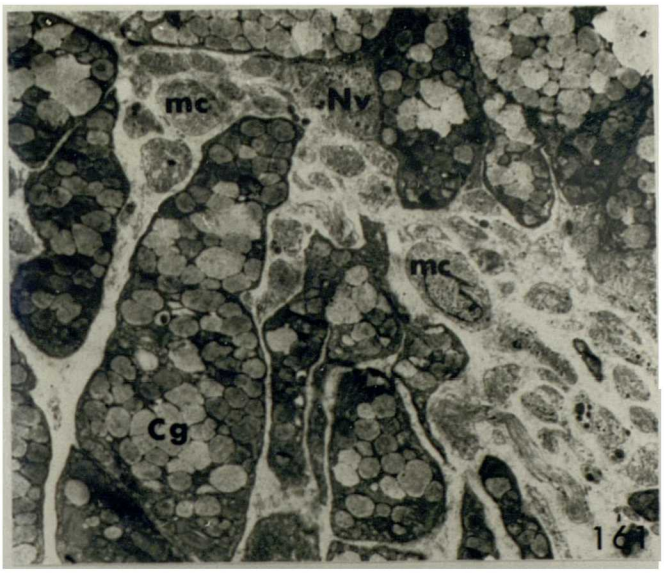
mc
Nv
mc
Cg
161

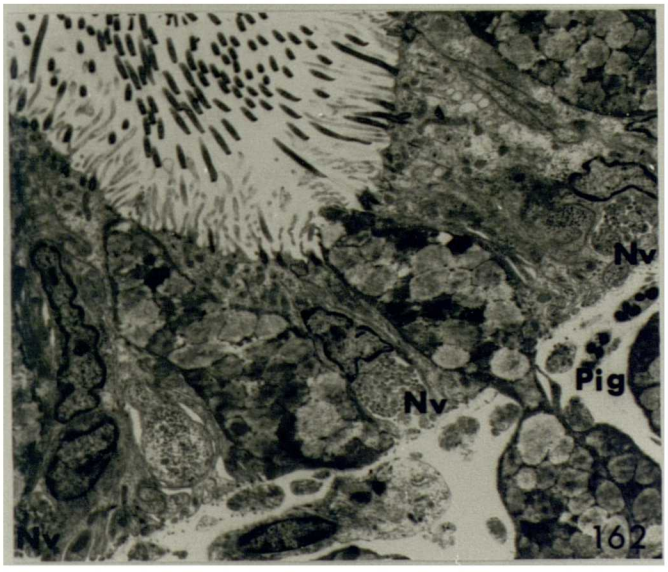
Nv
Pig
Nv
Nv
162


Nv
163

A.hortensis, connective tissue surrounding the carrefour at the junction of the albumen gland ducts and common duct.

Fig. 164 Nerve, muscle and pigment cells (x6K). Arrows indicate possible neuromuscular junctions.

Fig. 165 Neuromuscular junction indicated by the left arrow in Fig. 164 (x35K).

Fig. 166 The relationship of the nerves and epithelial cells (x9K).

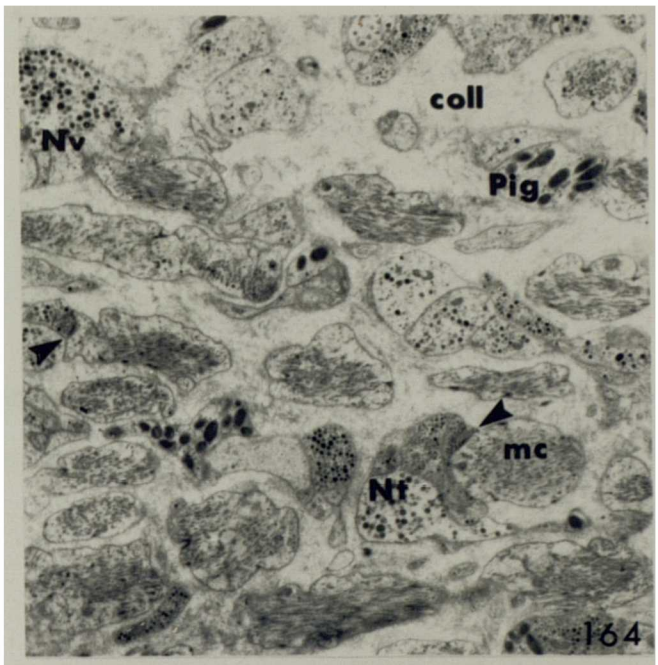

164

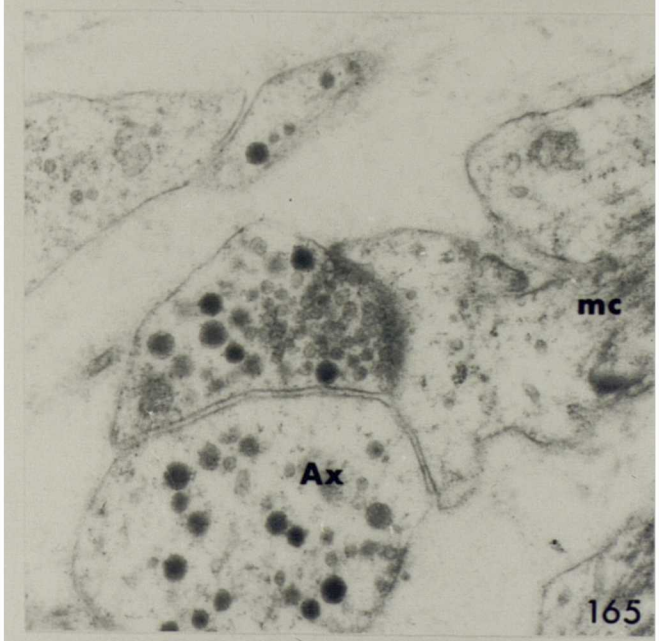

165

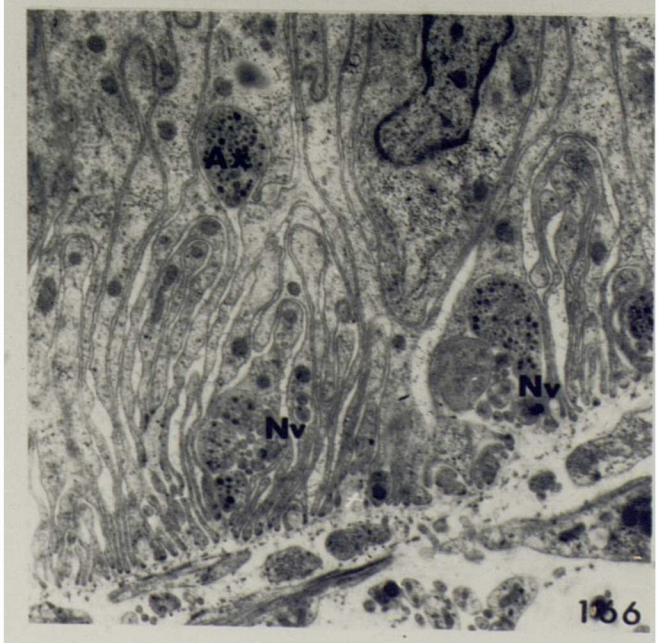

166

A.hortensis, connective tissue surrounding the carrefour at the junction of the albumen gland ducts and common duct.

Fig. 167 Relationship of sensory neuron with underlying nerve plexus (x9K).

Fig. 168 Detail of a typical neuron in the region of the Golgi apparatus (x37.5K).

Fig. 169 Detail of a typical nerve (x22.5K).

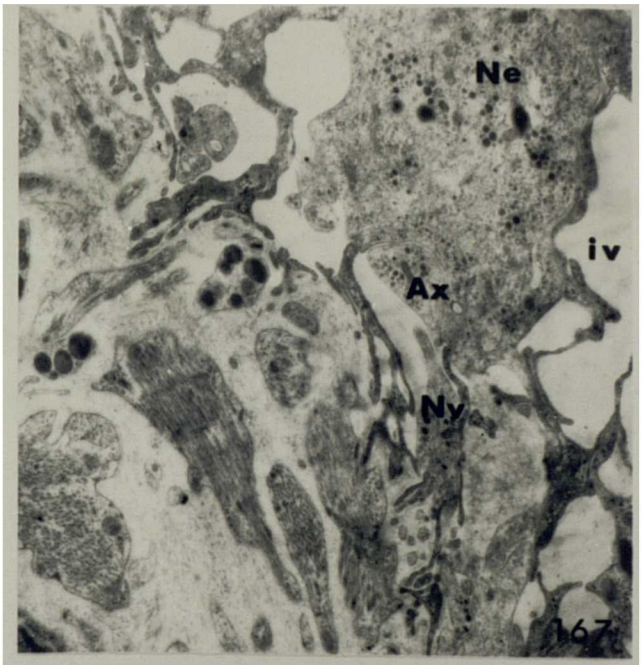
Ne
iv
Ax
Ny
167

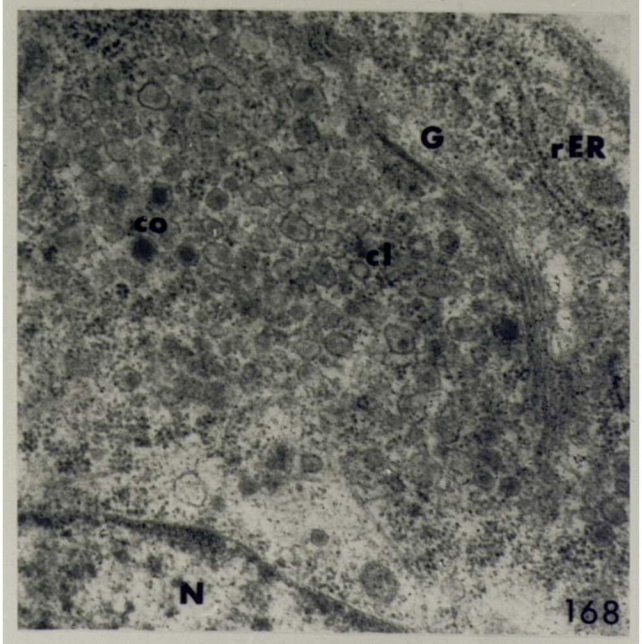
G
rER
co
cl
N
168

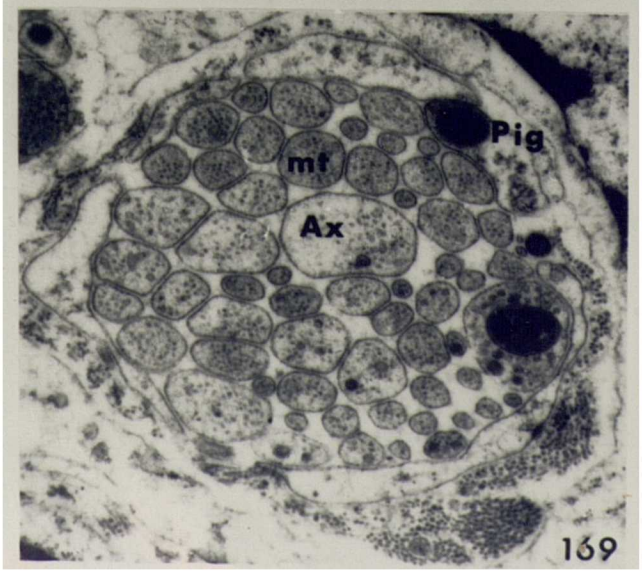
Pig
mf
Ax
169

Fig. 170 Diagram showing the variety of form of the stylommatophoran carrefour.

a. D.reticulatum

b. Helix pomatia

c. Pellicula depressa

d. Succinea putris

e. Succinea pfeifferi

f. Trichia hispida

g. Triodopsis multilineata

h. A.hortensis

i. Aillya camerunensis

Key: F = finger-like diverticulum in D. reticulatum and its equivalent structure in other Stylommatophora.

ρ = pouch-like diverticulum in D. reticulatum and its equivalent structure in other Stylommatophora.

arrows indicate the level of section.

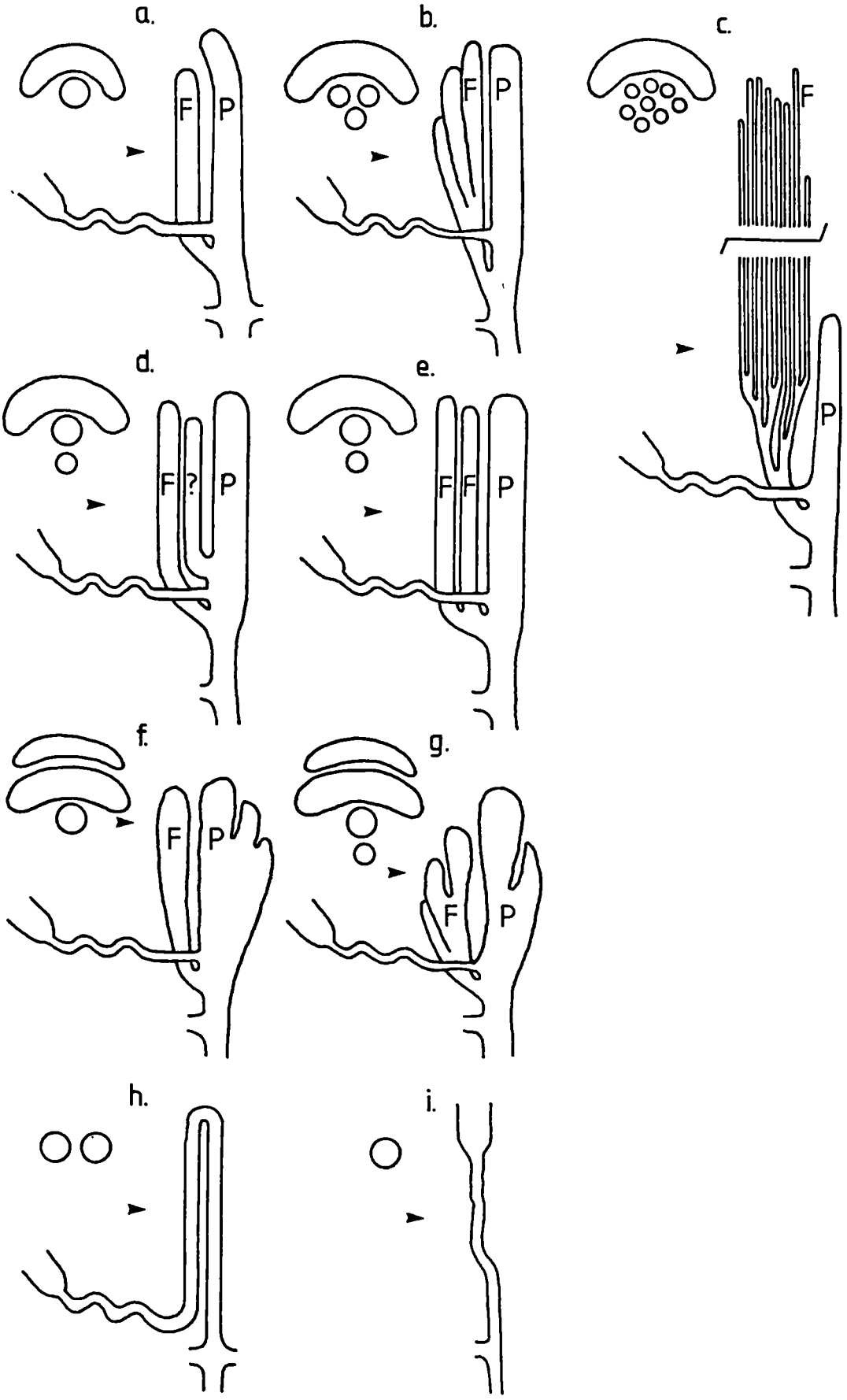

Fig. 170

Fig. 171 Diagram of the penial mass and anterior genital ducts of D.reticulatum.

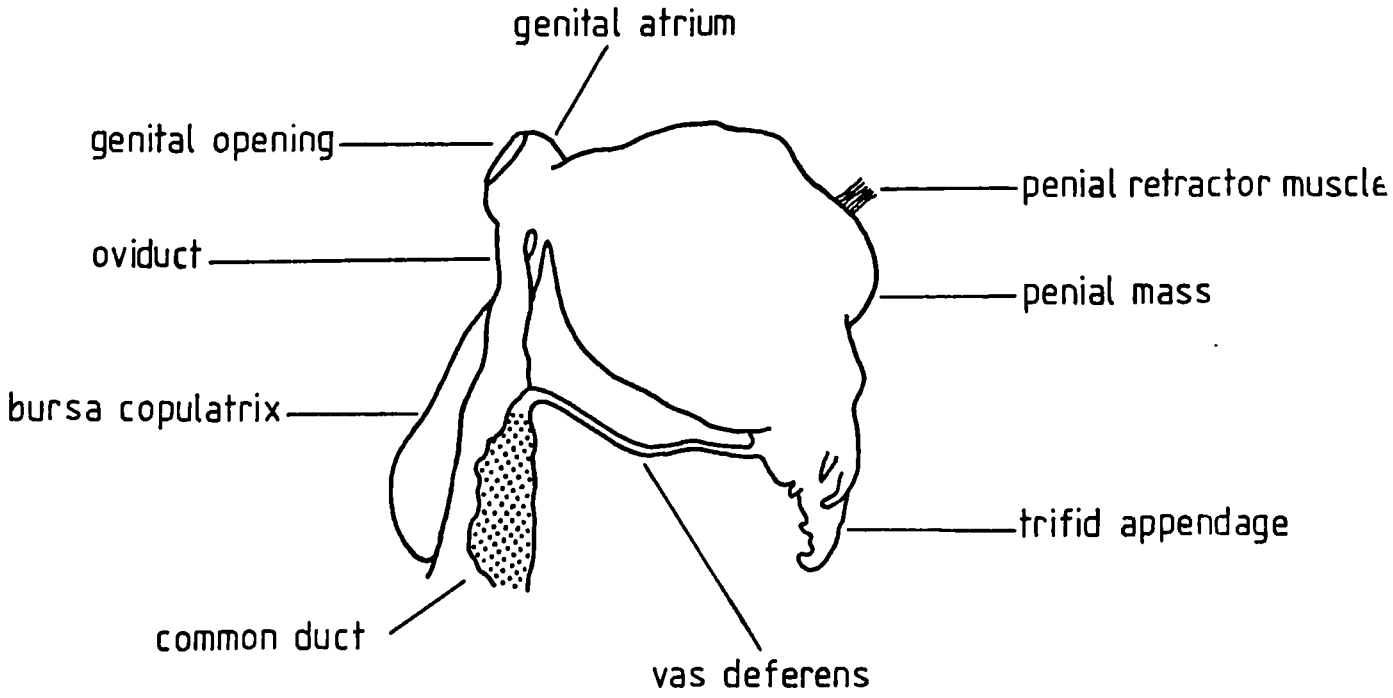
genital atrium
genital opening
oviduct
bursa copulatrix
common duct
vas deferens
penial retractor muscle
penial mass
trifid appendage

Fig. 171

Fig. 172 Longitudinal section through the trifid appendage of D.reticulatum (x100).

Fig. 173 Diagram showing the variety of form of the trifid appendage in D.reticulatum.

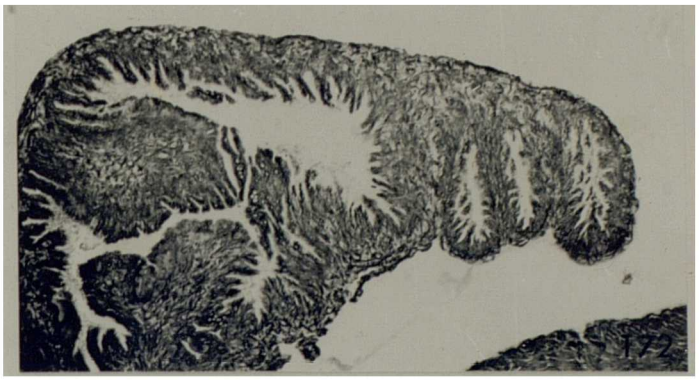

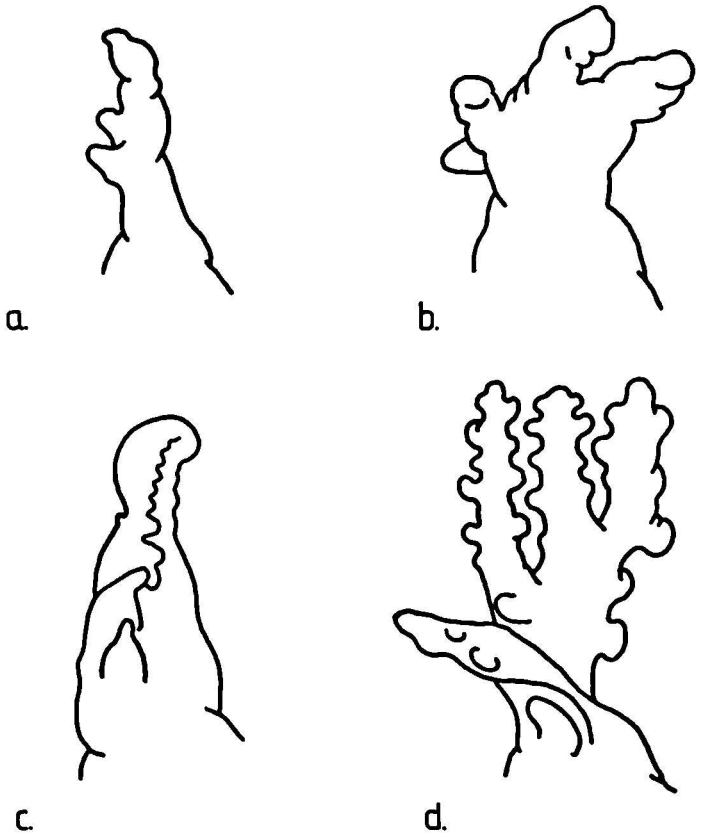

Fig. 173

Fig. 174 D.reticulatum, typical form of trifid appendage (x250).

Fig. 174

Fig. 175 Drawing of the dissected penial mass and anterior gential ducts of D.reticulatum . Arrows indicate point of dissection.

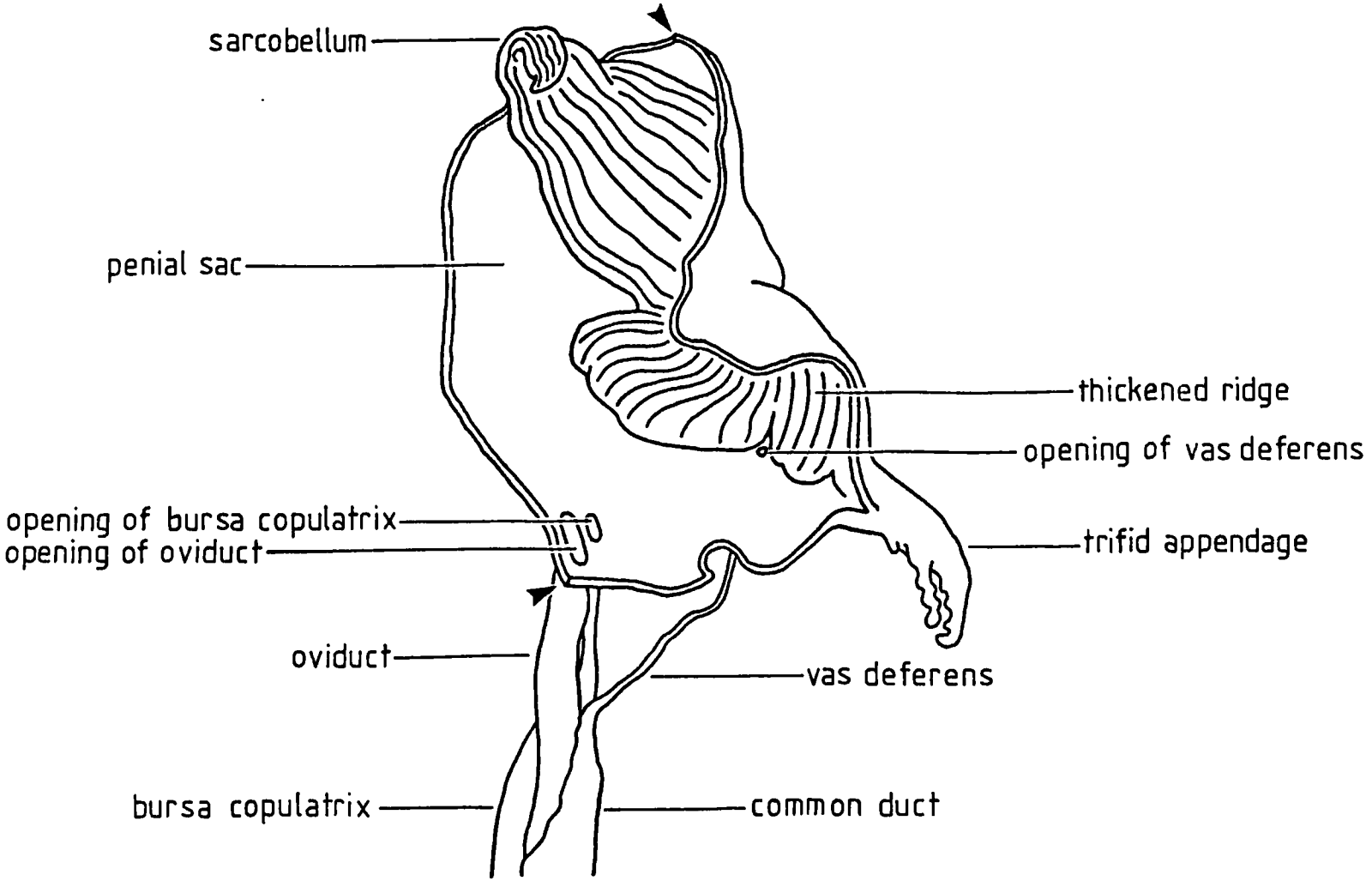
sarcobellum
penial sac
thickened ridge
opening of vas deferens
opening of bursa copulatrix
opening of oviduct
trifid appendage
oviduct
vas deferens
bursa copulatrix
common duct

Fig. 175

D.reticulatum, penial mass and anterior genital ducts.

Fig. 176 L.S. through the penial mass (x42). Stage D.

Fig. 177 L.S. through the penial mass (x34). Stage F.

Fig. 178 T.S. through the bursa copulatrix, oviduct and vas deferens (x160).

Fig. 179 T.S. through the bursa copulatrix and common duct (x34).

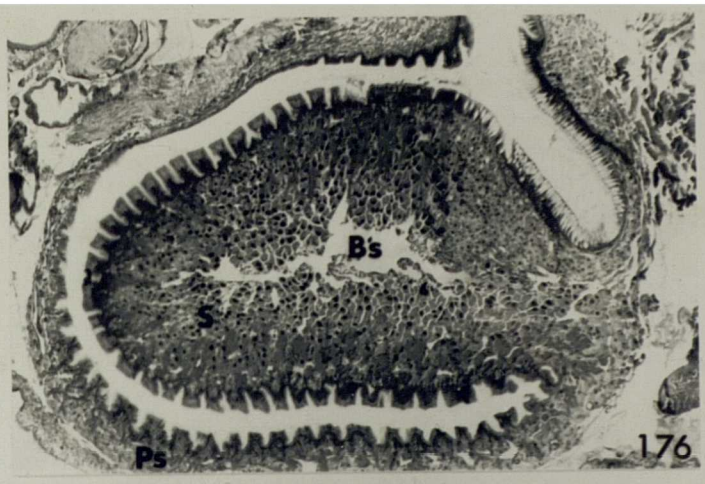

176

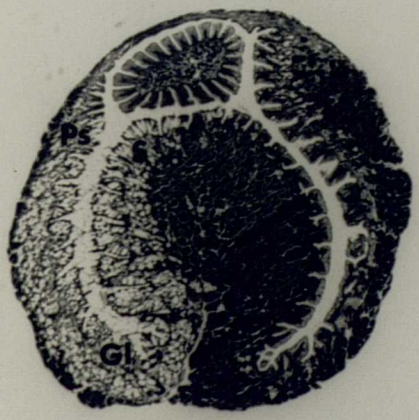

177

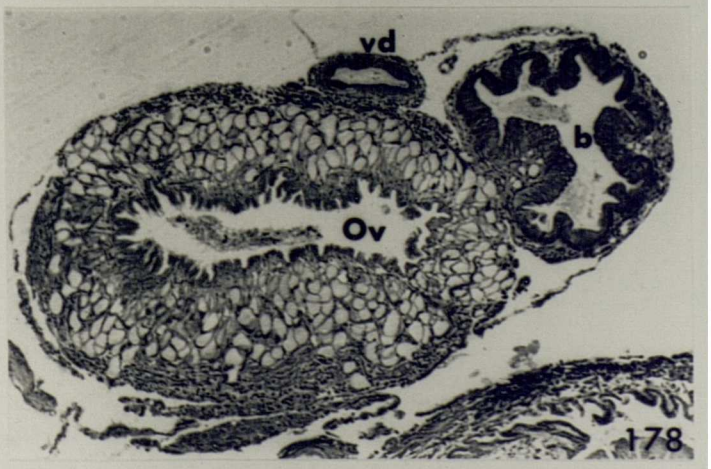

178

179

Fig. 180 Vascularization of the penial mass and anterior genital ducts of D.reticulatum, front (a) and rear (b) views.
Drawn from dissection. Blood vessels injected with Indian ink by A. Duval.
Regions of the penial mass are labelled in Fig. 171.

Fig. 181 Innervation of the penial mass and anterior genital ducts of D.reticulatum.
Drawn from dissection. Regions of the penial mass are labelled in Fig. 171.

a. front

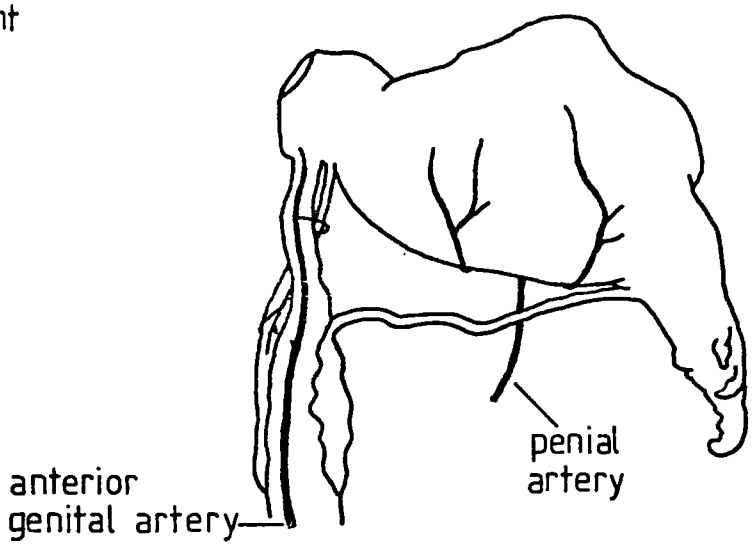

b. rear

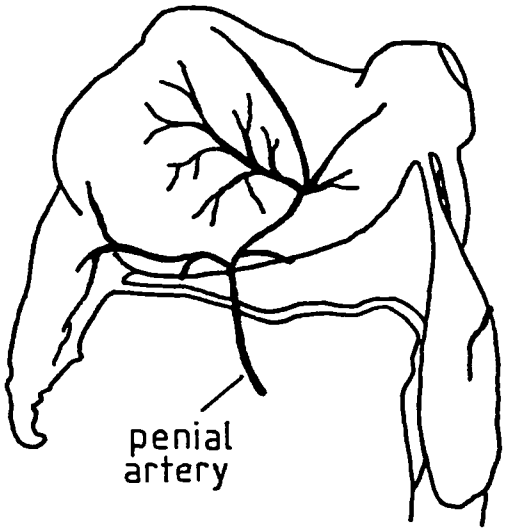

Fig. 180

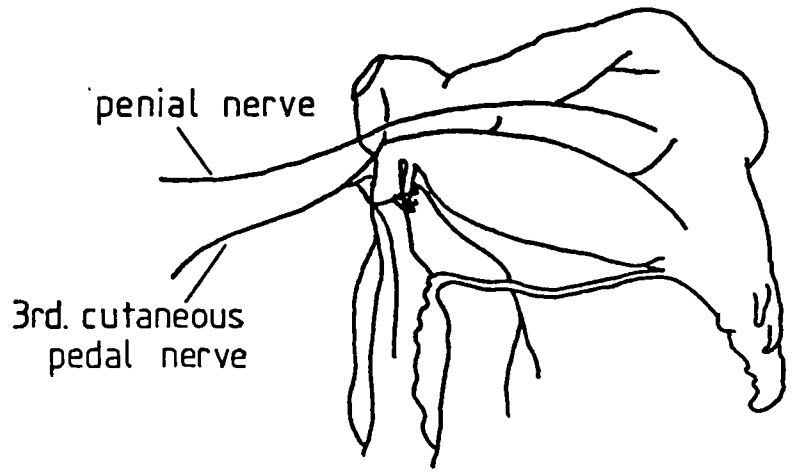

Fig. 181

D.reticulatum, penial mass and anterior genital ducts.

Fig. 182 T.S. through the reproductive tract in the region of the genital atrium (arrowed) (x550). Early A-stage.

Fig. 183 T.S. through the genital atrium (x550). Late A-stage.

Fig. 184 T.S. through the genital atrium and penial mass (x150). Early B-stage.

Fig. 185 T.S. through the penial mass and anterior genital ducts (x150). Early B-stage.

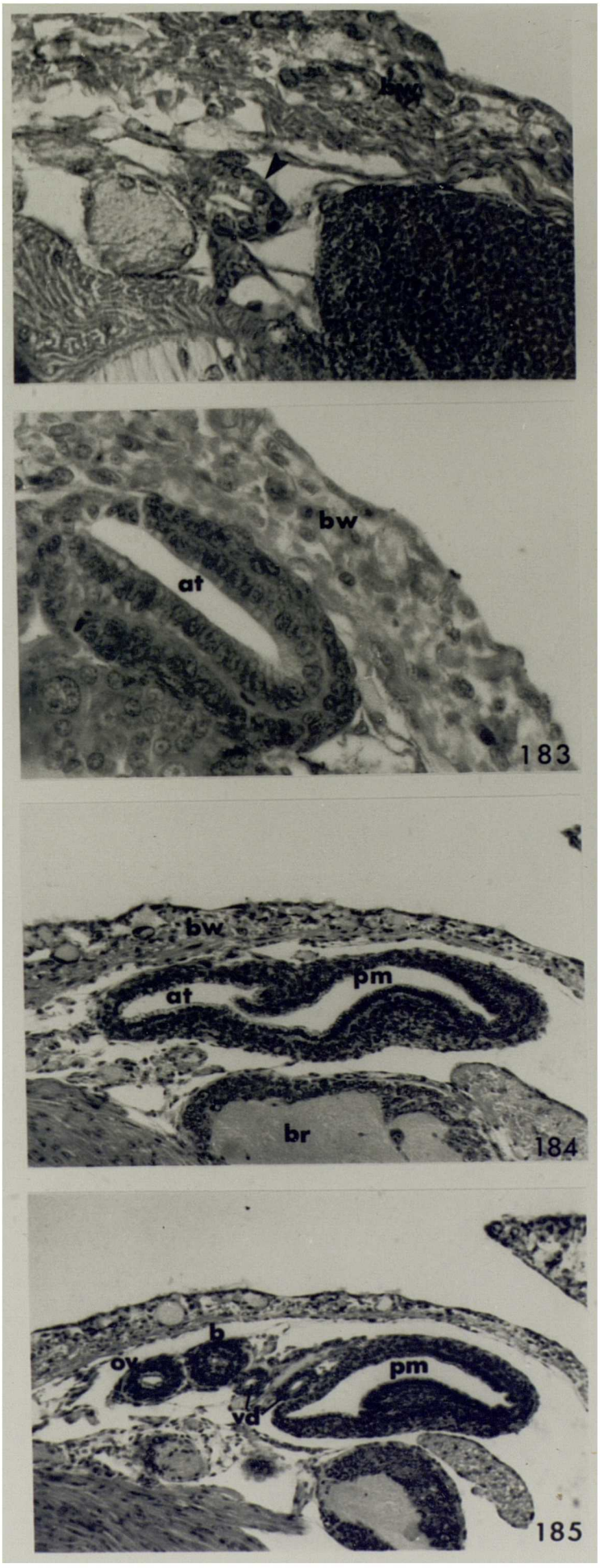
bw
bw
at
183
bw
at
pm
br
184
b
oy
pm
yd
185

D.reticulatum, penial mass and anterior genital ducts.

Fig. 186 T.S. through the common duct (arrowed) (x150). Early B-stage.

Fig. 187 L.S. through the penial mass and genital atrium (x180). Late B-stage.

Fig. 188 L.S. through the trifid appendage (x158). Late B-stage.

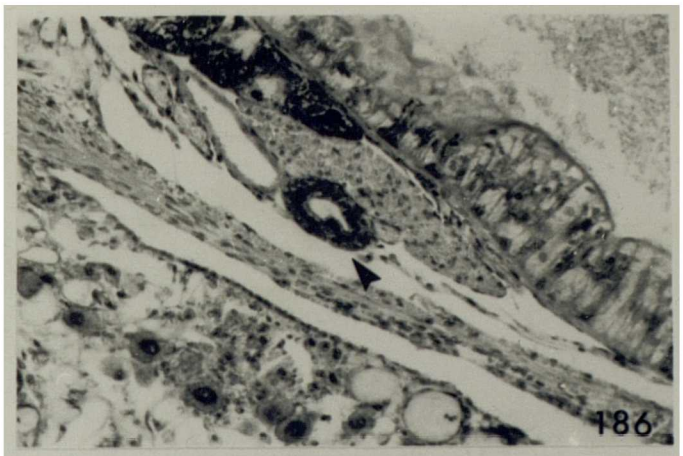

186

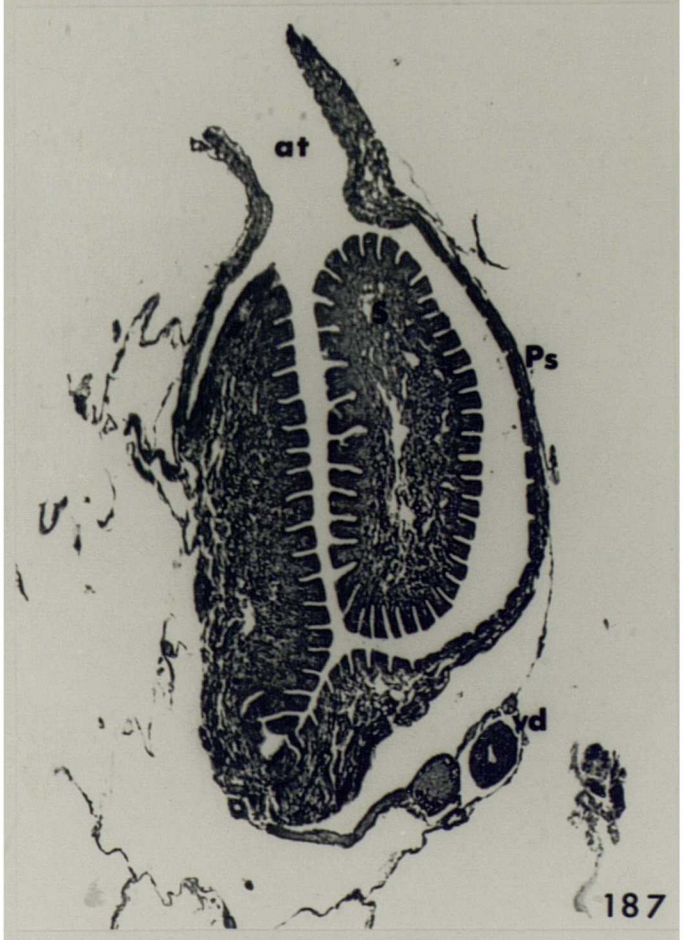

187

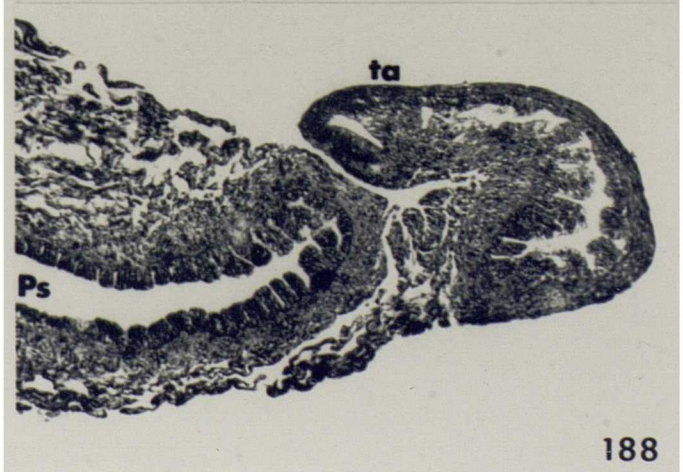

188

Fig. 189 Diagram of the anterior genital ducts of A.hortensis.

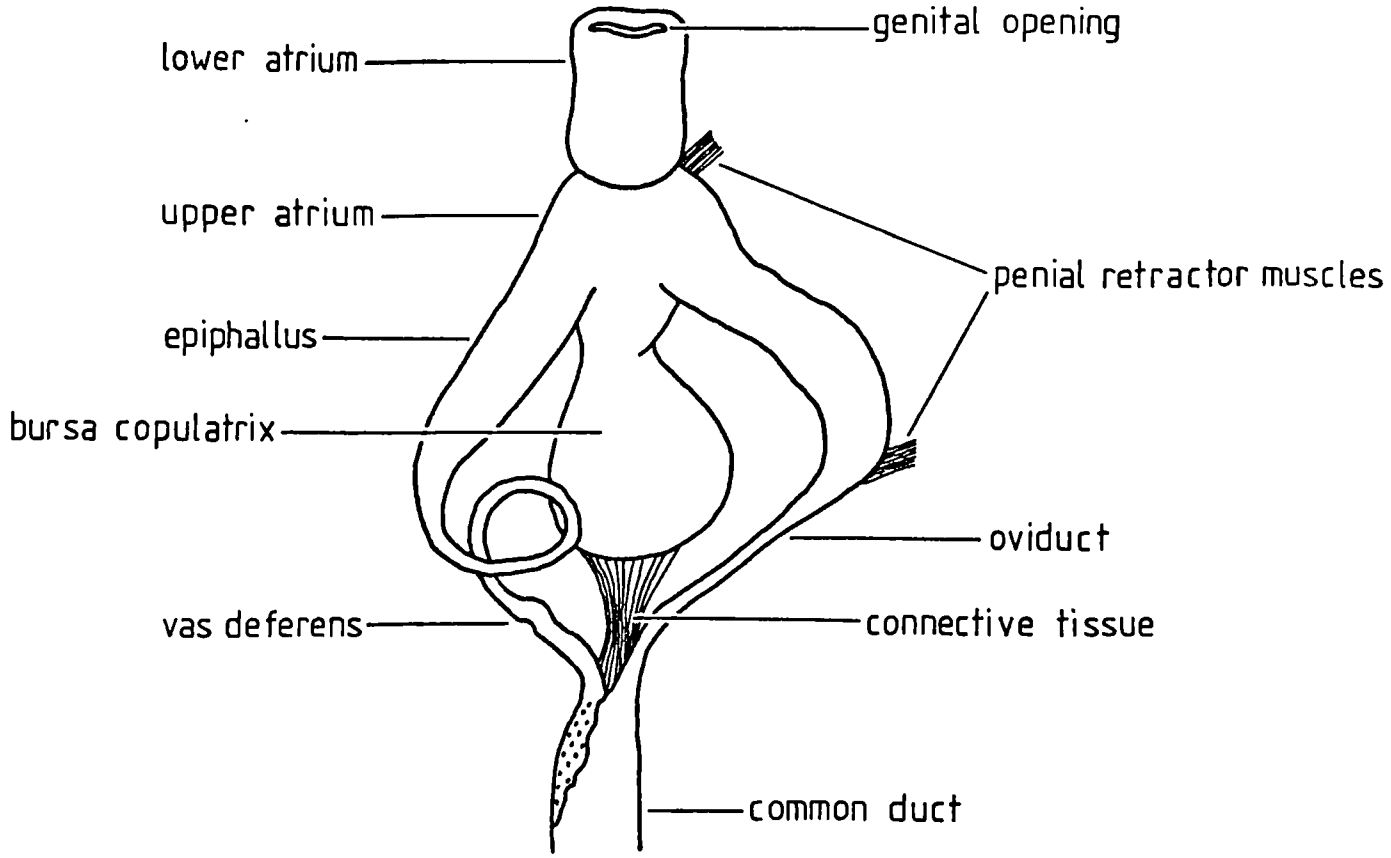
genital opening
lower atrium
upper atrium
penial retractor muscles
epiphallus
bursa copulatrix
oviduct
vas deferens
connective tissue
common duct

Fig. 189

A.hortensis, anterior genital ducts.

Fig. 190 L.S. through the lower and upper atria (x26).

Fig. 191 T.S. through the lower atrium (x34).

Fig. 192 T.S. through the upper atrium (x50).

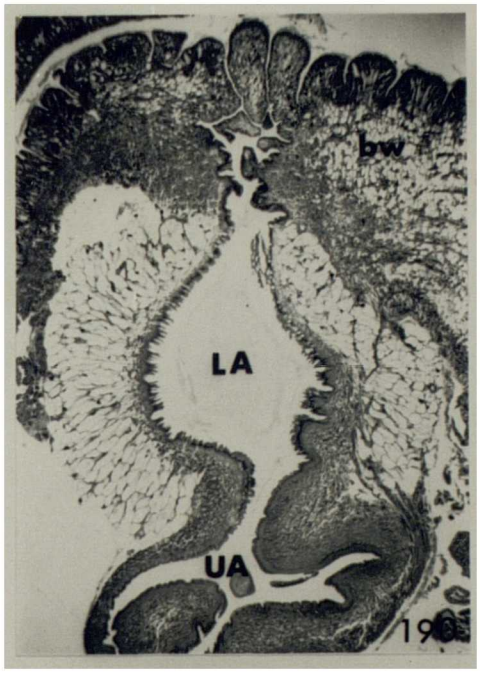
bw
LA
UA
190

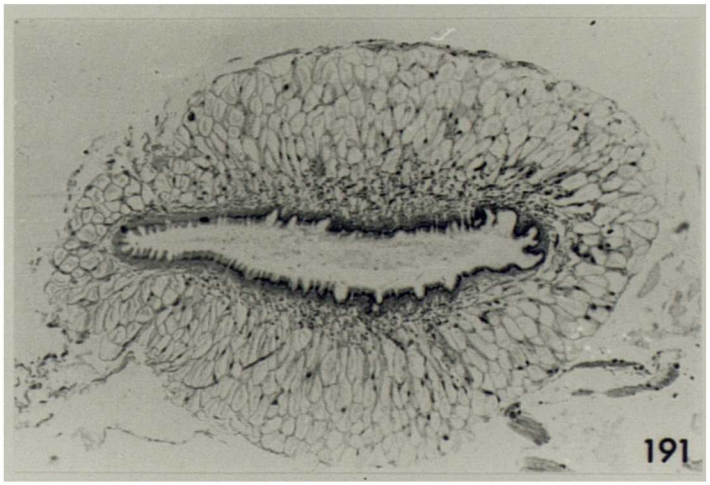
191

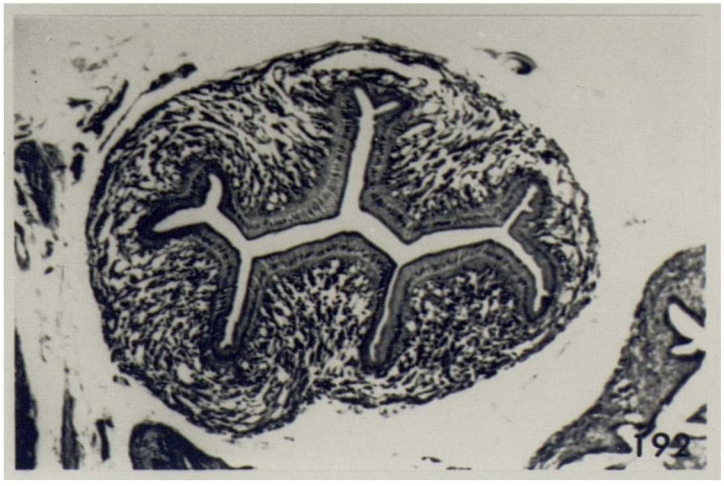
192

A.hortensis, anterior genital ducts.

Fig. 193 T.S. through the thick oviduct (x120).

Fig. 194 T.S. through the thin oviduct (x120).

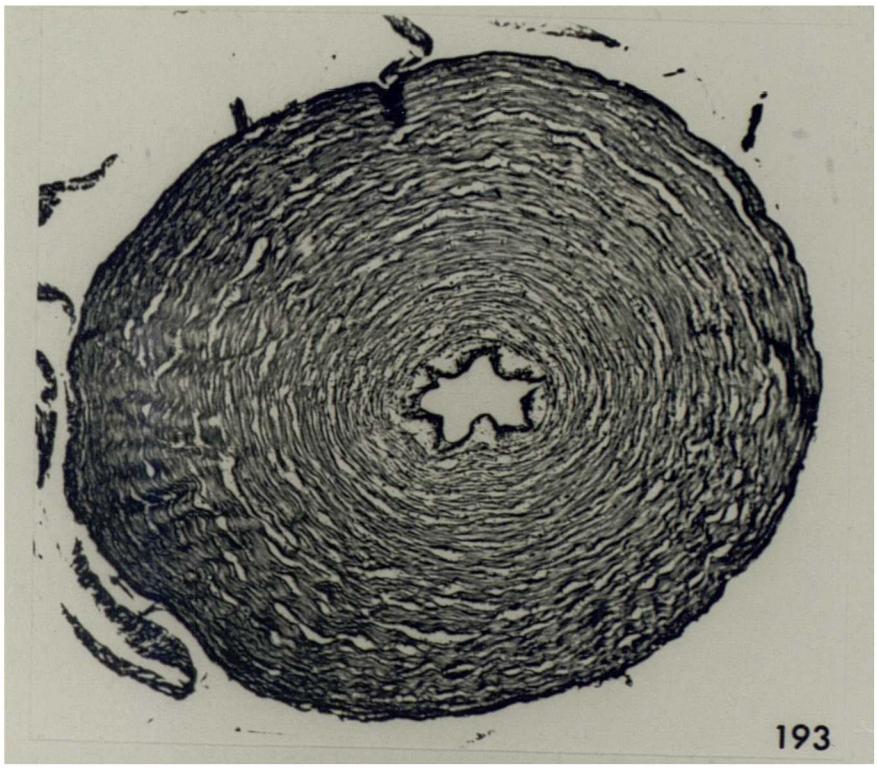

193

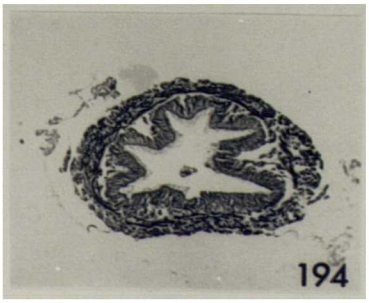

194

A.hortensis, anterior gential ducts.

Fig. 195 T.S. through the epiphallus (x190).

Fig. 196 L.S. through the epiphallus (x125).

Fig. 197 L.S. through the cone at the entrance of the epiphallus (x112).

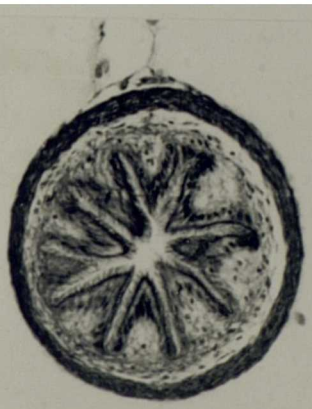

195

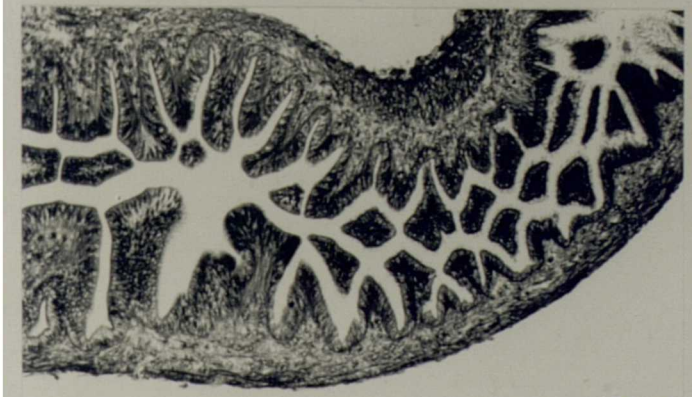

196

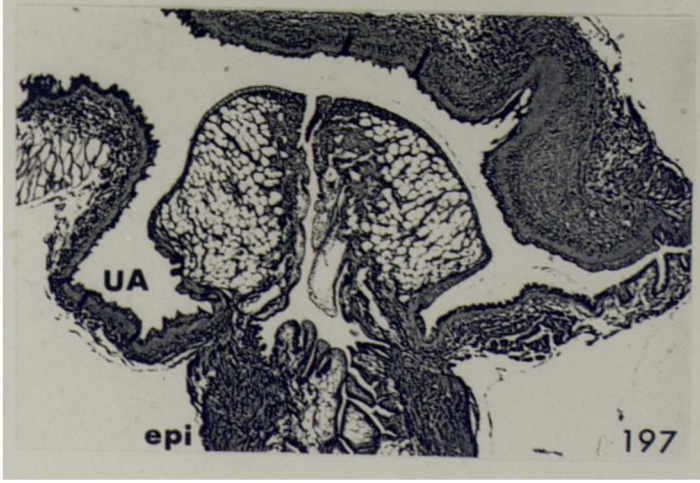

197

A.hortensis, anterior genital ducts.

Fig. 198 T.S. through the vas deferens (x288).

Fig. 199 T.S. through the duct of the bursa copulatrix (x124).

Fig. 200 L.S. through the bursa copulatrix (x42).

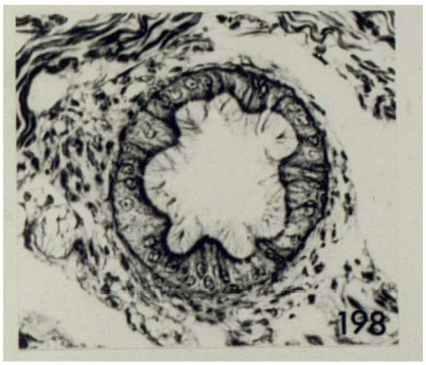
198

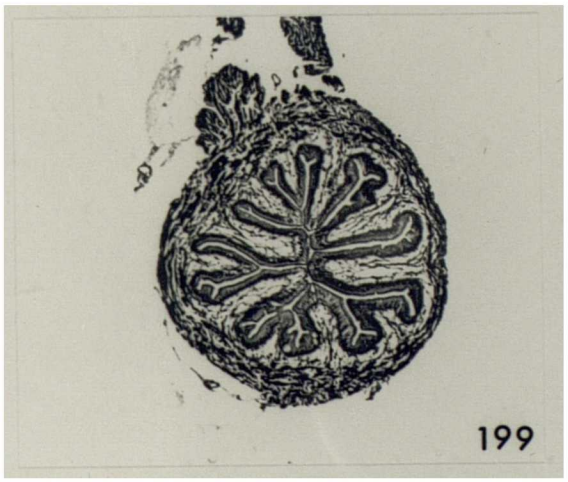
199

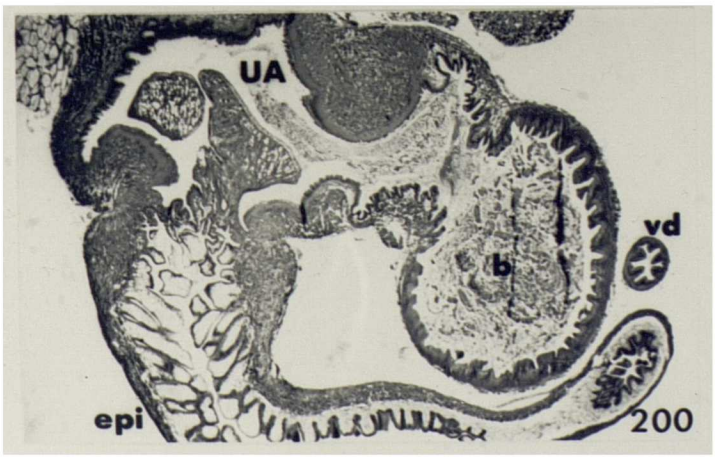
UA
vd
b
epi
200

Fig. 201 Vascularization of the anterior genital ducts of A.hortensis, front (a) and rear (b) views. Drawn from dissection. Blood vessels injected with Indian ink by A. Duval.
Regions of the anterior genital ducts are labelled in Fig. 189.

a. front

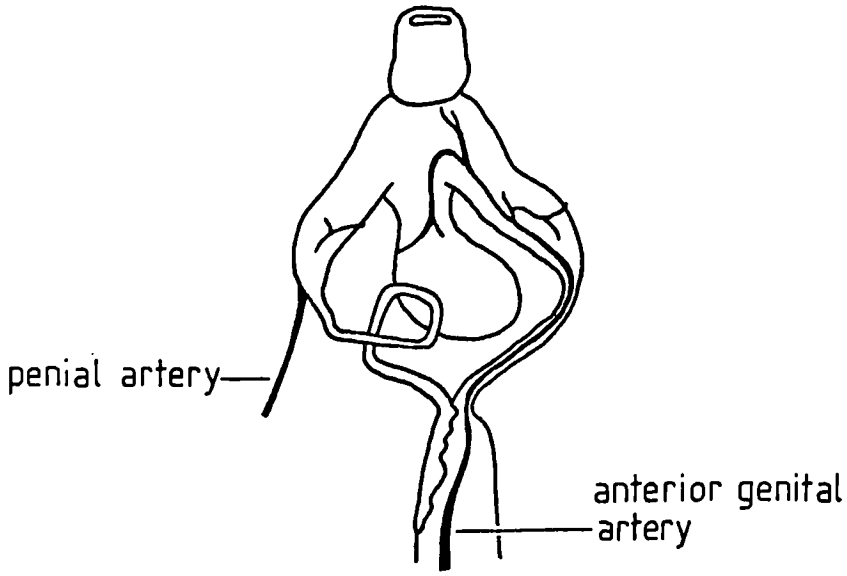

b. rear

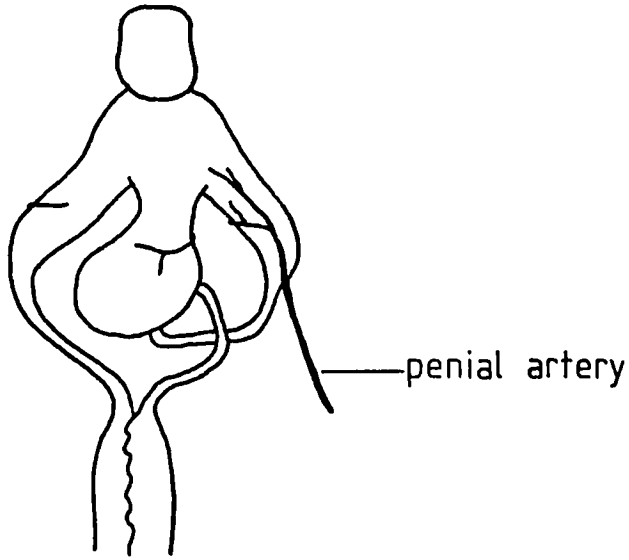

Fig. 201

A.hortensis, anterior genital ducts.

Fig. 202 T.S. through the reproductive tract in the region of the genital atrium (arrowed) (x680). Early A-stage.

Fig. 203 T.S. through the genital atrium (x680). Late A-stage.

Fig. 204 T.S. through the genital atrium (x180). Early B-stage.

Fig. 205 T.S. through the anterior genital ducts (x680). Early B-stage.

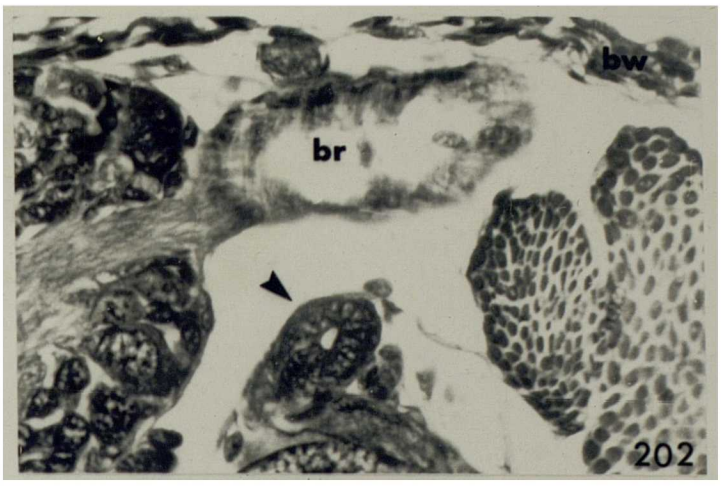
bw
br
202

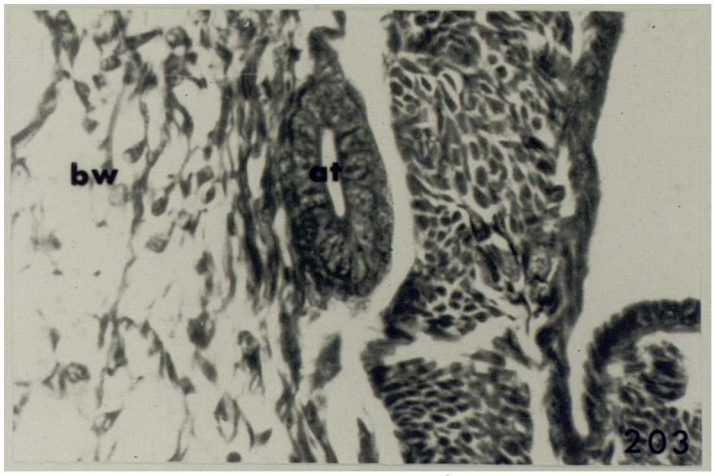
bw
at
203

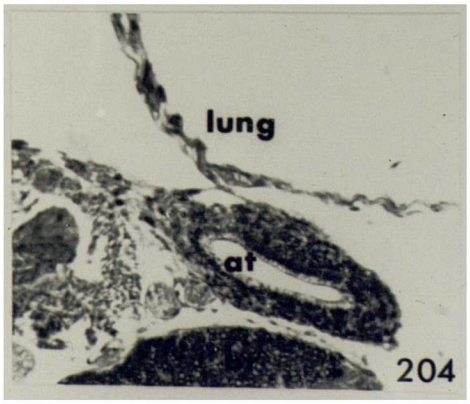
lung
at
204

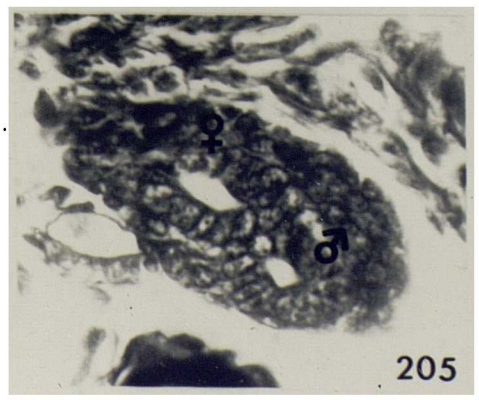
♀
♂
205

A.hortensis, anterior genital ducts.

Fig. 206 T.S. through the anterior genital ducts (x250). Late B-stage.

Fig. 207 T.S. through the common duct (x250). Late B-stage.

Fig. 208 T.S. through the anterior genital ducts (x100). Early C-stage.

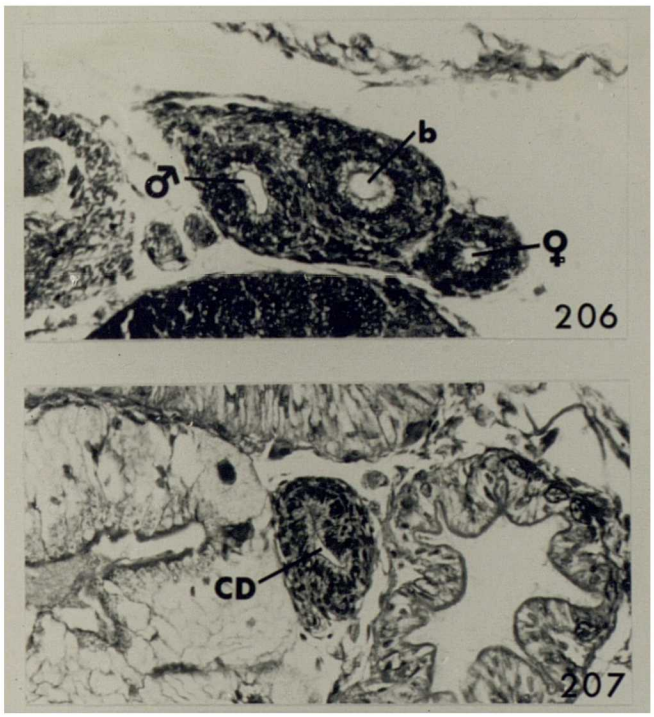
b
♂
♀
206
CD
207

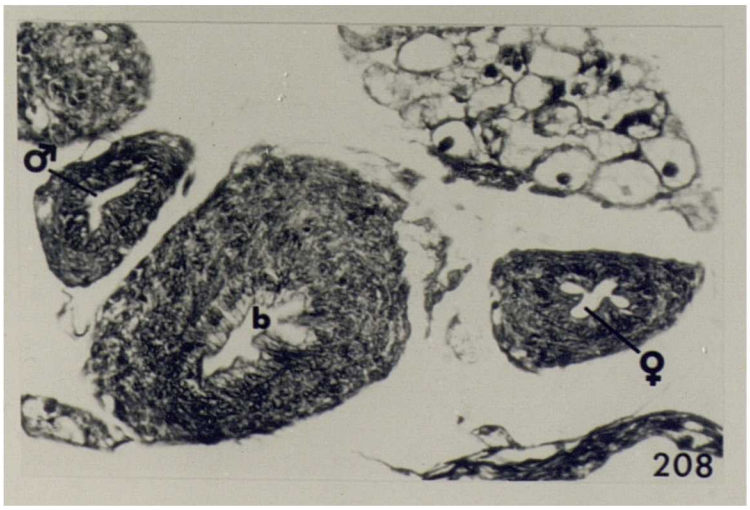
♂
b
♀
208